Chelated fluoroboron cations. Synthesis and multinuclear nmr studies

James A. Winston Shoemaker, B.A., B.Sc. (Hons.)

Brock University

A thesis submitted to the Department of Chemistry

in partial fulfillment of the requirements for the degree of

Master of Science.

Brock University

St. Catharines, ON

April, 1999

Abstract

The preparation of chelated difluoroboron cations $(DD)BF_2^+$, where DD is a saturated polydentate tertiary-amine or polydentate aromatic ligand, has been systematically studied by using multinuclear solution and solid state nuclear magnetic resonance spectroscopy and fast atom bombardment mass spectrometry. Three new methods of synthesis of $(DD)BF_2^+$ cations are reported, and compared with the previous method of reacting a chelating donor with $Et_2O.BF_3$. The methods most effective for aromatic donors such as 1,10-phenanthroline are ineffective for saturated polydentate tertiary-amines like N,N,N',N",N"-pentamethyldiethylenetriamine.

Polydentate tertiary-amine donors that form 5-membered rings upon bidentate chelation were found to chelate effectively when the BF_2 source contained two leaving groups (a heavy halide and a Lewis base such as pyridine = pyr or isoxazole = ISOX), i.e., $pyr.BF_2X$ (X = Cl or Br), $ISOX.BF_2X$ and $(pyr)_2BF_2^+$. Those that would form 6-membered rings upon chelation do not chelate by any of the four methods. Polydentate aromatic ligands chelate effectively when the BF_2 source contained a weak Lewis base, e.g., $ISOX.BF_3$, $ISOX.BF_2X$ and $Et_2O.BF_3$. Bidentate chelation by polydentate tertiary-amine and aromatic donors leads to nmr parameters that are significantly different then their $(D)_2BF_2^+$ relatives (D = monodentate t-amines or pyridines).

The chelated haloboron cations $(DD)BFCl^+$, and $(DD)BFBr^+$ were generated from $D.BFX_2$ adducts for all ligands that form BF_2^+ cations above. In addition, the $(DD)BCl_2^+$ and $(DD)BBr_2^+$ cations were formed from $D.BX_3$ adducts by the chelating aromatic ligands, except for the aromatic ligand 1,8-bis(dimethylamino)naphthalene, which formed only the $(DD)BF_2^+$ cation, apparently due to its extreme steric hindrance.

Chelation by a donor is a two-step reaction. For polydentate tertiary-amine ligands, the two rates appear to be very dependent on the two possible leaving groups on the central boron atom. The order of increasing ease of displacement for the donors was: pyr < Cl <

Br < ISOX. The rate of chelation by polydentate aromatic ligands appears to be dependent on the displacement of the first ligand from the boron. The order of increasing ease of displacement for the donors was: pyr < Cl < ISOX ≈ Br < Et_2O.

Acknowledgments

I wish to thank my supervisor, Dr. J. Stephen Hartman for his support, advice and understanding during this project.

Thanks to Professors Alex Janzen (University of Manitoba); I. D. Brindle, J. McNulty, and M. F. Richardson (supervising committee); H.L. Holland and J. M. Miller for helpful discussions.

My deepest thanks to T. R. B. Jones for all his assistance with nmr and ms instrumentation. Thank you Dr. J. Lakshmi (PDF) and Dr. D. Wails (PDF) for assistance with the solid state MAS nmr instrumentation (Brock University); and Dr. D. Hughes and B. Sayer for assistance with the 11.7 Tesla nmr instrument (McMaster University); Dr. A. Pirani and Professor G. J. Schrobilgen (McMaster University) for technical advice; Frank Bosco (President of New Era Enterprises, Inc., Vineland, New Jersey, U.S.A.) and Dr. Peter Heard (Birkbeck College, University of London, London, U.K.) for donating the Teflon 5 mm nmr tube inserts and oxazole-based tridentate ligands ($(MeOxz)_2py$, $(iPrOxz)_2py$, and $(BzOxz)_2py$) respectively.

To members of the Hartman research group (HRG), a huge thank you for making H202 so enjoyable in the summer. Specifically, thank you to P. Ragogna for technical assistance with low temperature solution nmr experiments; W. R. Szerminski for assistance in the synthesis of $(pyr)_2BF_2^+.PF_6^-$; and S. V. Withers for help with the Schlenk lines.

Finally, thanks to the rest of the students, staff and faculty of the Department of Chemistry and the Faculty of Mathematics and Science for making Brock such an enjoyable place to pursue knowledge.

Table of Contents

List of Figures

List of Tables

Chapter 1:
Introduction

1.1: Boron trihalide adducts and dihaloboron cations.

Boron trihalides (BX_3) are sp^2 trigonal planar Lewis acids in which the central boron atom has an empty $2p_z$ orbital, with which adduct formation with a Lewis base can readily occur [reaction **1.1**] (1,2). The resulting adduct has a tetrahedral structure. The

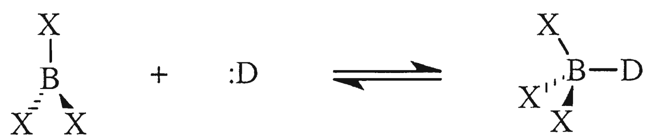

[**1.1**]

adduct's stability tends to be dependent on the donor (D) site in the ligand, specifically: the type of donor atom, the steric hindrance surrounding the donor atom, and the electronic nature of the donor (3). Adducts of boron trihalides have been studied extensively through the past 50 years, the first review appearing in 1954 (4).

Any two boron trihalides in solution can undergo exchange reactions, in which mixed boron trihalides are believed to occur through dimer formation [reaction **1.2**] (1).

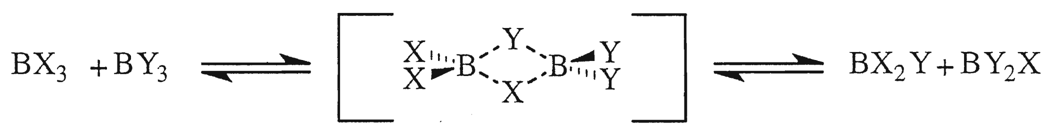

[**1.2**]

Exchange also occurs between a Lewis acid-base adduct D.BX_3 and a Lewis acid BY_3 [reaction **1.3**]. This is believed to occur though three possible mechanisms (5,6): 1) dimer

$$D.BX_3 + BY_3 \rightleftharpoons D.BX_2Y + BY_2X \rightleftharpoons \text{etc} \qquad [\mathbf{1.3}]$$

formation in which the adduct's boron becomes 5 coordinate; 2) through ion pairing D.BX_2^+.BY_3X^- [reaction **1.4**] in systems where the Lewis base was very basic (ie. an amidine, $pK_b = 0.5$ to 1.1 (7)); 3) the D.BX_3 disassociates to D.BX_2^+ and X^-, allowing the cation and BY_3 to exchange via a dimer bridge [**1.2**]. In 1 [**1.3**] and 3 [**1.2**], the

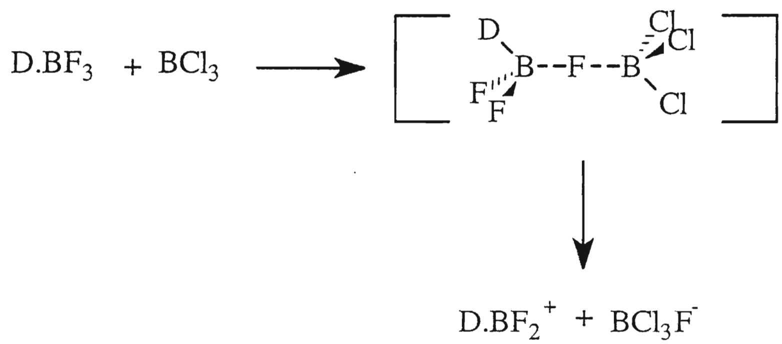

[**1.4**]

original coordination numbers were maintained at the end of the reaction. The coordination numbers in reaction **1.4** have switched, and the $D.\dot{B}F_2^+$ species will quickly react with an adduct, free Lewis base, or anion. $D.BF_2^+$ has not been detected in solution due to its expected high reactivity and these three mechanisms have been dealt with in much greater detail elsewhere (5,6,8).

In the above systems, unless the Lewis acid-base bond of the adducts were very weak (9), a slight molar excess of Lewis base stopped the exchange reactions within the systems. The resulting $D.BX_nY_{3-n}$ mixed adduct system's distribution of $D.BX_3$, $D.BX_2Y$, $D.BXY_2$ and $D.BY_3$ adducts tend to be dependent on the halides and the Lewis base used. In systems where the base was moderately strong (ie. pyridine, $pK_b = 8.8$ (10)) and the halides are fluorine and chlorine, the distribution of adducts was very close to statistical. In systems where the Lewis base was weak (ie. isoxazole, $pK_b = 12.5$ (10)) or soft and the halides are fluorine and bromine, the distribution of adducts was far from statistical, favouring the unmixed-halogen over the mixed-halogen adducts. The unmixed-halogen adducts are much more stable than the mixed fluorine-bromine ones, a consequence of Pearson's "symbiotic principle" that has been discussed in reference (5).

A $D.BF_nX_{3-n}$ mixed adduct system, with a D-B bond of adequate strength so that the adducts do not undergo rapid exchange, undergo the following reactions [**1.5**, **1.6** and **1.7**] on addition of a suitable D' (where D' = D, or another Lewis base). These reactions

$$D.BF_2X + D' \longrightarrow (D)(D')BF_2^{+} + X^{-} \qquad [\mathbf{1.5}]$$

$$D.BFX_2 + D' \longrightarrow (D)(D')BFX^{+} + X^{-} \xrightarrow{D'} (D)(D')_2BF^{+2} + X^{-} \qquad [\mathbf{1.6}]$$

$$D.BF_3 + D' \longrightarrow D'.BF_3 + D \qquad [\mathbf{1.7}]$$

have been the basis of a great deal of research in this lab over the past 20 years (11,12). The following trends tend to control the formation of mixed $(D)(D')BF_2^+$ cations, $(D)(D')_2BF^{+2}$ cations and $D'.BF_3$ adducts.

The formation of dihaloboron cations tends to be dependent on the steric hindrance of D' and especially D (13). Tertiary-amine systems (where D and D' are both NR_3), due to their steric hindrance, tend to need the heavy halide bromine (rather than chlorine, which is harder to displace) as the X species in order for them to form $(D)(D')BF_2^+$ cations from $D.BF_2X$ [**1.5**] (14). Yet, when D was of low steric hindrance (ie., pyridine), tertiary-amines as D' can readily form $(D)(D')BF_2^+$ cations with chlorine being the X species (13,15). Bicyclic amidines and pyridines, due to their low steric hindrance, react very readily in order to form $(D)(D')BF_2^+$ cations from $D.BF_2Cl$ (6,15).

Both amidines and pyridines can undergo reaction **1.6** to form $(D)(D')_2BF^{+2}$ cations from $D.BFX_2$ (6,15). The more basic and more sterically hindered amidines (relative to pyridine) tend to do so much more readily, whereas pyridine needs the X species to be bromine (15). Tertiary-amines do not, due to their steric hindrance, form $(D)(D')_2BF^{+2}$ cations under our conditions, even though they are in general much more basic then pyridines (14,16).

Reaction **1.7** behaves very much like **1.5**, in that D displacement by D' from D.BF_3 tends to be dependent on the steric hindrance of D' and especially D is not too great (13). Thus, tertiary-amines displace all other donors from D.BF_3, while they tend to not be displaced themselves. Amidines, pyridines and other donors do displace all but tertiary-amines. The other adducts in the mixed D.BF_nX_{3-n} adduct systems do not undergo this reaction as readily.

The (D)(D')BF_2^+ cations formed above, can be isolated as PF_6^- salts (12,13,17). These BF_2^+ cations have been reacted with various donors, as the subject of various studies (6,12,13), especially the $(pyr)_2BF_2^+$ cation (6,13). The results are not simple, but the reaction involves the displacement of a pyridine atom in the same vein as reaction **1.5**, to form a (pyr)(D')BF_2^+ cation. The advantage to this method is that reactions **1.6** and **1.7** are not occurring at the same time.

1.2: Bi and tridentate ligands.

Chelate comes from the Greek word *chelos*, meaning claw. Chelation of an atom by a polydentate ligand is generally due to the entropy of a chelated species being favourable in comparison to two or more monodentate ligands coordinating to the same atom (18). The products of chelation are generally more kinetically and thermodynamically stable to reaction after formation (19). In addition, the products of chelation can have very different structures then species that have monodentate ligands solely coordinated to the central atom (19).

A wide variety of bi and tridentate ligands were used in this work, but they can be broken down into three groups: tertiary-amine (table 1.1A); aromatic (table 1.1B); and miscellaneous (table 1.1C). The seven main ligands: Me_4en (20); Me_5dien (21); Me_4pn (22); bipyr (23); 1,10-phen (24); terpyr (25); and 1,8-BDN (26); have been coordinated to various transition and main group elements. More importantly, these seven

Table 1.1A: Tertiary-amine bi and tridentate ligands.

ethylenediamine (en)

N,N,N',N'-tetramethylethylenediamine (Me_4en)

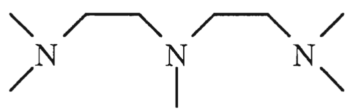

N,N,N',N'',N''-pentamethyldiethylenetriamine (Me_5dien)

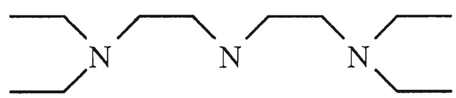

N,N,N'',N''-tetraethyldiethylenetriamine (Et_4dien)

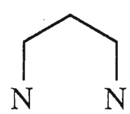

propanediamine (pn)

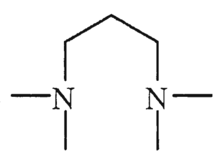

N,N,N',N'-tetramethylpropanenediamine (Me_4pn)

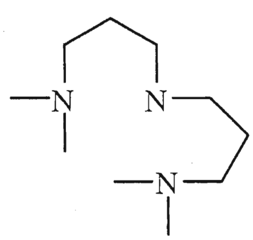

N,N,N'',N''-tetrtamethyldipropanetriamine (Me_4dipn)

Table 1.1B: Aromatic bi and tridentate ligands.

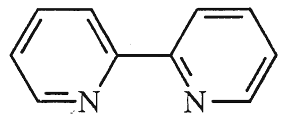

2,2'-bipyridine (bipyr)

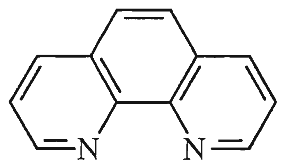

1,10-phenanthroline (1,10-phen)

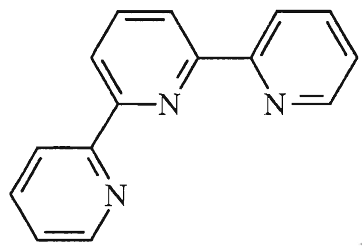

2,2',6',2''-terpyridine (terpyr)

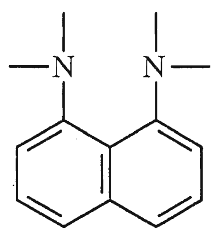

1,8-bis(dimethlyamino)naphthalene (1,8-BDN)

Table 1.1C: Miscellaneous type bi and tridentate ligands.

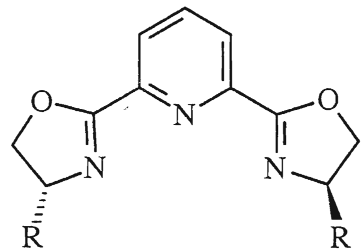

R = Me, iPr, Bz

2,6-bis[4-(S)-methyloxazolin-2-yl]-pyridine ((MeOzx)$_2$py)

2,6-bis[4-(S)-isopropyloxazolin-2-yl]-pyridine ((iPrOxz)$_2$py)

2,6-bis[4-(S)-phenyloxazolin-2-yl]-pyridine ((BzOxz)$_2$py)

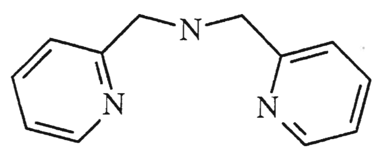

di-(2-picolyl)amine ((pyr)$_2$dien)

have been coordinated to boron (27-33), though not always in a chelated form (34,35). These structural differences can be readily studied by nmr spectroscopy.

1.2.1: Formation of chelated dihaloboron cations. The formation of chelated difluoroboron species has been reported in the literature (28-30,32,36-38) several times over the past thirty years, with ligands of both tertiary-amine, and aromatic amine type. The synthetic approach for both types of ligands has been the same: add $Et_2O.BF_3$ (30,34-36,38) or BF_3 (28,29,34) to a dry ether (34-36), benzene (28), toluene (28) or $CHCl_2F$ (29) solution containing a bidentate ligand. Typically, the solutions to which $Et_2O.BF_3$ was added, were stirred for an hour at room temperature. The solutions that used BF_3, started with condensed material at -196°C and were slowly warmed to room temperature. During this period, fluorine exchange must occur, between two BF_3 units, causing the formation of a BF_2^+ cation and BF_4^- anion [reaction **1.8**].

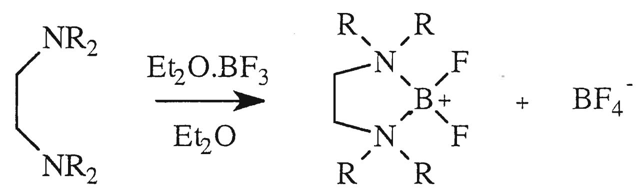

R = H or Me

[**1.8**]

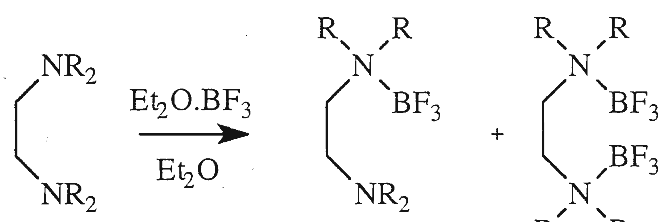

R = H or Me

[**1.9**]

The success of this method was mixed for t-amine ligands. In N. Wiberg and J. W. Buchler's (36) and T. Onak et al's (29) papers, the desired BF_2^+ species were formed successfully. In H. C. Brown and B. Singaram's (34,35) various attempts, only the mono and bis BF_3 adducts of the ligands were formed from en and Me_4en [reaction **1.9**]

As for the aromatic chelating ligands, the formation of desired BF_2 species was more successful than for the t-amine types. All reported attempts were successful (28,30,37) and the ligands used either had two nitrogen atoms (28,30), two oxygen atoms (37), or one of each (38).

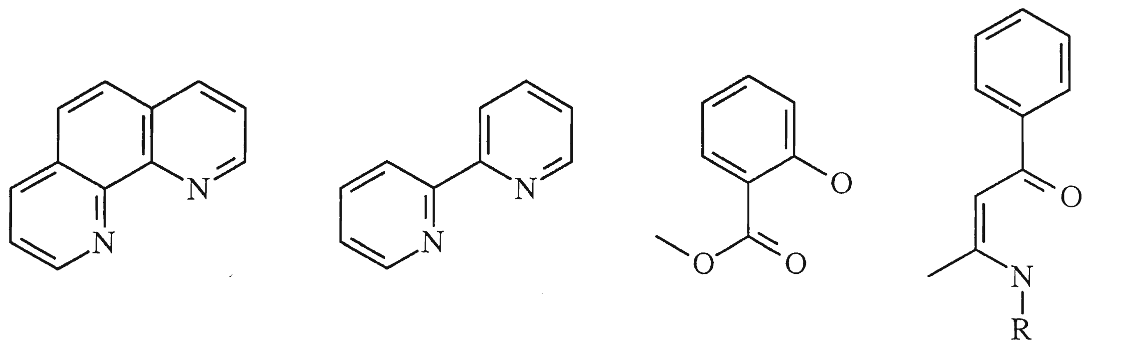

R = Bz, MeBz

Other dihaloboron cations of boron have not been studied as extensively (28,31). They have been formed by the same methodology as the difluoro species: add gaseous BX_3 to solutions of bidentate ligand and gently warm to room temperature. Only the $BX_2^+.X^-$ salts of bipyr and 1,10-phen have been reported (28,31).

1.3: Nuclear magnetic resonance spectroscopy.

1.3.1: Basic principles. Nuclear magnetic resonance (nmr) spectroscopy is possible because certain nuclei have an inherent spin angular momentum (P). This angular momentum can be quantized:

$$P = [I(I + 1)]^{-1/2}(h)/2\pi) \qquad \{\mathbf{1.1}\}$$

where I is the spin quantum number, and h is Planck's constant (39,40). The spin quantum number can have values of 0, 1/2, 1, ... 6 (40). If $I = 0$, the nucleus has no spin, yet if I is > 0, the nucleus possesses a magnetic moment (μ). This μ, and P, are proportional to one another and possess vector quantities:

$$\mu = \gamma \boldsymbol{P} \qquad \{\mathbf{1.2}\}$$

γ is a nucleus' gyromagnetic ratio and it is different for each isotope (40).

A nucleus can assume $2I+1$ nuclear spin states in a magnetic field, and in the absence of any magnetic field, all orientations of a nucleus are of the same energy. Upon placement in an applied (uniform) magnetic field (B_0), the various orientations have different energies. In the case of a nucleus such as ^{19}F that has $I = 1/2$, its -1/2 spin state orients antiparallel to the B_0 (high energy), while its +1/2 spin state orients parallel to the B_0 (low energy). The difference in energy (ΔE) between these states is dependent on μ and the strength of B_0 (40):

$$\Delta E = (h\,\gamma B_0)/2\pi \qquad \{\mathbf{1.3}\}$$

A nucleus in lower energy state may absorb radiofrequency radiation at the frequency corresponding to the ΔE between the two states. Upon absorption, the nucleus is flipped into the higher energy state, and this transition is detected electronically by the nmr instrument. This ΔE is calculated for each isotope of an element. If the γ and B_0 are large, the ΔE is greater, and therefore easier to detect by an nmr instrument.

The electron cloud surrounding a nucleus is modified when placed in a magnetic field B_0. This causes the magnetic field (B_{local}) that is experienced by the nucleus to be different then the applied field:

$$B_{local} = B_0(\,1 - \sigma) \qquad \{\mathbf{1.4}\}$$

where σ is the shielding constant and is small. Shielding (σ) is the ability of electrons to alter the magnetic field at a nucleus (40). Since the electronic environment of the same isotope in different chemical environments can differ greatly, the field experienced by nuclei differs as well. This leads to a wide range of chemical shifts of resonance frequency for a given nucleus, which can be applied to a wide range of chemical problems (41). Nmr can be used on a wide range of nuclei and this makes it an excellent choice for monitoring reactions observed in this project.

1.3.2: Two-dimensional nmr experiments. The majority of nmr spectra acquired within this work are in the one-dimensional (1-D) frame. Yet, 1-D nmr experiments cannot provide sufficient insight into many questions that arise. Typical 1-D spectra have frequency plotted along the x-axis, while the two-dimensional (2-D) experiments used in this work have frequency information plotted along both the Y and X axis. Between the two axes is a contour-plot displaying interactions that are not readily visible within a 1-D nmr frame. Much more detailed treatment of 2-D nmr can be found elsewhere (40,41,42), but it works on the following general principles: 1) nuclei of interest undergo an excitation phase were they are initially pulsed; 2) then a variable time delay occurs called an evolution phase; 3) and then the results of the experiment are detected. It is the second phase that is the key to the majority of information gained, for during this period, the nucleus relaxes or evolves. This evolution can give a variety of information to the experimenter. To gain further information, additional mixing pulse(s) can be applied during the evolution period. The two types of 2-D experiments that were performed in this work were correlation spectroscopy: ^{1}H-^{1}H and ^{19}F-^{19}F homonuclear correlation spectroscopy (COSY) which displays interactions between coupled H or F nuclei; and ^{11}B-^{19}F heteronuclear correlation (HETCOR) nmr which displays interactions between bonded B and F nuclei.

1.3.3: Solid state nuclear magnetic resonance spectroscopy. Nmr signals of solid samples are generally broad and any structural information is hidden within. Causes of the inherent broadness include chemical shift anisotropy (CSA). The chemical shift of a nucleus may be spread over a few or a few hundred ppm depending on orientation of the species in the magnetic field (41). All orientations to the B_0 are possible in a polycrystalline or amorphous solid and without a means of orienting the structural units in the same direction as in a single crystal, the chemical shift of the nuclei will be spread across a range. The chemical shift of a sample, when observed in solution, is an average of all the possible orientations due to rapid tumbling.

In solution, rapid tumbling eliminates another cause of broadening in solids: dipole-dipole interactions between nuclei (41,43,44). An insensitive nucleus undergoes dipole-dipole interactions through space (r_{IS}), depending on the direction of the angle ϕ between the nuclei relative to the magnetic field B_0, with the sensitive nucleus inducing broadening in the spectrum of the insensitive nucleus (41):

$$B_{local} = +/- \mu_S r_{IS}^{-3}(3\cos^2\phi_{IS} - 1) \qquad \{\mathbf{1.5}\}$$

Dipole-dipole broadening is directly dependent on the magnetic moment (μ_S) of the sensitive nucleus, and since ^{19}F has a strong magnetic moment and is 100 % abundant, it induces a great deal of dipole-dipole broadening in spectra of nearby nuclei, such as ^{11}B (41).

A third cause of broadening occurs when solid state nmr is performed on quadrupolar nuclei. Quadrupolar interactions (**Q**) are due to interactions between a quadrupolar nucleus' nuclear electric quadrupole moment (eQ) with the non-spherically symmetrical field gradient around the nucleus (**V**) (44):

$$\mathbf{Q} = (eQ/(2I(2I-1)h))\mathbf{V} \qquad \{\mathbf{1.6}\}$$

These interactions possess both direction and magnitude, and induce changes in the energy levels of the various Zeeman transitions. This is known as the first-order quadrupolar effect (43,44). With quadrupolar nuclei that have integral spins (I = 1, 2, ...) all spin-state transitions are altered relative to their original Zeeman transitions, leading to differing ΔE between states. This alteration in energy states leads to broadening within spectra acquired. Quadrupolar nuclei with non-integral spins (i.e.. 3/2, 5/2), undergo similar broadening due to first-order quadrupolar interactions (i.e., +1/2 to +3/2 transition), but these are not generally detected. The central m = +1/2 to -1/2 transition is not generally affected by first-order effects because the energy levels are altered to the same extent (see diagram below)[1] (44). The +3/2 to +1/2, etc. transitions are not observed for they are very broad. Quadrupolar nuclei with non-integral spins undergo a much smaller (in magnitude) second-order effect (44). The m = +1/2 to -1/2 transition is affected by this second-order effect, and it leads to broadening in the spectra acquired like its first-order relative. Since a nucleus' nuclear electric quadrupole moment (eQ) affects the first and second-order

[1]From page 125 of reference 44.

quadrupolar effects, the more symmetrical the molecule, the less the quadrupolar induced broadening.

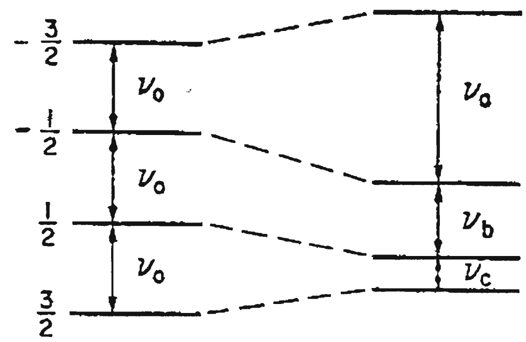

Solution **Solid State**

To combat broadening in solids, one can perform many types of experiments, including high-power decoupling of the nucleus inducing dipole-dipole effects, when the nucleus being observed is different. This technique is not suitable for homonuclear broadening. To reduce the effects of homonuclear broadening, and CSA, one can spin the sample at the magic-angle (55°44') to the magnetic field direction (41). Spinning at the magic angle mechanically induces similar narrowing to the rapid tumbling in solution, allowing for narrower, more resolved peaks, but very high spin rates (> 15 kHz) are required when the dipolar interactions are large. Quadrupolar broadening is reduced by high MAS spin rates, but due to quadrupolar interactions not being solely dependent on one directional interaction, they can not be eliminated by this method. One must spin the sample in two different directions mechanically (41) or perform multipulse experiments (i.e., multiple quantum transition MAS nmr) to lessen the broadening or detect species within the broaden regions of the spectrum. In addition, second-order quadrupolar effects can be reduced by using the highest possible magnetic fields, due to this interaction being inversely magnetic field dependent (41).

1.3.4: Nature of nuclei under study. Six nuclei were studied to varying degrees in this work (table 1.2). They span the range of nuclei types that can be studied by nmr, and the two primary nuclei studied (^{11}B and ^{19}F) are among the most sensitive of nuclei in comparision to ^{1}H. Even the less sensitive nuclei in the table are readily detectable with modern nmr instruments, so no isotopic substitution was necessary. ^{10}B was never directly observed in this research, but its $^{1}J_{BF}$ coupling was observed in some ^{19}F spectra. Only the boron nuclei are quadrupolar. They can behave very differently from their spin 1/2 counterparts, with faster relaxation times and poor $^{1}J_{BF}$ coupling constant resolution in solution nmr spectra.

All the species studied by ^{19}F nmr in this work have a central B atom, and terminal F atom(s). The effect of the ^{11}B isotope having $I = 3/2$, is to cause a 1:1:1:1 quartet to be visible in the ^{19}F spectrum for each individual species. This is due to the ^{11}B spin state having 4 equal populations. The well known $I = 1/2$ coupling pattern of the ^{19}F nuclei are visible in the companion ^{11}B spectrum. As the charge on the boron increases, or the number of fluorine atoms on the boron decreases, the $^{1}J_{BF}$ increases in magnitude (see table 2.1 as example) (11,12). This allows for ready identification of new species in solution, especially when combined with chemical shift information from the ^{11}B and ^{19}F spectra.

The chemical shift ranges of the two main nuclei under study in this work are very different. The chemical shift range of ^{11}B is approximately 200 ppm (46). Unfortunately the chemical shift ranges of the species under study in this research are within a 15 ppm window. This leads to difficulties, for peak overlap is very common at 64.2 MHz, the precession frequency of boron-11 in a 4.7 T nmr magnet (Brock). To overcome this problem, some samples have been studied at McMaster on their 11.7 T nmr instrument. The number of cycles per second (Hz) between signals in a 11.7 T nmr magnet is 2.5 times greater then that of a 4.7 T nmr magnet while J remains constant, causing multiplets that once overlapped, to be well separated. ^{19}F has a chemical shift range of 900 ppm (47) and the fluoroboron range is approximately 90 ppm. This allows monitoring of reactions readily on the 4.7 T nmr magnet at Brock. The only drawback to monitoring certain

Table 1.2: Nmr properties of nuclei under study (45).

Nucleus	Spin	Natural Abundance	Sensitivity (Relative)	Sensitivity (Nat. Abun.)
^{1}H	1/2	99.98	1.00	1.00
^{10}B	3	19.58	$1.99x10^{-2}$	$3.90x10^{-3}$
^{11}B	3/2	80.42	0.17	0.13
^{13}C	1/2	1.1	$1.59x10^{-2}$	$1.76x10^{-4}$
^{19}F	1/2	100	0.83	0.83
^{31}P	1/2	100	$6.63x10^{-2}$	$6.63x10^{-2}$

reactions with ^{19}F, is that not all the species present (ie., $D.BCl_3$) in some samples, contain fluorine.

Of the ligands that were successfully coordinated as BF_2 or BX_2 species (cations, neutrals and anions), few were studied by nmr in the past (28-31,36,38), and most studies had only scattered observations. Few papers reported the $^1J_{BF}$ of the species (29,36,38) and even fewer studied the samples by ^{19}F nmr (36,38). Other studies that were successful at coordinating ligands to BF_2 had solvolysis problems with DMSO-d_6 (28,30) and incorrectly identified the species they were studying via nmr. Thus, there is a great deal of information that could have been gained from nmr about chelation to boron (19), steric hindrance (section **1.1**), nuclei environment, etc., in these species that has yet to be determined. This lab is ideally suited to carry out this research, since the monodentate data needed to study the effects of chelation, steric hindrance, etc. has been carried out here (11,12,16).

1.4: Fast atom bombardment mass spectrometry.

Fast atom bombardment (FAB) mass spectrometry (ms) involves the striking of a liquid or liquid matrix of interest with a beam of neutral atoms (Xe or Ar) that are traveling at a great velocity. The impact of the neutral atoms causes the species within the matrix to be knocked into the gas phase, where once charged (if not charged in the solution), the species can pass through the mass spectrometer to the detector. FAB ms' application towards our systems (14,48,49) and others are best described elsewhere (48). FAB ms first was applied to fluoroboron cations in 1985 (11) and it has the been routinely applied to fluoroboron cations ever since (12). The key to FAB ms working for our haloboron cations is that this soft ionization method allows the cations to get into the gas phase so that they can be readily detected (50). It is certainly not the only ms method of studying fluoroboron systems (51,52), but these other methods (SIMS, and EI) are not available to us or suitable to our samples. With electron impact (EI) ms, the cations do not get into the gas phase, thus they can not be detected, because they are in the form of salts (thus, generally high melting or low decomposition points). As for mixed boron trihalide adducts that generally accompany the fluoroboron cations, they are not ionized by the FAB source in a means that allows for their ready detection nor interference. FAB ms, coupled with solution and/or solid state nmr, allows for rapid detection and identification of cation species.

Chapter 2:
Experimental

2.1: Equipment.

2.1.1: Nmr tubes. Glass 5 mm nmr tubes were washed with distilled water and acetone, dried with zero-grade nitrogen, heated to 120°C, dried again with zero nitrogen (while hot) and stored in desiccators over Drierite. Some tubes were also dried on the high vacuum line with a heating wire around the outside of the vacuum vessel. Teflon 5 mm nmr tube inserts were designed, made, and donated by Frank Bosco, President of New Era Enterprises, Inc., Vineland, New Jersey, U.S.A.. The Teflon inserts were not heated, but underwent two zero nitrogen gas purges before use.

2.1.2: Glassware. All Schlenk glassware was washed with distilled water, ether (to remove vacuum grease) and acetone before initial drying at between 120 and 200°C. The glassware was stored at 120°C. When needed, it was transferred hot to the glove box and assembled under nitrogen. 2 ml GC-ms clear crimp vials with rubber septum caps (from Hewlett Packard) were used for syntheses involving the ISOX.BF_nX_{3-n} systems and boron trifluoride.etherate. These vials were used as supplied and they were handled like the Schlenk glassware (after the washing steps).

2.1.3: Syringes. Gas tight Hamilton syringes were used for microscale transfer (0.5 ml or less) of bases and all gas containing solutions. The syringes were cleaned and dried in the same manner as the Teflon inserts above. Needles (16 to 22 gauge) and large ground glass syringes (1 ml and above) used for macroscale transfers and additions, were dried as described for the glass nmr tubes, with the addition of an ether wash.

2.1.4: Inert atmosphere devices. Glove bags were generally used under dynamic positive pressure of zero-grade nitrogen. The nitrogen was dried by passing through a tube of drierite before entering the bag. Phosphorus pentoxide was used in the bag to assist in removing moisture, especially if the bag was used under static positive pressure for preparing MAS nmr spinners or during short-term storage of samples. All glove bags had their original gloves replaced by black vacuum gloves before use. This greatly increased the glove bags' longevity and air tightness. In addition, one can handle the syringes much more easily with this improvement.

The vacuum glove box used zero nitrogen for its atmosphere. A blower that contained a bed of 4 Å Molecular Sieves and an open plate of phosphorus pentaoxide were used to dry the atmosphere. When the atmosphere was dry, the plate of phosphorus pentaoxide would last 4 months, whereas a glove bag's plate would last between one and two weeks. The glove box also contained a double trap air recirculation system, for the removal of solvent vapours, which was used weekly. The main box, and the entrance port could be placed under -100 kPa vacuum. All materials (except liquids) entering the box, were placed under vacuum twice before entering the main box (zero nitrogen was used as the make-up gas). Liquid containing vessels were purged under zero nitrogen for 15 minutes at between 30 to 60 kPa before entering the glove box.

The high vacuum line, glove box and the two Schlenk lines used Speedivac vacuum pumps. The Schlenk lines used zero-grade nitrogen as their purge gas.

2.2: Materials.

2.2.1: Solid reagents. Ammonium hexafluorophosphate (Aldrich, 95+%), bipyr (Aldrich, 99+%), 1,8-BDN (Aldrich, 99%), 1,10-phen (Aldrich, 99+%), and terpyr (Aldrich, 98%) were used without further purification. $(MeOxz)_2py$, $(iPrOxz)_2py$ and $(BzOxz)_2py$ were donated by Dr. Peter Heard (Birkbeck College, University of London, London, UK). They were used without further purification. All donated ligands were stored in a nitrogen atmosphere glove box dried under 4 Å Molecular Sieves and phosphorus pentoxide.

2.2.2: Liquid reagents. $(Pyr)_2dien$ (Aldrich, 99%), en (J.T. Baker Chemical Company, 100.4%), ISOX (Aldrich, 99%), methylisoxazole (Aldrich, 97%), Me_5dien

(Aldrich, 99%), pn (Aldrich 99+%), pyr (Aldrich, 99.5%), pyridine, 4-methyl (Aldrich, 98.0%), Et_4dien (Aldrich, 90.0%), Me_4en (Aldrich 99%), Me_4pn (Aldrich 99%), and Me_4dipn (Aldrich, 97.0%), were used without further purification. All bases were dried over 3 Å Molecular Sieves that had been heated in a muffle furnace at 400°C for more than 3 hours and cooled over a period of 0.5 hours in a vacuum desiccator.

2.2.3: Boron trihalides. Boron trifluoride (Aldrich, 99.5%), boron trichloride (Matheson, 99.5%) boron tribromide (Aldrich, 99.9%), were all used without further purification. Boron trifluoride.etherate (Aldrich) was stored at -20°C until use.

2.2.4: Solvents. Acetone (Caledon, HPLC grade), acetone-d_6 (Aldrich, 99.5% and Cambridge Isotope Laboratories, 99.8%), acetonitrile-d_3 (Cambridge Isotope Laboratories, 99.8%), chloroform (Caledon, hydrocarbon stabilized, 99.8%), chloroform-d_1 (Cambridge Isotope Laboratories, 99.8%), nitromethane (Fisher Scientific Company), and sulpholane (BDH) were all dried over 3 Å Molecular Sieves. Benzene (Caledon, 99.0%) and hexane (Caledon, HPLC grade) were dried over sodium wire. All solvents were used without further purification.

2.2.5: Miscellaneous chemicals. Hexafluorobenzene (Aldrich, 99.5%), 3-nitrobenzyl alcohol (Aldrich, 98%), trimethyl borate (Aldrich, 98+%), and tetramethylsilane (Cambridge Isotope Laboratories, 99.98%) were used without further purification.

2.3: Mixed boron trihalide adduct systems.

2.3.1: Formation of BF_3 adducts. The formation of adducts, D.BF_3 (D = Lewis base) occurs via the following process: first, a Schlenk vessel is assembled in the glove box; then between 1 to 3 g of D is placed in the tared flask; once the weight of the D has been determined, a 1.0 M solution of D in hexane is created; from here, the flask is taken from the glove box and placed in a chloroform bath that is between -15 and -20°C; nitrogen is flushed into the flask via a Schlenk line (through the side arm) and a septum cap is placed on the top the flask. In advance, the BF_3 addition system in the fumehood is purged for two hours with nitrogen to clear the system of moisture. The Schlenk vessel is transferred to the hood (still in the bath) and the syringe at the end of the boron trifluoride addition system is plunged through the septum, with the tip placed under the surface of the hexane solution. A pressure release needle is inserted at the same time. With the purge nitrogen keeping the pressure in the vessel positive, the BF_3 lecture bottle is turned on and at a rate of about 3 to 5 bubbles a second, the gas is carried by the nitrogen flow into the flask for about the next 20 minutes. A thick stream of white $BF_3.H_2O$ forming at the interface between the release needle and the fume hood's atmosphere indicates that the reaction is finished and the BF_3 is turned off. The flask is then taken back to the Schlenk line, where any excess BF_3 is removed under vacuum (takes about 10 seconds). A positive nitrogen atmosphere is applied to the vessel, and the contents are allowed to settle. After approximately an hour, the majority of the hexane and unreacted D are removed with a syringe. The newly formed $D.BF_3$ is white, and the ground glass top is placed back on the vessel. The adduct is dried for another one to two hours by vacuum on the Schlenk line. The product's identity is confirmed via ^{19}F nmr in $CDCl_3$, and the average yield is between 60 and 80 %.

2.3.2: Formation of boron mixed trihalide adduct systems. A 0.5 M solution of the $D.BF_3$ adduct in $CDCl_3$ is made up in a 5 mm nmr tube or B-19 flask (depending on quantity required), and cooled in a -63°C chloroform slush bath in a glove bag. Y moles of BX_3 (from a 1.0 to 2.0 M chloroform solution) are added via a gas tight syringe to the solution. The solution is mixed thoroughly, so that the adduct and BX_3 will form mixed halide compounds. When thorough mixing does not occur, the BF_3 and BX_3 adducts tend to be the majority of the species in solution. Y moles of D are added to the solution, while thorough mixing is occurring. The solution is removed from the chloroform slush and allowed to warm to room temperature. If the solution starts to bubble or fume, this indicates that it is not quenched, and must have a small amount of D added to coordinate the free Lewis acids. Depending on the base used, the solution is ready for reaction with D or a D', to form fluoroboron cations within minutes or hours of reaching room temperature. Before any experiments, a ^{11}B or ^{19}F nmr spectrum is normally obtained to confirm formation of the mixed boron trihalide adducts at the desired ratio.

The pyr.BF_nCl_{3-n} system (11), produced as described above, is colourless in chloroform. Its ^{11}B and ^{19}F nmr parameters are available in reference 15.

ISOX.BF_3 and ISOX.BF_nX_{3-n} were made as described above. ISOX.BF_3 is white. The ISOX.BF_nCl_{3-n} system is light yellow and the ISOX.BF_nBr_{3-n} system is light brown in colour in chloroform. ^{11}B and ^{19}F nmr parameters of the ISOX.BF_nX_{3-n} system in chloroform are found in table 2.1.

2.4: Formation and isolation of $(pyr)_2BF_2^+.PF_6^-$.

The synthesis of $(pyr)_2BF_2^+.PF_6^-$ was first reported in 1985 (17). All previous work (6,12,13,15) used salt prepared in 1985 by the late M.J. Farquharson. The synthesis has been refined by the work of the author and W. R. Szerminski, via methods included in Z. Yuan's M.Sc. and the author's B.Sc. theses (12). From a pyr.BF_nCl_{3-n} (F:Cl = 1:1.5) system, the $(pyr)_2BF_2^+$ cation is maximized from the pyr.BF_2Cl adduct. At room temperature, an ethanol solution, with a 1.5 molar ratio of $NH_4^+.PF_6^-$ to the amount of cation calculated to exist in the solution is prepared. The ethanol solution is then made up to an equal volume as the chloroform solution containing the desired $(pyr)_2BF_2^+$ cation. Under nitrogen, the ethanol solution is added, and the white precipitate of the $(pyr)_2BF_2^+.PF_6^-$ salt immediately forms. This solution is stirred for approximately one hour before being filtered out of solution by a Hirish funnel in the open air. The solid is washed with cool chloroform to remove any adducts or uncomplexed base present. The salt can then be dried further on a Schlenk line if desired. There are two keys to this method working: 1) the amount of pyr.BF_3 used should not exceed 1.5 g, for the amount of BCl_3 added to make the 1:1.5 F:Cl ratio above this mass, tends to cause the reaction to violently

Table 2.1: Nmr parameters of $D.BF_nCl_{3-n}$ and $D.BF_nBr_{3-n}$ systems (D = ISOX).

	$D.BF_3$	$D.BF_2Cl$	$D.BFCl_2$	$D.BCl_3$	$D.BF_2Br$	$D.BFBr_2$	$D.BBr_3$
^{19}F (ppm)	-149.0	-130.9	-123.4		-124.3	-117.3	
^{11}B (ppm)	-0.6	2.6	4.9	4.9	0.4	-3.1	-13.4
$^{1}J_{BF}$ (Hz)	a	32.9	61.0		45.1	81.4	

[a]not resolved

fume (even at -63°C); 2) the amount of pyr added to maximize the desired cation should just be adequate to the task, or the undesired $(pyr)_2BFCl^+$ cation will also be formed in solution.

While the $(pyr)_2BF_2^+$ cation's ^{11}B and ^{19}F nmr data in chloroform-d1 has been reported in the literature (15), the PF_6^- salt's has not. Nmr parameters for the $(pyr)_2BF_2^+.PF_6^-$ salt in acetone-d_6: ^1H, 9.16 ppm (s), 8.70 ppm [$^3J_{HH}$ = 7.22 Hz] (t), and 8.20 ppm [$^3J_{HH}$ = 6.97 Hz] (t); ^{11}B, 3.0 ppm [$^1J_{BF}$ = 23.2 Hz]; ^{13}C, 147.5 ppm, 144.8 ppm, and 128.9 ppm; ^{19}F, -70.6 ppm [$^1J_{FP}$ = 707.2 Hz], and -153.4 ppm [$^1J_{BF}$ = 23.2 Hz]; and ^{31}P, -140.8013 [$^1J_{FP}$ = 707.2 Hz]. The salt decomposes rapidly above 95°C. The salt decomposes over two weeks, if stored in an environment (under nitrogen) where the temperature is at 28°C or above. Yet, the salt prepared by the author and the late M.J. Farquharson have been stored successfully at room temperature for 8 months and 12 years respectively without decomposition.

2.5: General reaction procedures.

2.5.1 Reactions with pyr.BF_nCl_{3-n}. 5-mm nmr tubes containing solutions of the pyr.BF_nCl_{3-n} were prepared for each reaction. The chelating DD were added via syringe (either in a lump amount, or in small quantities) to the tube under a nitrogen atmosphere. The solution was mixed via a long mixing rod to ensure vertical mixing. Reactions were monitored by ^{19}F nmr (by a kinetics monitoring program), and were generally complete after 16 hours. Solutions were continued to be monitored via ^{19}F nmr, for slow secondary reactions took place over a period of 2 to 10 days. Any precipitates were separated by centrifuging the nmr tube, and analyzed by + FAB ms.

2.5.2 Reactions with ISOX.BF_nX_{3-n} systems. 10 ml of a chloroform solution of ISOX.BF_nCl_{3-n} or ISOX.BF_nBr_{3-n} was prepared in a vessel with a B-19 ground glass joint. 1-ml amounts of the solutions were added to GC-ms vials containing the chelating donors in 0.5 ml of chloroform. Precipitation of desired products occurred within seconds in most cases, but the solutions were allowed to sit for 16 hours to ensure complete reaction. The vials were then centrifuged, and both the mother liquor and precipitate analyzed by nmr and + FAB ms.

2.5.3 Reactions with $(pyr)_2BF_2^+.PF_6^-$. Acetone solutions (20 mg/ml) of the salt were prepared and 0.5 ml portions were added to nmr tubes containing neat liquid chelating donors, or solid chelating donors in 0.5 ml acetone solutions. The reactions were monitored by ^{19}F nmr, and took between 24 hours and 3 weeks (at room temperature) to complete. Systems that were heated to 50°C or higher were finished reacting in 24 hours. Any precipitates were separated by centrifuging the nmr tube, and analyzed by + FAB ms analysis.

2.5.4 Reactions with $Et_2O.BF_3$. Various amounts of $Et_2O.BF_3$ were added via gas tight syringe to GC-ms vials or sealed round bottom flasks containing the chelating donors in 1 to 15 ml chloroform or 1:1 ether:acetone or benzene solutions (with stirring when required). Precipitation of desired products normally occurred within seconds in most cases, but the solutions were allowed to sit for 1 to 16 hours to ensure complete reaction. The vials were then centrifuged, and both the mother liquor and precipitate analyzed by nmr and +/- FAB ms.

2.6: Instrumentation.

2.6.1: Nuclear magnetic resonance spectroscopy. Most ^{19}F, ^{11}B $\{^1H\}$ and all ^{31}P $\{^1H\}$ nmr spectra were obtained on a Bruker AC-200 4.7 Tesla multinuclear Fourier transform nmr spectrometer operating at 188.31 MHz (^{19}F), 64.20 MHz (^{11}B) and 81.01 MHz (^{31}P), using 5 mm nmr tubes. ^{19}F spectra were obtained with 16K FID's, 16K zero-filling, spectral windows of up to 35,000 Hz, with between 256 and 4096 30° pulses and relaxation delay of 1.0 s. The 90° pulse duration was 6.6 μs. ^{19}F chemical shifts are accurate to $\pm$ 0.1 ppm and were internally referenced to C_6F_6 as a secondary standard (-162.7 ppm from $CFCl_3$), and are reported in ppm from $CFCl_3$. $^1J_{BF}$ coupling constants are accurate to $\pm$ 1 Hz. ^{11}B {^{1}H} spectra were obtained with 16K FID's, 16K zero-filling, and spectral windows of up to 6400 Hz, with between 256 and 4096 30° pulses and relaxation delays of between 0.5 and 10 s. The 90° pulse duration was 17.1 μs. ^{11}B chemical shifts are accurate to $\pm$ 0.1 ppm and were externally referenced to $Et_2O.BF_3$. ^{31}P {^{1}H} spectra were obtained with 16K FID's, 16K zero-filling, and spectral windows of up to 36,000 Hz, with between 4096 and 64K 30° pulses and relaxation delays of between 0.5 and 1.0 s. The 90° pulse duration was 17.1 μs. ^{31}P chemical shifts are accurate to $\pm$ 0.1 ppm and were externally referenced to 85% H_3PO_4.

Some ^{19}F, ^{11}B, $^{11}B\{^{19}F\}$, $^{19}F\{^{11}B\}$, ^{19}F-^{19}F COSY and ^{11}B-^{19}F HETCOR nmr spectra were obtained at 30°C on a Bruker DRX-500 11.7 Tesla multinuclear Fourier transform nmr spectrometer (McMaster University) operating at 470.53 MHz (^{19}F) and 160.46 MHz (^{11}B) using between 40 and 128 30° pulses with 32K FID's. The 90° pulse durations were 7.5 μs (^{19}F) and 15.0 μs (^{11}B). Spectral windows of 42,016 Hz (^{19}F) and 40,000 Hz (^{11}B) were used. $^{11}B\{^{19}F\}$ and $^{19}F\{^{11}B\}$ decoupling experiments used selective and broad band decoupling pulse power between 25 and 35 dB. ^{19}F-^{19}F COSY experiments were performed using the Bruker cosy45 pulse program, with a 2.0 s relaxation delay. ^{11}B-^{19}F HETCOR experiments used the Bruker hxcocp pulse program, with the BIRD sequence removed. Removal of the BIRD sequence was due to there being no $^{3}J_{HB}$ or $^{4}J_{HF}$ coupling visible, and the sequence induced T_1 artifacts in our spectra. The relaxation delay was 1.0 second.

^{1}H, ^{1}H-^{1}H COSY, ^{1}H nOe difference and ^{13}C {^{1}H} nmr spectra of the samples were obtained on a Bruker DPX300 7.05 Tesla multinuclear Fourier transform nmr spectrometer (Brock University) operating at 300.13 MHz (^{1}H) and 75.45 MHz (^{13}C), using 5 mm nmr tubes in a QNP probe. ^{1}H samples were run for 16 to 64 scans, and ^{13}C {^{1}H} samples were run for 256 to 2048 scans with relaxation delay of approximately 1.0 seconds. TMS was used as the internal standard, with its chemical shift being set to 0.0 ppm. ^{1}H-^{1}H COSY experiments were performed using the Bruker cosy45 pulse program, with 2.0 s relaxation delays. ^{1}H nOe difference spectra used saturation pulse power between 45 and 55 dB and a relaxation delay of 2.0 seconds.

^{11}B, $^{11}B\{^{1}H\}$ and ^{19}F (depth) solid state magic angle spinning (MAS) nmr spectra of the samples were obtained on a Bruker DPX300 7.05 Tesla multinuclear Fourier transform nmr spectrometer (Brock University) operating at 96.29 MHz (^{11}B) and 282.41 MHz (^{19}F). The MAS probe (Bruker) used 4 mm spinners (capacity ~100 mg). Spin rates were between 5 to 15 KHz. Samples were run for 256 to 2048 scans, with relaxation delays of between 0.5 to 5.0 seconds and 32 K of data points were obtained and Fourier transformed with 5 - 15 Hz of line broadening. For ^{11}B, trimethyl borate was used as the external standard, with its chemical shift being set to 18.3 ppm, while Teflon (-123.01 ppm) was the external standard for the ^{19}F spectra. The depth program used to suppress the background signals of fluorine (contained in the MAS probe), did not work except for a few rare cases. Therefore, little data could be gained by this technique.

2.6.2: Fast atom bombardment mass spectrometry. Positive and negative ion FAB spectra were obtained on a Concept 1S double beam mass spectrometer, with 8 KV accelerating voltage using Xe collision gas at 7.5 KeV/n energy. 3-nitrobenzyl alcohol (NBA) was used as a liquid matrix. Data were collected on a Kratos DART data system with SUN Sparcstation 10, using XMACH3 software.

2.6.3: Molecular modeling. Semi-empirical molecular orbital calculations at the PM3 level were performed via MacSpartan 1.7.1 software on an Apple 7600 Power PC with a 233 MHz processor.

Chapter 3:
Chelating Donor Reactions with Pyr.BF_nCl_{3-n}

3.1: Introduction.

Previous studies of pyr.BF_nCl_{3-n} mixed-halogen adducts (11,13,15), display that they will undergo a wide range of reactions with monodentate ligands (see chapter 1). The formation of mixed monodentate (pyr)(D)BF_2^+ cations from pyr.BF_2Cl via chloride displacement [**1.5**] appears to be a very promising first step towards forming chelated BF_2^+ cations. If a polydentate ligand (DD) is added to a chloroform solution of pyr.BF_nCl_{3-n}, the donor could first displace the chloride ion from pyr.BF_2Cl and then displace the pyridine atom from the mixed (pyr)(DD)BF_2^+ cation [**3.1**].

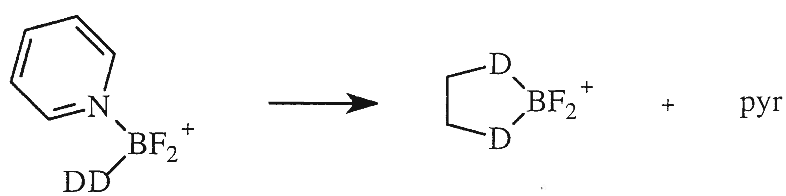

[**3.1**]

3.2: Results.

All reactions were carried out in chloroform, and the nmr parameters of products in this chapter can be found in chapter 7. A base like pyridine should not sterically hinder the chelating t-amine donors from displacing Cl^- and forming mixed non-chelated (pyr)(DD)BF_2^+ cations (13). The pyr.BF_nCl_{3-n} system unfortunately causes the formation of some unexpected products when one attempts the formation of mixed (pyr)(DD)BF_2^+ cations. Displacement of chloride from pyr.BF_2Cl [**1.5**] and pyridine from pyr.BF_3 [**1.7**] occur with the t-amine ligands, but reaction **1.7** was much faster then **1.5**.

3.2.1: Pyr.BF_nCl_{3-n} + Me_4pn: maximizing the formation of non-chelated (pyr)(DD)BF_2^+ cations. Me_4pn does not chelate, making it the ideal DD to display the maximization of (pyr)(DD)BF_2^+, the first step in a two step bidentate chelation. In figure

3.1, approximately 80 % of the pyr in the form of BF_3 adduct has been displaced by the Me_4pn in the first 2.4 hours of the reaction. Only 25 % of the pyr.BF_2Cl species has reacted over the same time period to give $(pyr)_2BF_2^+$ and $(pyr)(Me_4pn)BF_2^+$. Due to reaction **1.7** being so fast, a great deal of pyr was released into the solution. Pyridine can then compete with the DD ligand to react with pyr.BF_2Cl, thereby leading to the formation of massive amounts of $(pyr)_2BF_2^+$ in solution (figure 3.1). To combat these undesirable reactions, one can do two things: 1) add enough DD so that it can compete with the displaced pyr; 2) limit the amount of pyr.BF_3 that exists in the solution at the time of DD addition. In figure 3.2, the amount of unchelated mixed $(pyr)(Me_4pn)BF_2^+$ that forms is approximately double that figure 3.1, because the amount of DD added was increased from 1.5 mol equivalent to 2.5 mol equivalent. Yet the key factor is the amount of pyr.BF_3 in the initial solution. In figure 3.3, the ratio of pyr.BF_2Cl to pyr.BF_3 is 1.5:1 versus 1:1 in figure 3.2. This leads to a near tripling of the amount of unchelated mixed $(pyr)(Me_4pn)BF_2^+$ that is formed. Positive ion FAB ms confirms the presence of $(pyr)(Me_4pn)BF_2^+$ in solution: 258 m/z.

When Me_4pn is added in one large quantity, a white foam like material occurs on the top of the solution. This is $Me_4pn.BF_3$ (identified by ^{19}F nmr), which forms instantly on addition to the solution. When Me_4pn was added in small amounts over time, no $Me_4pn.BF_3$ appears to precipitate from solution. Instead, the solution just turns from colourless to yellow, which is common for chloroform solutions of $D.BF_nCl_{3-n}$ in the presence of excess Lewis base (12b).

Me_4pn also displaces pyridine from pyr.BF_2Cl to form the $Me_4pn.BF_2Cl$ adduct. This reaction is very slow and has not previously been observed when t-amine ligands react with pyr.BF_2Cl (11,13-15).

Me_4pn reacts with the $(pyr)_2BF_2^+$ cation when the solution is left standing over several days, leading to the formation of more $(pyr)(Me_4pn)BF_2^+$ in solution. Over this period of days, it also reacts with pyr.$BFCl_2$ adduct in similar ratios to how it reacts with

Figure 3.1: The limited formation of $(pyr)(Me_4pn)BF_2^+$ due to mole ratio 2:1.5 of pyr:Me_4pn (pyr.BF_nCl_{3-n} mole ratio pyr:BF_3:BCl_3 = 2:1:1).

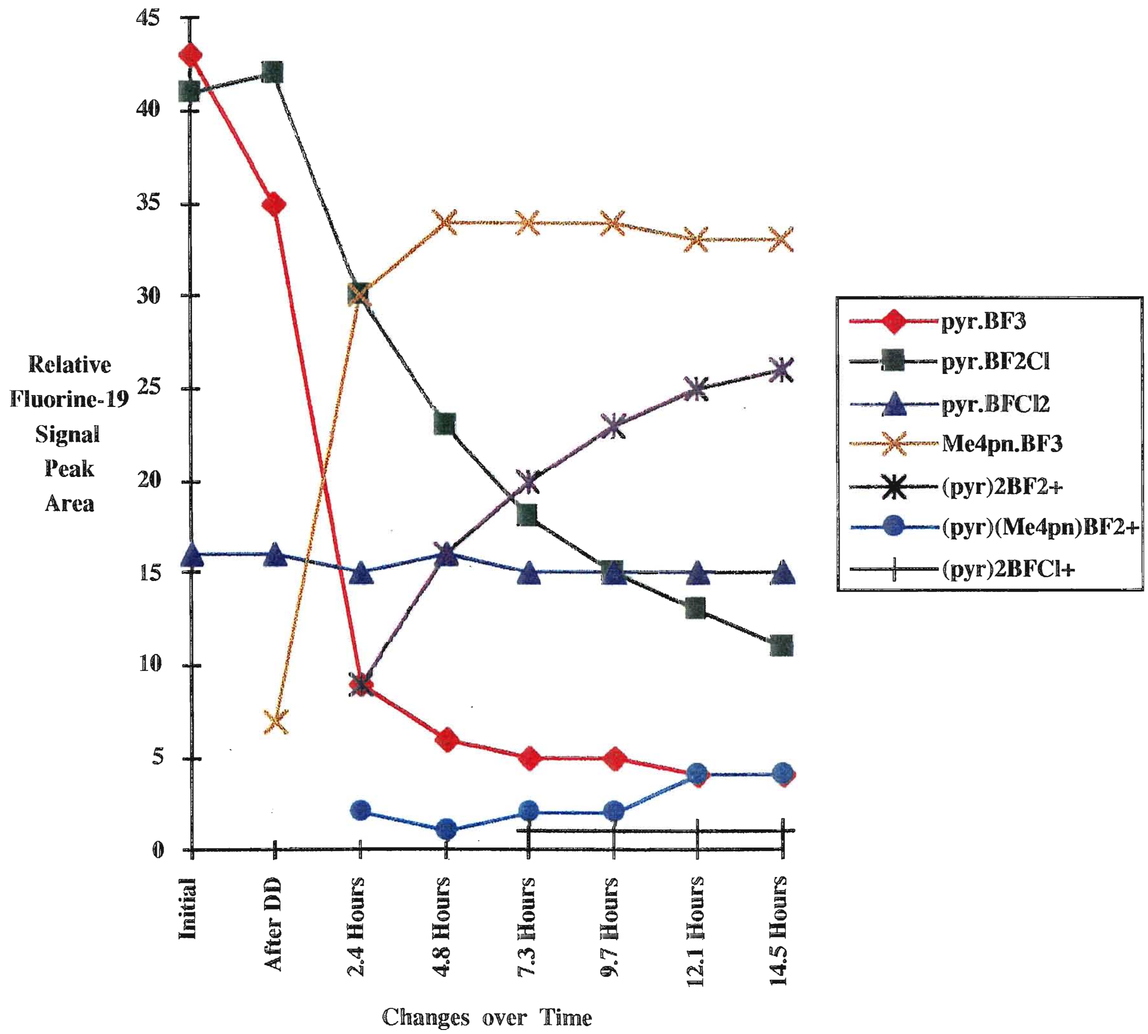

Figure 3.2: The increased formation of (pyr)(Me_4pn)BF_2^+ due to mole ratio 2:2.5 of pyr:Me_4pn (pyr.BF_nCl_{3-n} mole ratio pyr:BF_3:BCl_3 = 2:1:1).

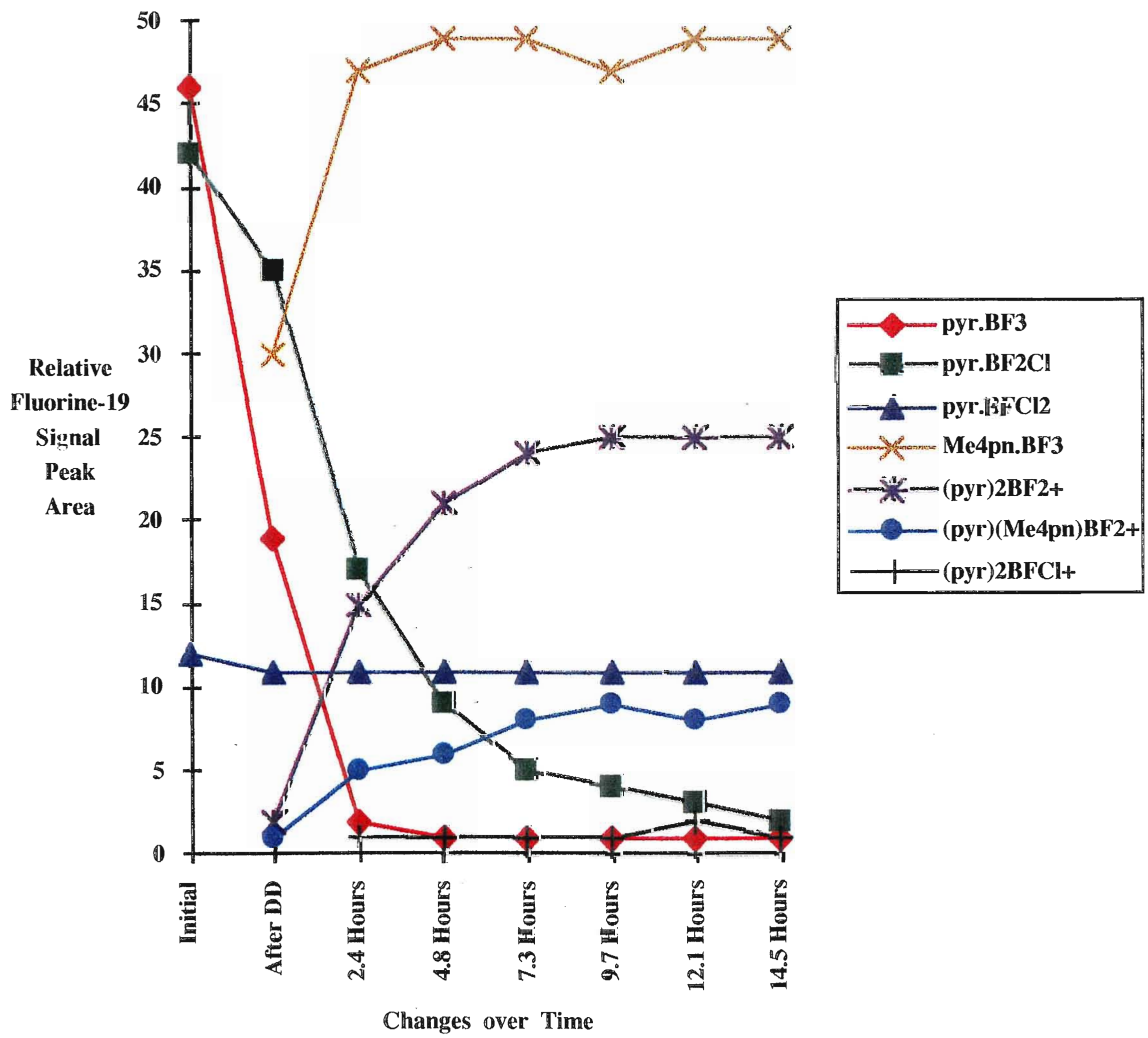

Figure 3.3: The increased formation of $(pyr)(Me_4pn)BF_2^+$ due to limiting the amount of reactive $pyr.BF_3$ in solution ($pyr.BF_nCl_{3-n}$ mole ratio $pyr:BF_3:BCl_3 = 2.5:1:1.5$).

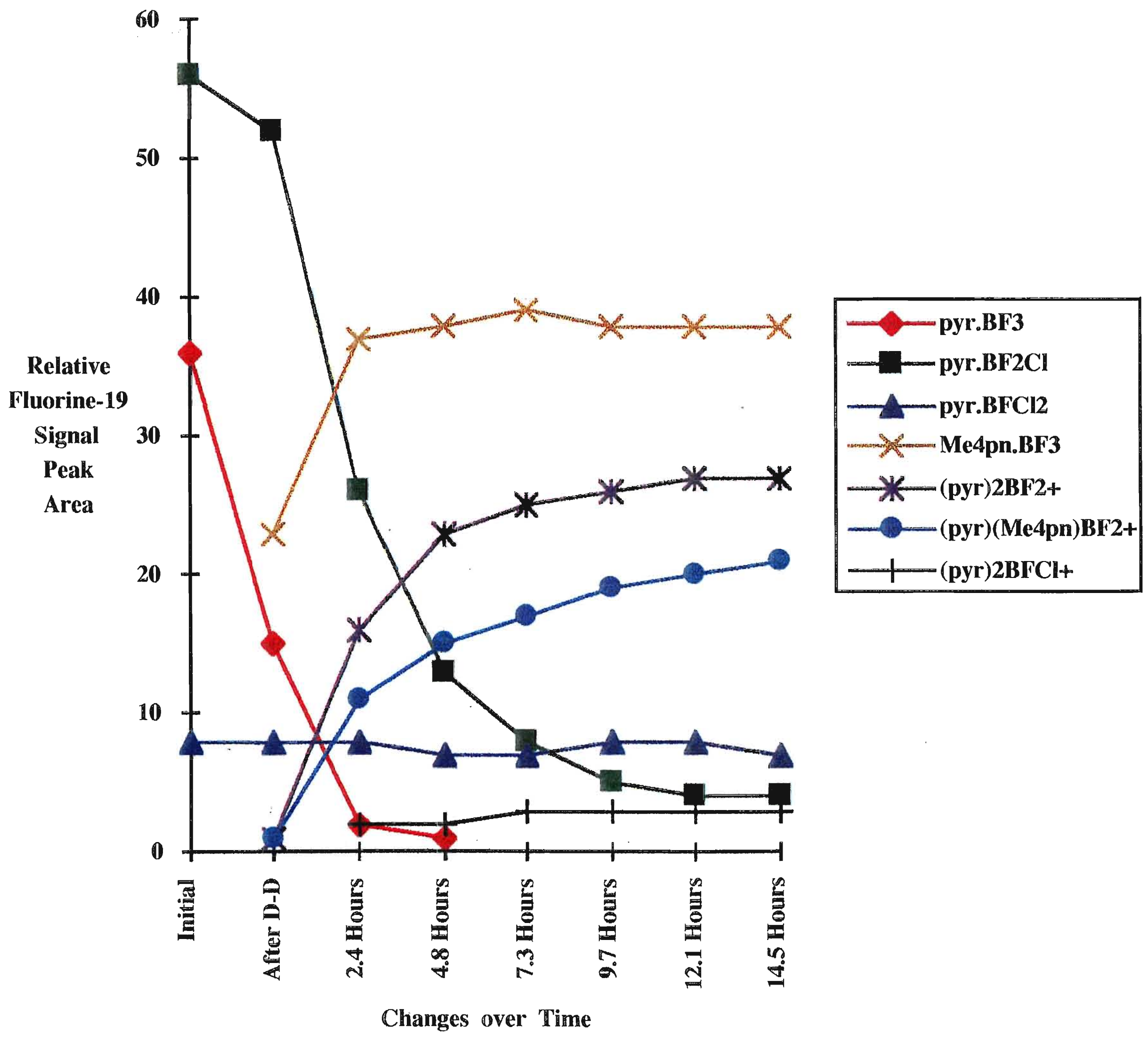

the pyr.BF_2Cl adduct. The major of product is (pyr)(Me_4pn)$BFCl^+$ and the minor product is Me_4pn.$BFCl_2$. Me_4pn does not displace pyridine from (pyr)(Me_4pn)$BFCl^+$ or a chlorine atom from pyr.$BFCl_2$ to form the chelated $BFCl^+$ cation.

3.2.2: Pyr.BF_nCl_{3-n} + Me_4en. Addition of 2.5 molar equivalents of Me_4en to a pyr.BF_nCl_{3-n} (BF_3:BCl_3 = 1:1.5) solution leads to the formation of unchelated mixed (pyr)(Me_4en)BF_2^+ from pyr.BF_2Cl [**1.5**]. The Me_4en then readily displaces the pyr from that mixed cation, leading to the formation of the desired chelated (Me_4en)BF_2^+ cation [**3.1**]. (Me_4en)BF_2^+ is not very soluble in chloroform, and after it reaches approximately 10 % of the total ^{19}F signal intensity, it begins to precipitate from solution (figure 3.4) as the white chloride salt, identified by its + FAB mass spectrum: (Me_4en)BF_2^+ [165 m/z (100 %)] and ((Me_4en)BF_2^+)$_2$(Cl^-) [365 m/z (5.6 %)] (figure 3.5). Expansion of the vertical scale by a factor of 20 (inset of figure 3.5) shows the higher mass clusters: ((Me_4en)BF_2^+)$_3$(Cl^-)$_2$ [565 m/z] and ((Me_4en)BF_2^+)$_4$(Cl^-)$_3$ [767 m/z]. Elemental analysis confirms the species: C calculated = 35.97 %, detected = 36.13 %; N calculated = 13.98 %, detected = 14.09 %; H calculated = 8.05 %, detected = 8.30 %.

Me_4en displaces pyr from pyr.BF_3 [**1.7**], forming the monodentate Me_4en.BF_3 adduct (figure 3.4). Although both nitrogen atoms of Me_4en can coordinate to BF_3 (34) (see chapter 6) only the mono-BF_3 adduct forms in detectable amounts by displacement of pyr from pyr.BF_3. This reaction leads to a great deal of free pyr in solution, which behaves as described in section **3.2.1**.

On standing for several days at room temperature, the $(pyr)_2BF_2^+$ formed from free pyr and pyr.BF_2Cl, reacts with Me_4en, and the (Me_4en)BF_2^+ cation continues to precipitate as the chloride salt. This is consistent with our successful use of $(pyr)_2BF_2^+.PF_6^-$ as a reagent to form (DD)BF_2^+ cations (chapter 5). A positive ion FAB mass spectrum of the mother liquor after a week confirms this, for only the (Me_4en)BF_2^+ and (Me_4en)$BFCl^+$ cations are detected. Thus there are rapid initial reactions, followed by

Figure 3.4: The formation of $(Me_4en)BF_2^+$ from $pyr.BF_2Cl$ and precipitation of $(Me_4en)BF_2^+.Cl^-$ from chloroform (mole ratio $pyr:BF_3:BCl_3:Me_4en$ = 2.5:1:1.5:2.5).

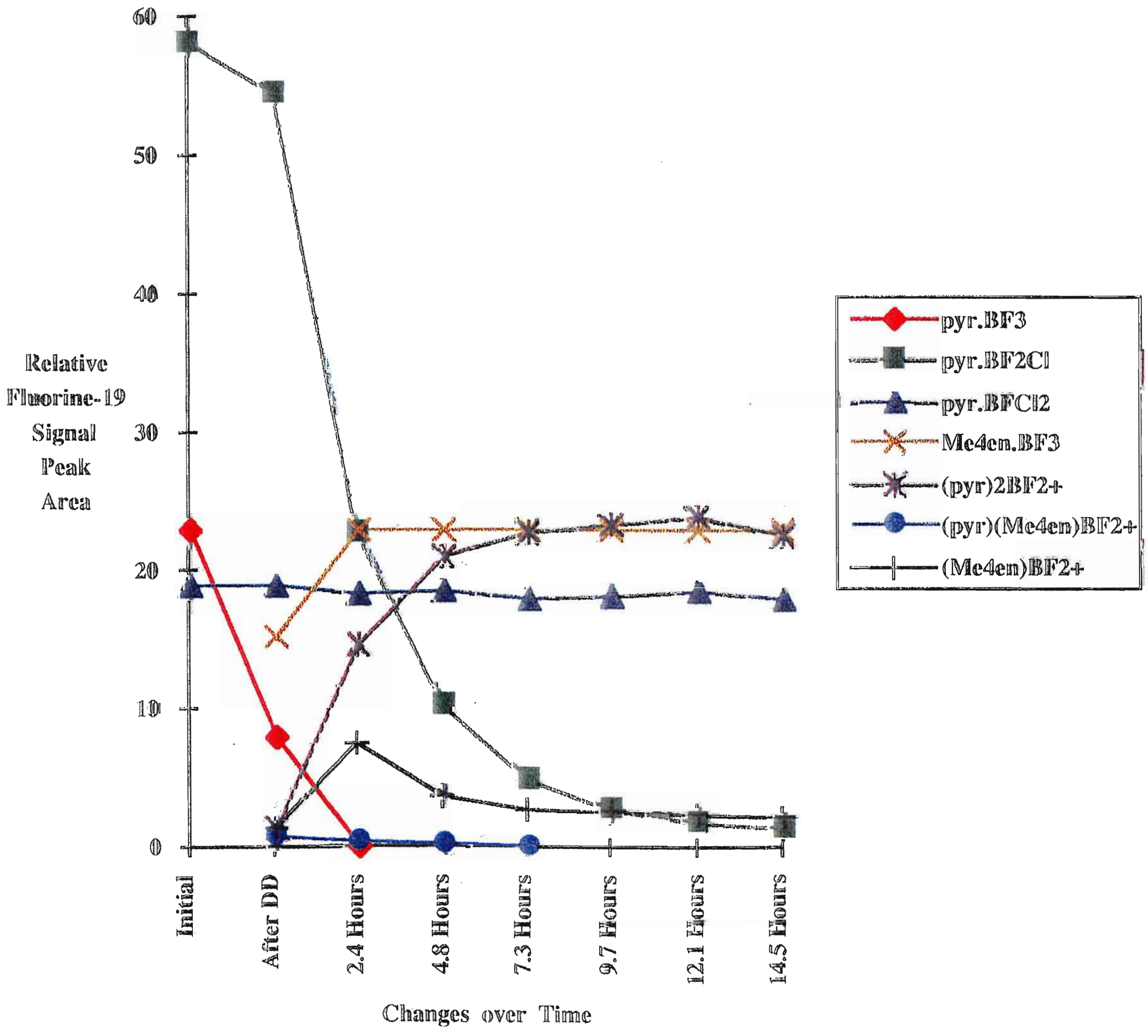

Figure 3.5: Positive ion FAB mass spectrum of $(Me_4en)BF_2^+.Cl^-$. C = $(Me_4en)BF_2^+$, A = Cl^-

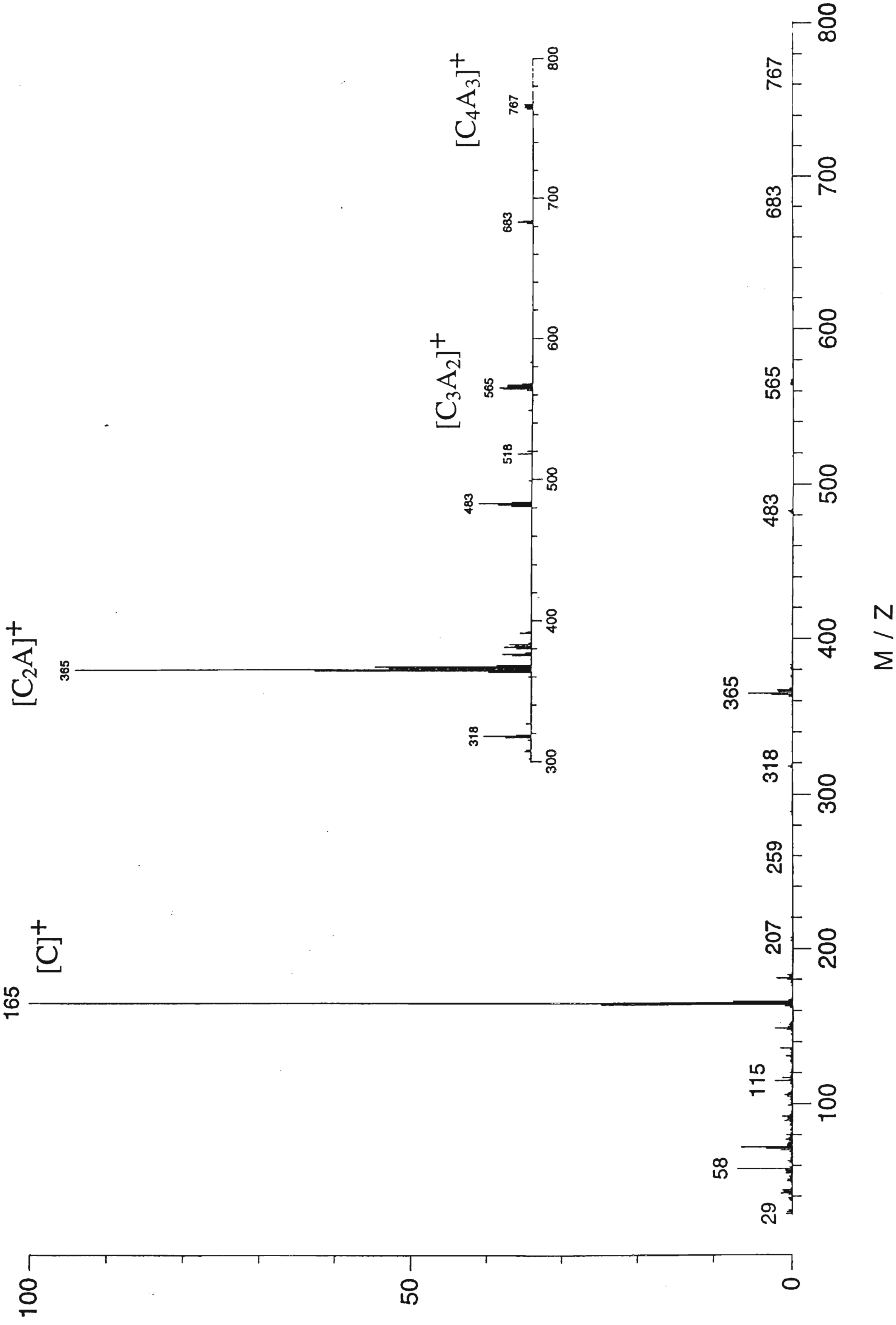

much slower reactions, as we have noted before in other haloboron adduct/cation systems (13).

As well as the slow formation of more $(Me_4en)BF_2^+$ in solution, there is also the slow formation of $(Me_4en)BFCl^+$ from $pyr.BFCl_2$, and again there is competition from free pyr: $(pyr)_2BFCl^+$ also forms from $pyr.BFCl_2$: confirmed by its nmr data (15) and by a weak + FAB peak at 223 m/z, obtained from the mother liquor after standing for one week.

3.2.3: $\underline{Pyr.BF_nCl_{3-n} + Me_5dien}$. Me_5dien is a potentially tridentate ligand, but it behaves towards $pyr.BF_nCl_{3-n}$ like the bidentate ligands. Me_5dien is affected by the same reaction conditions as discussed in section **3.2.1**, and unlike Me_4en, its various products are completely soluble in chloroform, making nmr monitoring of the reactions more straight forward.

Me_5dien readily undergoes reaction **1.7** with $pyr.BF_3$ (figures 3.6 and 3.7), and when it does, it has two possible bonding sites with the BF_3. Though two sites are available, the ^{19}F data suggests that only the end nitrogen site readily displaces pyr from BF_3 (see section **3.3.1**). Like Me_4en, the displacement of pyr from the BF_3 adduct by Me_5dien gives free pyr in solution and leads to the formation of $(pyr)_2BF_2^+$ and $(pyr)_2BFCl^+$ (figures 3.8 and 3.9). The formation of these cations makes it difficult to precipitate the desired BF_2^+ cation of Me_5dien.

Me_5dien readily undergoes reaction **1.5**, leading to the formation of $(pyr)(Me_5dien)BF_2^+$, and then displaces the pyr (reaction **3.1**), leading to the formation of the desired $(Me_5dien)BF_2^+$ cation (figures 3.6 and 3.7). The centre nitrogen on Me_5dien becomes chiral upon formation of the +1 cation, making the BF_2 fluorines prochiral and magnetically nonequivalent. This leads to a complex ^{19}F spectrum (figure 3.6), rather then the typical 1:1:1:1 quartet due to ^{11}B-^{19}F coupling that all the other species have in figure 3.6 (This is discussed in chapter 7). $(Me_5dien)BF_2^+$ was also detected from the chloroform

Figure 3.6: 188.31 MHz ^{19}F nmr monitoring of the formation of $(pyr)_2BF_2^+$ and $(Me_5dien)BF_2^+$ from pyr.BF_2Cl (mole ratio pyr:BF_3:BCl_3:Me_5dien = 2.5:1:1.5:2.5). **A** = initial solution; **B** = after Me_5dien addition; **C** = 2.3 hours; **D** = 13.8 hours.

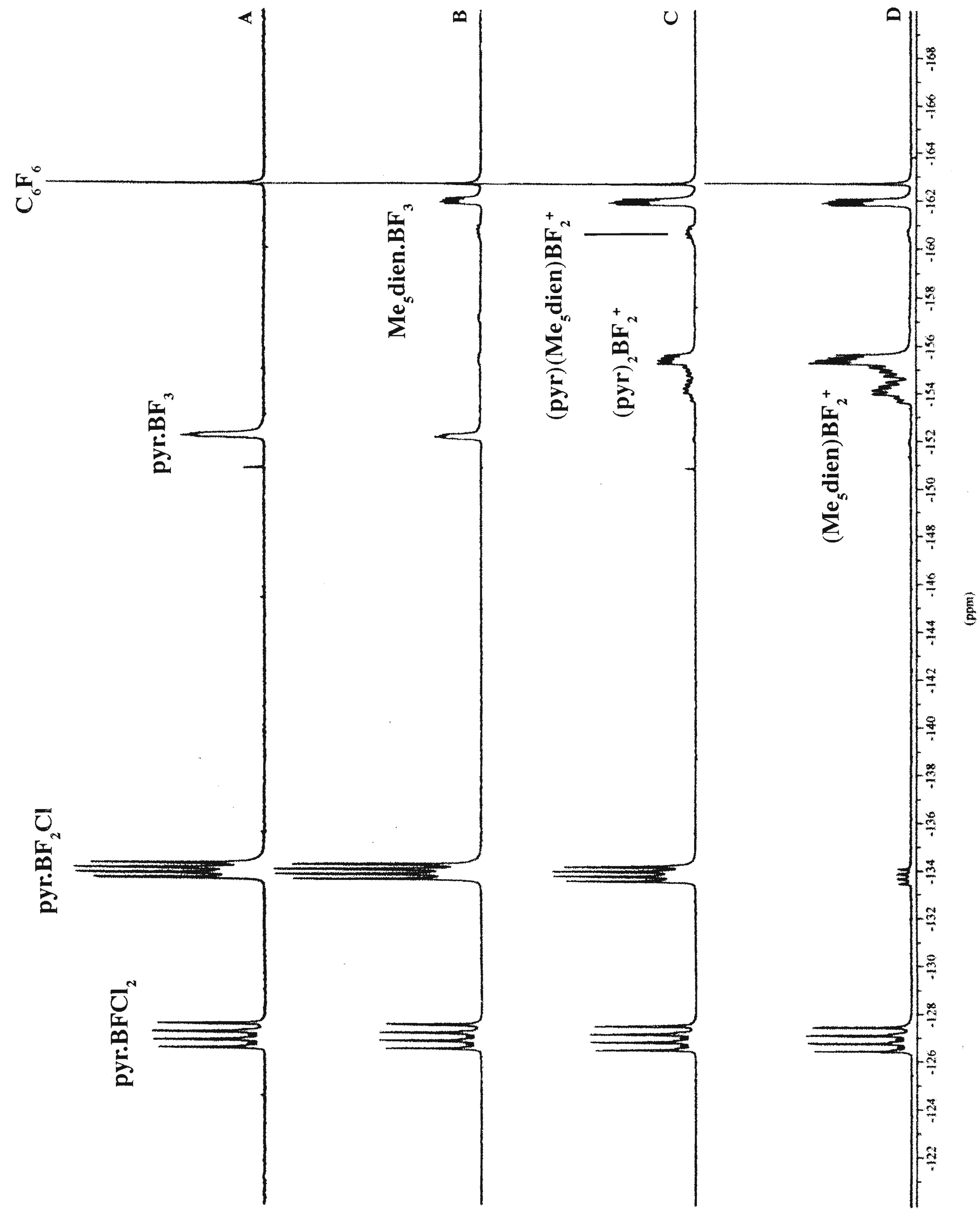

Figure 3.7: Primary reactions caused by addition of Me_5dien to a solution of $pyr.BF_nCl_{3-n}$ (mole ratio pyr:BF_3:BCl_3:Me_5dien = 2.5:1:1.5:2.5).

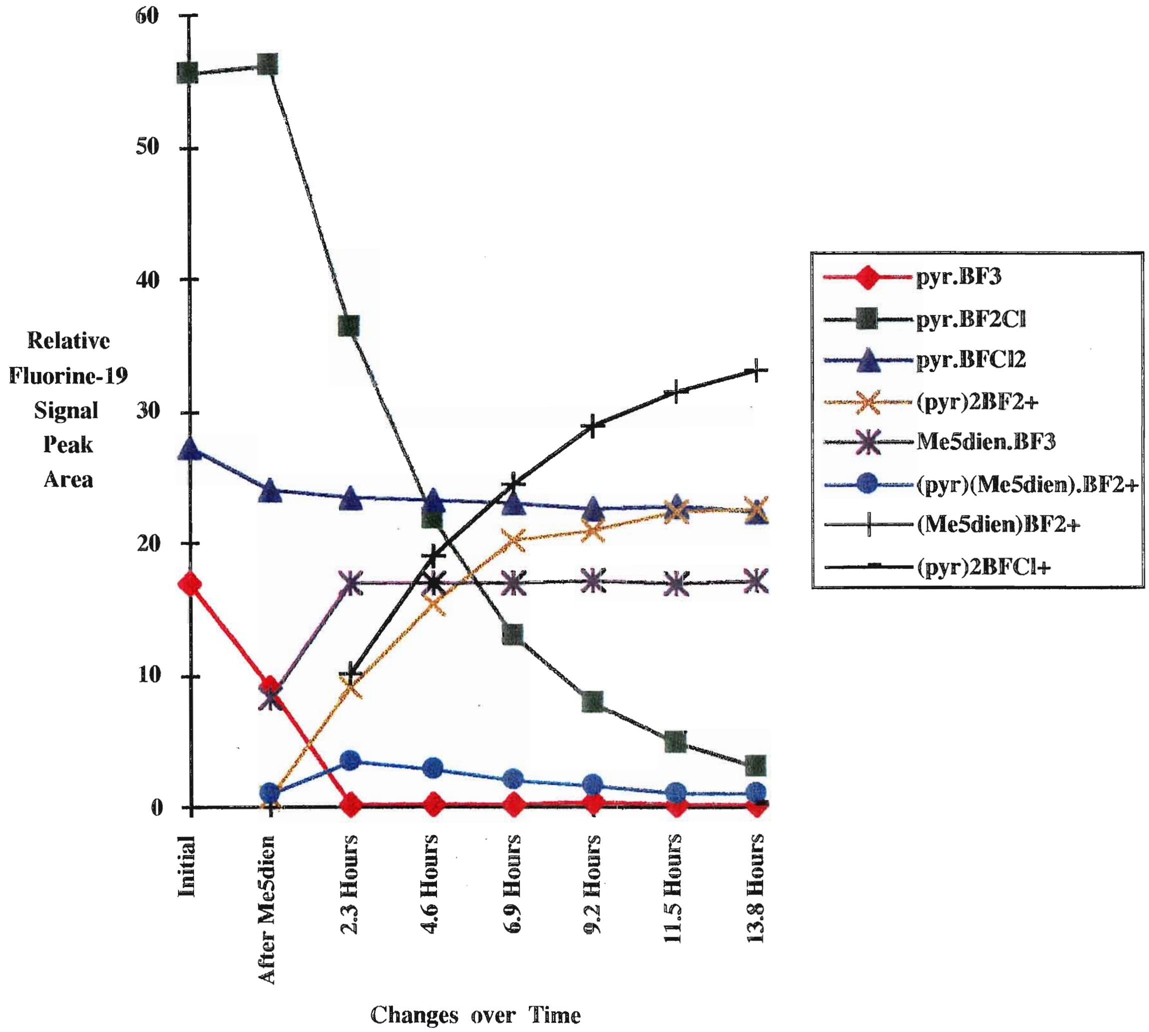

solution via + FAB ms: parent ion at 221 [12.5 %] and 222 [49.7 %] m/z; $Me_5dien.H^+$ was the ion of greatest intensity.

Over a period of days, Me_5dien reacts with the pyr.$BFCl_2$ adduct to form the $(Me_5dien)BFCl^+$ cation (figures 3.8 and 3.9). The reason for two ^{19}F chemical shifts is that the boron, in addition to the centre nitrogen atom on the Me_5dien, are chiral on formation of this cation. The diastereomers form at a ratio of about 1:3 (-137.5ppm:-140.5 ppm (^{19}F chemical shifts)). The presence of $(Me_5dien)BFCl^+$ is confirmed by a positive ion FAB mass spectrum obtained directly from the chloroform solution: 237 [2.4 %] and 238 [8.2 %] m/z.

The figures 3.8 and 3.9 display another trend that are not seen in the initial reaction displayed in figures 3.6 and 3.7: over time, the Me_5dien displaces both pyridines from $(pyr)_2BF_2^+$, until the only BF_2^+ cation in solution is $(Me_5dien)BF_2^+$.

3.2.4: Pyr.BF_nCl_{3-n} + bipyr. Bipyr reacts with pyr.BF_2Cl over a period of days, to form $(bipyr)BF_2^+$. No $(pyr)(bipyr)BF_2^+$ or bipyr.BF_2Cl intermediate is detected by nmr. Along with the + 1 cation, ^{19}F signals of BF_4^- and $(pyr)_2BF_2^+$ appear. The pyr.BF_nCl_{3-n} solution changes to a pink colour over time, with white crystals forming. During crystal formation, the ^{19}F total intensities decrease and the ratios of $(bipyr)BF_2^+$:$(pyr)_2BF_2^+$ alter, suggesting that both precipitate. Positive ion FAB ms of the solution: pyr.H^+ [3.1 %] 80 m/z, bipyr.H^+ [100 %] 157 m/z, $(bipyr)BF_2^+$ [2.1 %] 205 m/z, $(pyr)_2BF_2^+$ [8.6 %] 207 m/z; and the white crystals bipyr.H^+ [100 %] 157 m/z, $(bipyr)BF_2^+$ [63.2 %] 205 m/z $(pyr)_2BF_2^+$ [47.8 %] 207 m/z. These crystals were soluble in sulpholane, but $^1J_{BF}$ was not visible for $(bipyr)BF_2^+$ at room temperature (likely due to the greater viscosity of the solvent). $(bipyr)BF_2^+$ appeared at -154.4 ppm in the fluorine-19 spectrum. In a 3:1 acetone:sulpholane the $^1J_{BF}$ is visible (23.4 Hz).

Bipyr does not displace pyr from pyr.BF_3 like the t-amine ligands discussed above, nor does it react with pyr.$BFCl_2$.

Figure 3.8: 188.31 MHz ^{19}F nmr spectra of the formation of $(pyr)_2BFCl^+$ and $(Me_5dien)BFCl^+$ from $pyr.BFCl_2$ (mole ratio $pyr:BF_3:BCl_3:Me_5dien = 2.5:1:1.5:2.5$). **A** = 2 days; **B** = 4 days; **C** = 6 days; **D** = 8 days; **E** = 10 days.

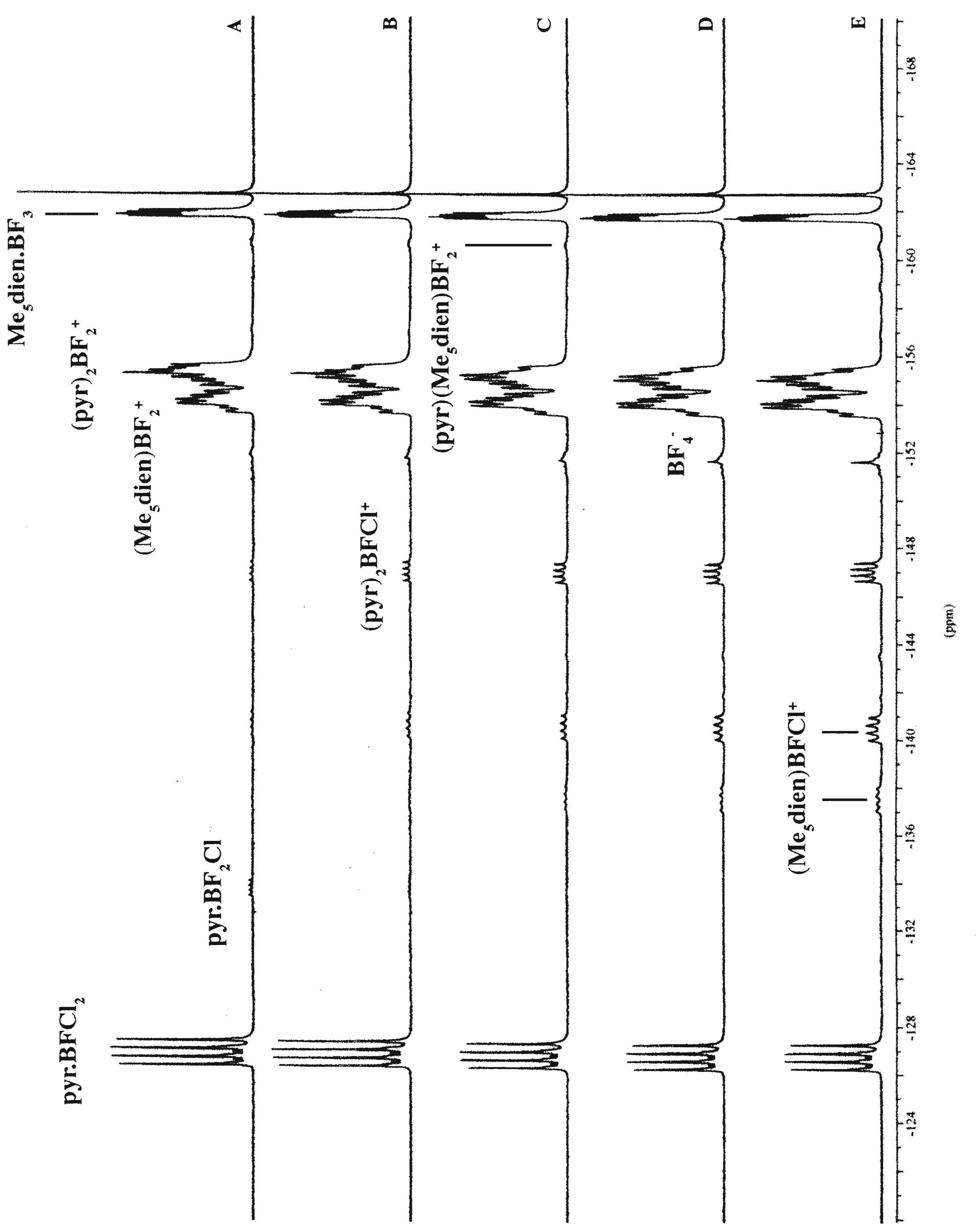

Figure 3.9: Secondary reactions caused by addition of Me_5dien to a solution of $pyr.BF_nCl_{3-n}$ (mole ratio $pyr:BF_3:BCl_3:Me_5dien = 2.5:1:1.5:2.5$).

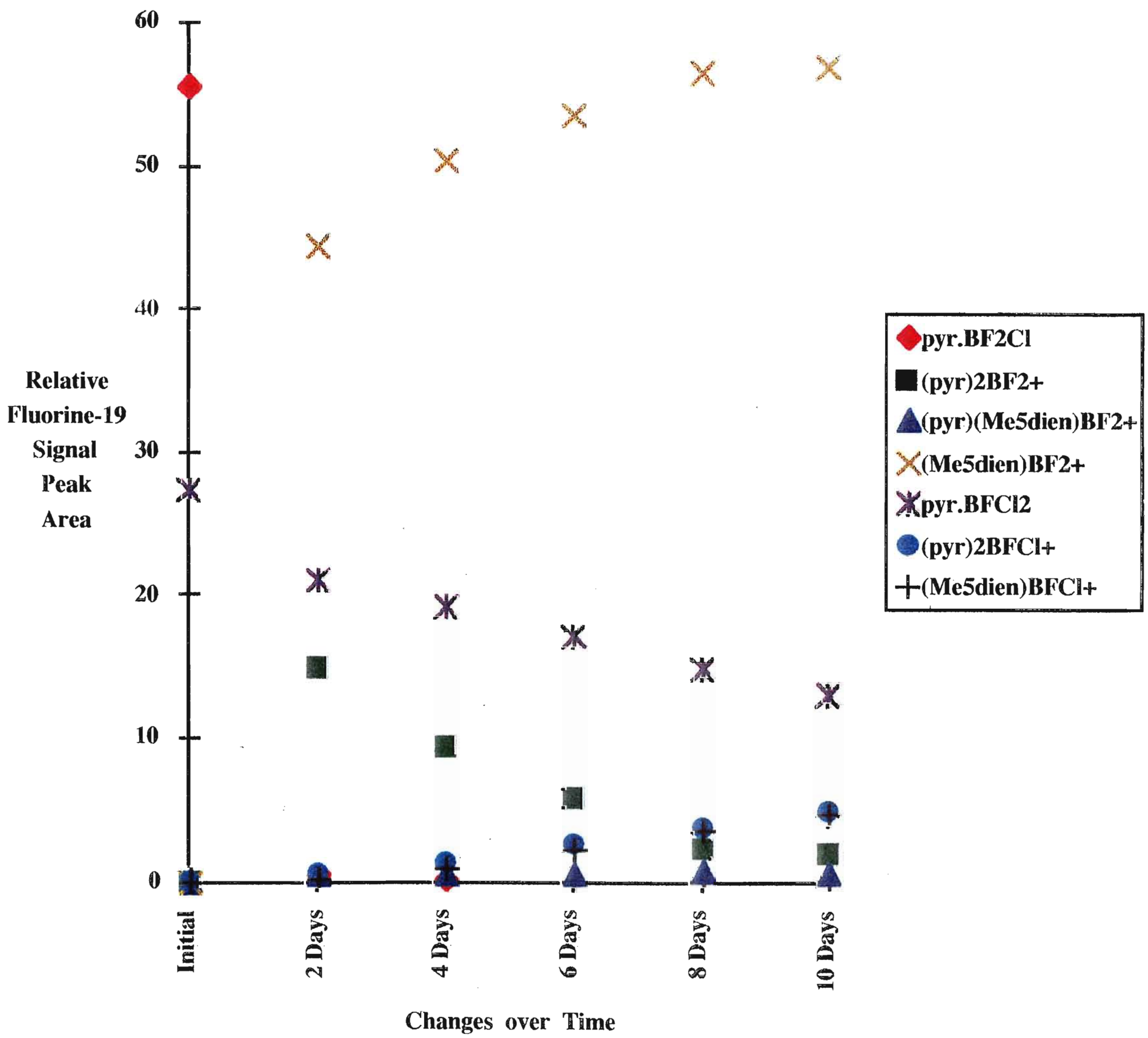

3.2.5: Pyr.BF_nCl_{3-n} + 1,10-phen. 1,10-Phen does not displace pyr from pyr.BF_3. No (pyr)(1,10-phen)BF_2^+ or 1,10-phen.BF_2Cl intermediate is detected by ^{19}F nmr, but after 10 days pyr.BF_2Cl reacts to give the (1,10-phen)BF_2^+ cation along with BF_4^- and $(pyr)_2BF_2^+$. Aside from pyr.BF_2Cl the other pyr.BF_nCl_{3-n} species in solution do not undergo any change in intensity over time. White crystals precipitate over the ten days. Positive ion FAB ms of the crystals and reaction solution did not give a detectable (1,10-phen)BF_2^+ signal, but only 1,10-phen.H^+ and $(pyr)_2BF_2^+$.

3.2.6: Pyr.BF_nCl_{3-n} + terpyr. Terpyr like the other aromatic ligands, does not displace pyr from pyr.BF_3. No (pyr)(terpyr)BF_2^+ or terpyr.BF_2Cl intermediate is detected in solution by nmr. The ^{19}F signal assigned to (terpyr)BF_2^+ appears along with BF_4^- and $(pyr)_2BF_2^+$ after 48 hours. Indicating pyr and Cl displacement from pyr.BF_2Cl since the other pyr.BF_nCl_{3-n} species in solution do not undergo any change in intensity over time. White crystals precipitate over the ten day period. During crystal formation, the ^{19}F intensities decrease and the ratios of (terpyr)BF_2^+:$(pyr)_2BF_2^+$ alter, suggesting that both cations precipitate. Positive ion FAB ms of the solution: terpyr.H^+ [100%] 234 m/z, (terpyr)BF_2^+ [~ 2%] 282 m/z $(pyr)_2BF_2^+$ [5.4%] 207 m/z; and the white crystals: terpyr.H^+ [100%] 234 m/z, (terpyr)BF_2^+ [4.3%] 282 m/z $(pyr)_2BF_2^+$ [12.4%] 207 m/z. Terpyr does not appear to react with pyr.$BFCl_2$.

3.2.8: Pyr.BF_nCl_{3-n} + 1,8-BDN. 1,8-BDN does not react with any of the pyr.BF_nCl_{3-n} species (2.5:1:1.5:2.5 pyr:BF_3:BCl_3:1,8-DBN) over ten days.

3.3: Discussion.

3.3.1: Reactions with pyr.BF_3. All three tertiary-amine chelating ligands (Me_4en, Me_4pn, and Me_5dien) can displace pyr from pyr.BF_3 [**1.7**] and form non-chelated Me_4en.BF_3, Me_4pn.BF_3, and Me_5dien.BF_3 adducts. This is consistent with monodentate tertiary-amine ligands being able to displace pyr from pyr.BF_3 (6,13,15). This may be due to the lower steric hindrance around the B-N bond of the BF_3 adduct, compared to those with a mixture or all heavy halides or due to BF_3 being the weakest Lewis base of the series (54), and thus, it is more easily displaced. The large majority (>> 95 %) of the polydentate tertiary-amines coordinate to only one BF_3, and this is likely due to the excess of these ligands versus BF_3 in the reaction solutions. It was very rare to see the bis adducts of Me_4en, Me_4pn, and Me_5dien. In solutions where equal amounts of tertiary-amine chelating ligands versus BF_3 are present, bis (tris) adducts occur readily (chapter 6).

Me_5dien only displayed one of its mono BF_3 adduct isomers, with the coordinated nitrogen being the end nitrogen (see chapter 6). This is likely due to the steric hindrance of the centre nitrogen (which is surrounded by a methyl and two dimethlyamineethyl groups), and this has important effects on the formation the desired (Me_5dien)BF_2^+ cation (section **3.3.2**).

The four other ligands do not react with pyr.BF_3. This is not surprising when one notes their sterically hindered structures (see chapter 1). If these bases were able to displace the pyridine from pyr.BF_3, these new adducts would likely rapidly lose a fluorine from the BF_3 (via possible halide exchange methods from chapters 1 and 6), leading to the (aromatic DD)BF_2^+.Y^- salt in solution.

3.3.2: Reactions with pyr.BF_2Cl. All bases except 1,8-BDN react with pyr.BF_2Cl, leading to five cases where the desired (DD)BF_2^+.Cl^- formed. The two-step chelation of boron by the t-amine ligands has a visible (pyr)(DD)BF_2^+ intermediate. The two cations (pyr)(Me_4pn)BF_2^+, and (pyr)(Me_5dien)BF_2^+ are of most interest, because they provide a great deal of information about the chelation of boron by tertiary-amine chelating ligands. Since (pyr)(Me_4pn)BF_2^+ never forms the desired (Me_4pn)BF_2^+ cation, the chelation of boron involving a six membered ring is not favoured (this will be discussed in chapter 5). In addition, Me_4pn does also displace pyridine from pyr.BF_2Cl to form Me_4pn.BF_2Cl, but the ligand does not then displace the chloride in order to form the desire cation. Since this reaction is slow (days), it suggests that this is not the mechanism in which the (DD)BF_2^+ cations form for the other two chelating tertiary-amine ligands.

(Pyr)(Me$_5$dien)BF_2^+, could have two isomers, yet only one ^{19}F signal, for the isomer with one of the two end nitrogen atoms coordinated is visible in the spectra. With the evidence from section **3.3.1**, this makes sense, for the other isomer would be too hindered to form. With this information, and the fact that displacement of pyridine from pyr.BF_2Cl by a tertiary-amine donor is a very slow reaction: the pathway for the formation of (Me$_5$dien)BF_2^+ from pyr.BF_2Cl is as follows [**3.2**]:

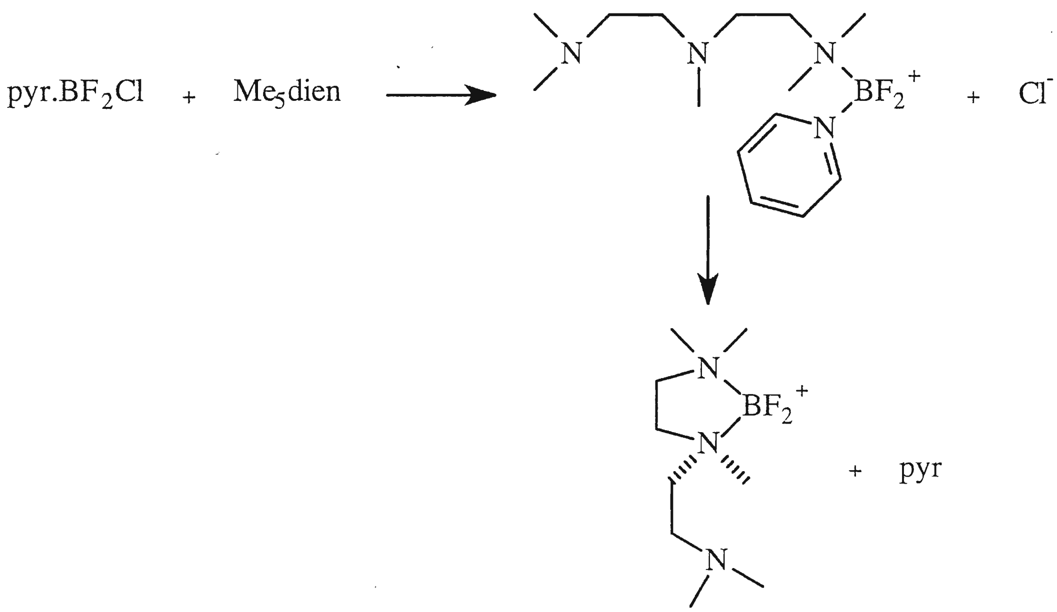

[**3.2**]

The three aromatic chelating ligands react with pyr.BF_2Cl to form (bipyr)BF_2^+, (terpyr)BF_2^+, and (1,10-phen)BF_2^+, but much more slowly than the tertiary-amine chelating ligands and the yields are poor. This may be related to the lack of flexibility and/or steric hindrance of these ligands. These bases are fairly rigid in comparision to the tertiary-amine chelating ligands. In addition, they have a great deal of steric bulk, which interferes with their ability to displace the chlorine and pyridine from the pyr.BF_2Cl. Within these three ligands, the yield of cations, (bipyr)BF_2^+ > (terpyr)BF_2^+ > (1,10-phen)BF_2^+, follows relative steric hindrance/flexibility (bipyr < terpyr < 1,10-phen). In addition, the most sterically hindered/least flexible species: 1,8-BDN does not react with the pyr.BF_2Cl adduct at all.

3.3.3: Reactions with pyr.$BFCl_2$. Pyr.$BFCl_2$ is much less reactive then pyr.BF_2Cl with tertiary-amine chelating ligands. This is not surprising, for the D.$BFCl_2$ adduct is less reactive then its D.BF_2Cl counterpart (6,13,15,55). Over a period of days, a 2.5:1:1.5 (pyr:BF_3:BCl_3) chloroform solution of pyr.BF_nCl_{3-n} that is reacted with Me_4en or Me_5dien produces the (Me_4en)$BFCl^+$ or (Me_5dien)$BFCl^+$ cations from pyr.$BFCl_2$. It is likely that species form by chloride displacement, followed by pyridine displacement, from pyr.$BFCl_2$, though no intermediate has been detected for these two bases. Me_4pn does form the mixed (pyr)(Me_4pn)$BFCl^+$ cation, which supports this mechanism for the other two bases. Yet, Me_4pn also displaces pyridine from pyr.$BFCl_2$ to form Me_4pn.$BFCl_2$. This occurs over a similar timeline, so some formation of the (Me_4en)$BFCl^+$ or (Me_5dien)$BFCl^+$ cations may be due to initial pyridine displacement from pyr.$BFCl_2$ followed by chloride displacement.

Chapter 4:
Chelating Donor Reactions with ISOX.BF_nX_{3-n}

4.1: Introduction.

1-Methylimidazole (MIA), 2-methyl-2-oxazoline (MOZ) and 2-methyl-2-thiazoline (MTZ) are three bases that have been used by our group for the formation of fluoroboron

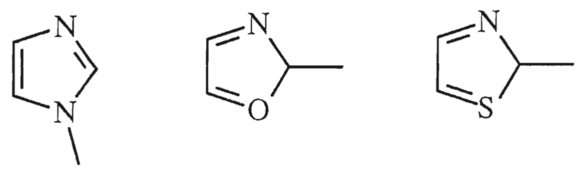

MIA MOZ MTZ

cations (12a,13,56). They undergo substitution reactions with a D' when they are in mixed boron trihalide adducts (D.BF_nX_{3-n}) or $(D)_2BF_2^+.PF_6^-$ salt forms, but tend to decompose if the D' is a strong base or if the D.BF_nX_{3-n} solutions are left standing for several days (56). As such, they are not suitable for reactions with chelating tertiary-amine based donors (strongly basic) and chelating aromatic donors (slow reacting). Thus, we moved to two bases that we thought would be more stable, and thus allow us to perform mixed adduct and $(D)_2BF_2^+.PF_6^-$ salt reactions as we had with pyridine (chapters 3 and 5). Isoxazole (ISOX) and 5-methylisoxazole (MISO) form mixed fluorochloroboron adducts but due to

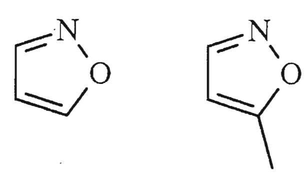

ISOX MISO

their weak basicity (ISOX (pK_b = 12.7) (10) and MISO (pK_b = 15.0) (10)) do not form BF_2^+ cations (56). As such, these bases can not be used for salt reactions, but the fact that they can not form cations was an unexpected benefit, because the side reaction that made using solutions of pyr.BF_nCl_{3-n} difficult (ie. the formation of $(pyr)_2BF_2^+$) does not occur (chapter 3). In addition, they have a basicity of 4 to 6 orders of magntude weaker then pyr, but have similar steric hindrance, meaning that they should readily allow substitution by both chelating t-amine and chelating aromatic donors. These studies involve ISOX, though preliminary studies indicate that MISO behaves similarly.

4.2: Results - Reactions with ISOX.BF_nCl_{3-n}.

Reactions of bi and tridentate ligands with ISOX.BF_nCl_{3-n} at ratios of 2:1:1:2 and 4:1:3:4 (ISOX:BF_3:BCl_3:DD) in chloroform were carried out. All nmr parameters of products in this section can be found in chapter 7.

4.2.1: Me$_4$en. The addition of ISOX.BF_nCl_{3-n} at both reaction ratios to chloroform solutions containing Me$_4$en caused orange solids to form on the top of the solutions, and the solutions themselves to turn from colourless to yellow. The yellow solutions were removed by syringe and analyzed by nmr. Me$_4$en.BF_3, Me$_4$en.$BFCl_2$, (Me$_4$en)$BFCl^+$ and Me$_4$en.BCl_3, were found in both solutions. In addition, the (Me$_4$en)BF_2^+ cation was detected in the chlorine-rich solution. The orange solids were dried on a Schlenk line for approximately 1 hour. Positive ion FAB ms were performed in the dried precipitates and the spectra contained: (Me$_4$en)BF_2^+ [165 m/z (100 %; 100 %)]; and (Me$_4$en)$BFCl^+$ [181 m/z (16.5 %; 43.4 %)] (% at 2:1:1:2; % at 4:1:3:4). The greater proportion of (Me$_4$en)$BFCl^+$ in the chlorine-rich sample is expected. The solid precipitates could be partly dissolved in a 3:1 acetone:sulpholane or completely dissolved in nitromethane. ^{11}B and ^{19}F nmr showed the same species as the yellow solution, plus (Me$_4$en)BF_2^+ (2:1:1:2 solution) and Me$_4$en.BF_2Cl (4:1:3:4 solution). Since (Me$_4$en)BF_2^+ is very insoluble in chloroform (chapter 3) it is not surprising that it was not detected in the (2:1:1:2) mother liquor. Me$_4$en.BF_2Cl is not normally detected in solution, due to the fact that chloride displacement normally occurs very quickly, leading to the formation of (Me$_4$en)BF_2^+. In this case, it was likely trapped by rapid precipitation before it had a chance to react.

4.2.2: Me$_5$dien. The addition of ISOX.BF_nCl_{3-n} at both reaction ratios to chloroform solutions containing Me$_5$dien caused red solids to form on the top of the solutions, and the solutions change from colourless to orange. Nmr of the solutions showed that $Me_5dien.BF_3$, $(Me_5dien)BF_2^+$, $Me_5dien.BFCl_2$, $(Me_5dien)BFCl^+$ and $Me_5dien.BCl_3$, were present. The ^{19}F spectrum also included 5 singlets in the BF_3 adduct (-150 to -160 ppm) range, arising from unknown species, with no counter parts in the ^{11}B spectrum. Positive ion FAB ms was performed on the 2:1:1:2 reaction solution and it contained: $Me_5dien.H^+$ [174 m/z (100 %)]; $(Me_5dien)BF_2^+$ [222 m/z (42.3 %)]; and $(Me_5dien)BFCl^+$ [238 m/z (13.3 %)]. The reaction vials with the red solids were dried on a Schlenk line for approximately 1 hour and gave positive ion FAB ms peaks of $Me_5dien.H^+$ [174 m/z (100 %; 100 %)]; $(Me_5dien)BF_2^+$ [222 m/z (62.1 %; 52.2 %)]; and $(Me_5dien)BFCl^+$ [238 m/z (23.9 %; 52.2 %)] (% values are for the 2:1:1:2 and 4:1:3:4 mole ratio solutions). The greater portion of $(Me_5dien)BFCl^+$ in the chlorine-rich sample is expected. As with Me_4en, the Me_5dien solid precipitates were studied by solution ^{11}B and ^{19}F nmr, and they contained the same species as the orange reaction solutions.

4.2.3: $\underline{Me_4pn}$. The addition of $ISOX.BF_nCl_{3-n}$ at both reaction ratios to chloroform solutions containing Me_4pn caused red solids to form on the top of the solutions, and the solutions themselves to turn from colourless to orange. Nmr of the orange solutions showed the presence of $Me_4pn.BF_3$, $Me_4pn.BFCl_2$, $Me_4pn.BFCl_2$ and $Me_4pn.BCl_3$, with the chlorine-containing species being more abundant in the 4:1:3:4 sample. The red solid gave positive ion FAB ms spectra showing the presence of $Me_4pn.H^+$ [131 m/z (100 %; 100%)] (% at 2:1:1:2; % at 4:1:3:4). Some of the solid precipitates were then placed in a nmr tube with 3:1 acetone:sulpholane (partly dissolved) or nitromethane (completely dissolved) and their ^{11}B and ^{19}F nmr showed that the same species were present as in the orange solutions.

This ligand, though unsuccessful again (see chapter 3) at forming the desired chelated BF_2^+ cation, does display an interesting trend. ISOX, with its weak basicity, is displaced from all four of its adducts by Me_4pn. Normally, when a D' is added to solution, only the BF_3 adduct has its D displaced by D' (13), or it takes days to displace the D from the other adducts (chapter 3). Due to the ease in displacement of ISOX, the reactions in this chapter occur so quickly.

4.2.4: Bipyr. The addition of ISOX.BF_nCl_{3-n} to chloroform solutions containing bipyr caused a pink precipitate to form. The colourless solutions gave ^{11}B nmr (and ^{19}F nmr in the case of the 4:1:3:4 sample) that indicated the presence of only very small amounts of (bipyr)BF_2^+, (bipyr)$BFCl^+$, (bipyr)BCl_2^+, and BF_4^-. The pink solids were dried on a Schlenk line for 1 hour, and gave positive ion FAB ms peaks for: (bipyr)BF_2^+ [205 m/z (100 %; 100%)]; (bipyr)$BFCl^+$ [221 m/z (29.1 %; 69.2 %)]; and (bipyr)BCl_2^+ [237 m/z (0.0%; 19.4 %)]. Again, there are greater amounts of (bipyr)$BFCl^+$ and (bipyr)BCl_2^+ in the chlorine-rich sample. The solids dissolved in 3:1 acetone:sulpholane or nitromethane were studied by ^{11}B (figure 4.1) and ^{19}F nmr: they both contained (bipyr)BF_2^+, (bipyr)$BFCl^+$, and BF_4^-, plus (in the 4:1:3:4 sample) (bipyr)BCl_2^+ and a large amount of BCl_4^- (7.7 ppm). The BF_4^-:BCl_4^- ratio is quite small in the chlorine-rich sample, showing that the ratio of fluorine:chlorine in solution not only affects the ratio of cation species formed, but the ratio of anions formed.

4.2.5: 1,10-Phen. The addition of ISOX.BF_nCl_{3-n} to chloroform solutions containing 1,10-phen caused an orange precipitate to form, and the solution turned yellow. The yellow solutions gave nmr spectra showing a very small amount of (1,10-phen)$BFCl^+$, (1,10-phen)BCl_2^+ (4:1:3:4 sample only), and BF_4^-. The orange solids gave positive ion FAB ms spectra containing: 1,10-phen.H^+ [181 m/z (100 %; 100 %)]; (1,10-phen)BF_2^+ [229 m/z (95.7 %; 85.8 %)]; (1,10-phen)$BFCl^+$ [245 m/z (25.7 %; 54.0 %)]; and (1,10-phen)BCl_2^+ [261 m/z (0.0%; 6.7 %)]. Both ^{11}B spectra and + FAB ms showed that the amount of (1,10-phen)BCl_2^+ was not as great as the amount of (bipyr)BCl_2^+ above (**4.2.4**). The solids that were dissolved in 3:1 acetone:sulpholane or nitromethane, gave ^{11}B and ^{19}F nmr signal of (1,10-phen)BF_2^+, (1,10-phen)$BFCl^+$, and BF_4^-, plus the 4:1:3:4 sample had (1,10-phen)BCl_2^+ and a large amount of BCl_4^-.

Figure 4.1: 64.20 MHz ^{11}B nmr spectra of $(bipyr)BX_nY_{2-n}^+$ cations formed from $ISOX.BF_nCl_{3-n}$. **A** 3:1 acetone:sulpholane solvent ($ISOX:BF_3:BCl_3$ = 2:1:1); **B** nitromethane solvent ($ISOX:BF_3:BCl_3$ = 4:1:3).

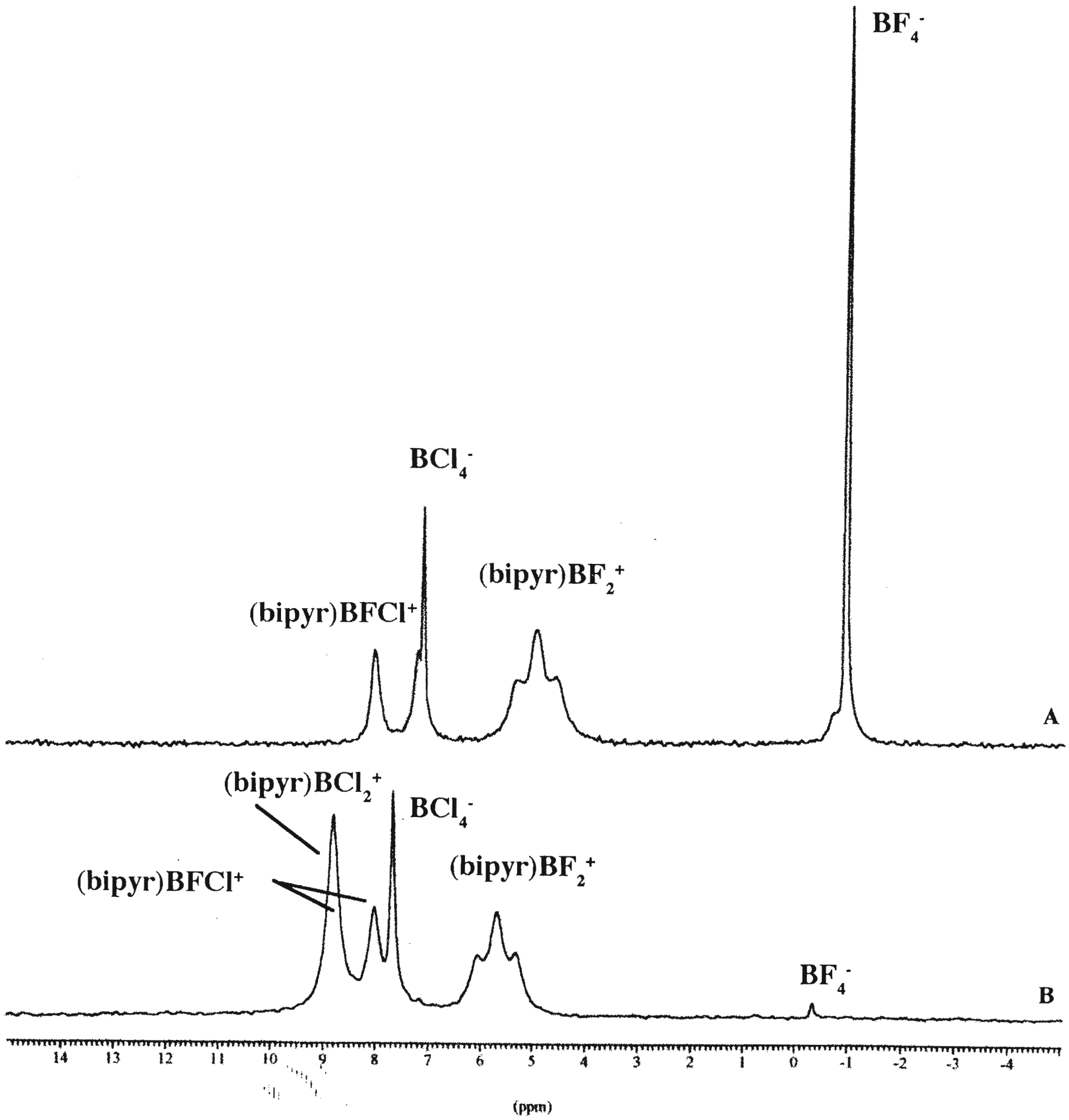

4.2.6: Terpyr. The addition of ISOX.BF_nCl_{3-n} at both reaction ratios to chloroform solutions containing terpyr caused a small amount of brown precipitate, and the solution turned yellow. The solutions gave ^{11}B nmr (and ^{19}F nmr in the case of the 4:1:3:4 sample) spectra containing (terpyr)BF_2^+, (terpyr)$BFCl^+$, BF_4^- and (terpyr)BCl_2^+ (in the 4:1:3:4 sample). The chloroform solution (2:1:1:2 sample) was analyzed by + FAB: terpyr.H^+ [234 m/z (100 %)]; (terpyr)BF_2^+ [282 m/z (90.1 %)]; and (terpyr)$BFCl^+$ [298 m/z (29.1 %)]. The solutions were dried on a Schlenk line for 1 hour. Positive ion FAB ms were performed in the dried material that remained, and it contained: (terpyr)BF_2^+ [282 m/z (100 %; 41.1 %)]; (terpyr)$BFCl^+$ [298 m/z (29.6 %; 100%)] and (terpyr)BCl_2^+ [314 m/z (0.0%; 14.9 %)]. Yet, the amount of (terpyr)$BFCl^+$ is much more significant in the + FAB ms than in the ^{11}B spectrum for the 4:1:3:4 sample. The dried materials were dissolved in 3:1 acetone:sulpholane or nitromethane. The solutions were studied by ^{11}B and ^{19}F nmr: they both contained: (terpyr)BF_2^+, (terpyr)$BFCl^+$, BF_4^-, plus the 4:1:3:4 sample had (terpyr)BCl_2^+ and a large amount of BCl_4^-.

4.2.7: 1,8-BDN. 1,8-BDN was reacted with only the 4:1:3:4 solution. Its results were very different from those of any of the other ligands. Upon addition of the ISOX.BF_nCl_{3-n} solution to the vial containing 1,8-BDN, the solution slowly turned quite a few colours yellow; orange; brown; red; gold; brown; and before settling on deep purple. This display of colour change is very much like that which the author found in his work with amidines (12b), and is apparently related to the strong basicity of 1,8-BDN [pK_b = 1.7] (29), which causes the formation of diclorocarbene (CCl_2) from chloroform. The formation of carbene leads to the formation of $BF_nCl_{4-n}^-$ anions as observed with amidines (6), with ligand.H^+ cations as the counterion. The majority of the ^{11}B signal arose from three species: BCl_4^- (6.9 ppm), $BFCl_3^-$ (7.0 ppm [$^1J_{BF}$ = 81.8 Hz]), and $BF_2Cl_2^-$ (5.0 ppm [$^1J_{BF}$ = 54.8Hz]) (6,57). A ^{19}F spectrum taken a day later confirmed that $BFCl_3^-$ and $BF_2Cl_2^-$ were indeed the major F species in the solution. The ^{11}B spectrum had a 1:2:1 triplet at 1.9 ppm, which we assign to (1,8-BDN)BF_2^+, in addition to some ISOX.BCl_3

and $ISOX.BFCl_2$. A + FAB ms displayed two significant species: $1,8\text{-BDN.H}^+$ [215 m/z (100 %)] and $(1,8\text{-BDN})BF_2^+$ [263 m/z (5.6 %)].

Since this system gave no precipitate like the other ligands, a solution of $ISOX.BF_nCl_{3-n}$ (4:1:3) was placed in an nmr tube, and a chloroform solution of 1,8-BDN was added to the solution in a series of additions and the changes were monitored by nmr. The formation of $BF_nCl_{4-n}^-$ anions was favoured over the formation of the $(1,8\text{-BDN})BF_2^+$ cation. Only after the system had an excess of 1,8-BDN to ISOX, and was heated at 50°C, did the system start to produce significant amounts of the desired $(1,8\text{-BDN})BF_2^+$ cation.

4.3: Results - Reactions with $ISOX.BF_nBr_{3-n}$.

Reactions of bi and tridentate ligands with $ISOX.BF_nBr_{3-n}$ at ratios of 2.5:1:1.5:2.5 and 4:1:3:4 ($ISOX:BF_3:BBr_3:DD$) were carried out in chloroform. All nmr parameters of products in this section can be found in chapter 7.

4.3.1: $\underline{Me_4en}$. In both reaction ratios, the reaction solution turned yellow on addition of the $ISOX.BF_nBr_{3-n}$, and a brown solid formed on the top. The vials were centrifuged, and the reaction solutions were studied by nmr. A small amount of $Me_4en.BF_3$ and $(Me_4en)BF_2^+$ was present, as well as some unreacted $ISOX.BF_3$ and a ^{19}F singlet at -151.3 ppm of an unidentified species. The samples were dried, and then the precipitates were analyzed by + FAB ms: 2.5:1:1.5:2.5 solid; $Me_4en.H^+$ [117 m/z (100 %)], $(Me_4en)BF_2^+$ [165 m/z (21.7 %)] and $Me_4en.H.HBr^+$ [197 m/z (5.4 %)]; 4:1:3:4 solid; $Me_4en.H^+$ [117 m/z (100 %)], $(Me_4en)BF_2^+$ [165 m/z (26.7 %)], $Me_4en.H.HBr^+$ [197 m/z (7.3 %)] and $(Me_4en)BFBr^+$ [225 m/z (5.4 %)]. Nitromethane was used in an attempt to dissolve the precipitate, but it was unsuccessful at dissolving anything that had not been detected by nmr before. Acetone, acetone:sulpholane and acetonitrile have been attempted as solvents as well, but without any success. Since the precipitates were insoluble, ^{11}B MAS nmr was carried out on the samples.

In the ^{11}B MAS nmr spectra of the precipitates (figure 4.2), there are a great deal of species in the BF_nBr_{3-n} adduct range (2 ppm to -10 ppm) (14). In addition, there are species in the $BF_nBr_{1-n}^+$ cation range (10 ppm to 2 ppm) (14). The spectrum for the 4:1:3:4 solid sample is much more complex in both regions, than the 2.5:1:1.5:2.5 solid sample. This is not surprising, considering that the + FAB ms suggests the same thing (i.e., higher intensities of cations). In particular, the cation species appear to be greater in number and intensity in the bromine rich system, and this is the system that had the $(Me_4en)BFBr^+$ cation according to the + FAB ms spectrum.

4.3.2: <u>Me_5dien</u>. In both reaction ratios, the reaction solution turned yellow on addition of the ISOX.BF_nBr_{3-n}, and a brown solid formed on the top. The vials were centrifuged, ^{19}F and ^{11}B nmr of the chloroform solutions gave a small signal of Me_5dien.BF_3, and other ^{19}F peaks (singlets) in the -150 to -160 ppm region arising from unknown species. The precipitates were analyzed by + FAB ms: 2.5:1:1.5:2.5 solid; Me_5dien.H^+ [174 m/z (100 %)], $(Me_5dien)BF_2^+$ [222 m/z (9.3 %)], Me_5dien.H.HBr^+ [254 m/z (17.7 %)] and possibly $(Me_5dien)BFBr^+$ [282 m/z (1.7 %)]; 4:1:3:4 solid; Me_5dien.H^+ [174 m/z (100 %)], $(Me_5dien)BF_2^+$ [222 m/z (5.9 %)], Me_5dien.H.HBr^+ [254 m/z (24.9 %)] and $(Me_5dien)BFBr^+$ [282 m/z (2.0 %)]. This second system was run in raw data collection mode to determine if the fully chelated tridentate $(Me_5dien)BF^{+2}$ cation existed, but nothing was detected in the 100 to 103 m/z range that would represent this cation. Nor were any high mass clusters detected of the $(Me_5dien)BF^{+2}$ cation. As with, Me_4en, the Me_5dien samples were insoluble in numerous solvents. The ^{11}B MAS nmr of the precipitates was very similar to those of the Me_4en samples, both in chemical shift ranges of species, and ratios of cations:adducts as an affect of F:Br concentration.

4.3.3: <u>Me_4pn</u>. The reaction solutions and their precipitates were identical in appearance as those reported for the other t-amines. Only a small amount of Me_4pn.BF_3, was detected in the reaction solutions by nmr. As with the other t-amines, the Me_4pn samples were insoluble in numerous solvents. ^{11}B MAS nmr was performed on the

Figure 4.2: 96.29 MHz ^{11}B MAS nmr spectra of species formed from Me_4en + $ISOX.BF_nBr_{3-n}$. **A** $ISOX:BF_3:BBr_3:Me_4en$ = 2.5:1:1.5:2.5, **B** $ISOX:BF_3:BBr_3:Me_4en$ = 4:1:3:4. [$BF_nBr_{1-n}^+$ cations = 10 ppm to 2 ppm, BF_nBr_{3-n} adducts = 2 ppm to -10 ppm]

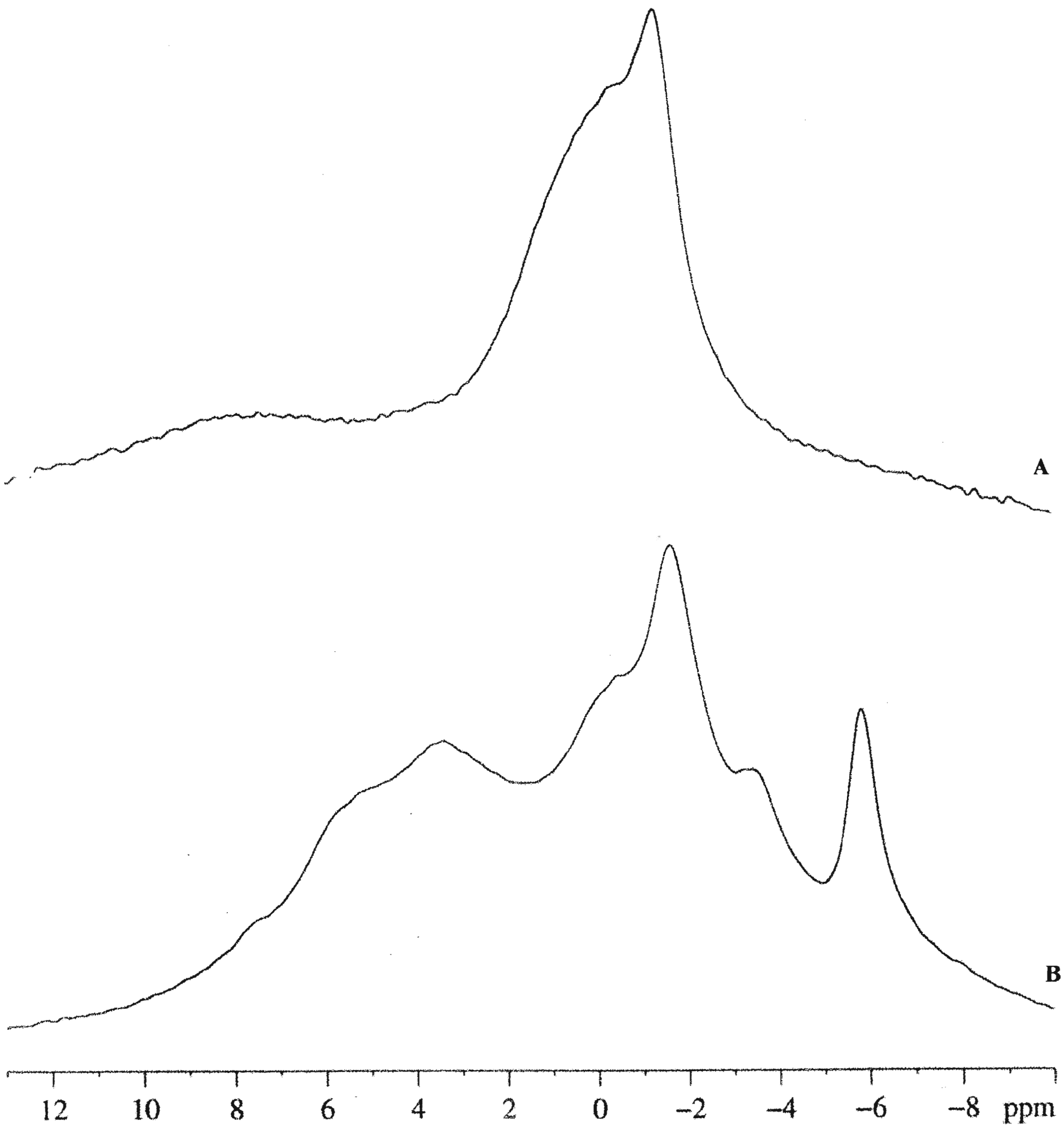

Figure 4.3: 96.29 MHz ^{11}B MAS nmr spectra of species formed from Me_4pn + $ISOX.BF_nBr_{3-n}$. A ISOX:BF_3:BBr_3:Me_4pn = 2.5:1:1.5:2.5, B ISOX:BF_3:BBr_3:Me_4pn = 4:1:3:4. [BF_nBr_{3-n} adducts = 2 ppm to -10 ppm]

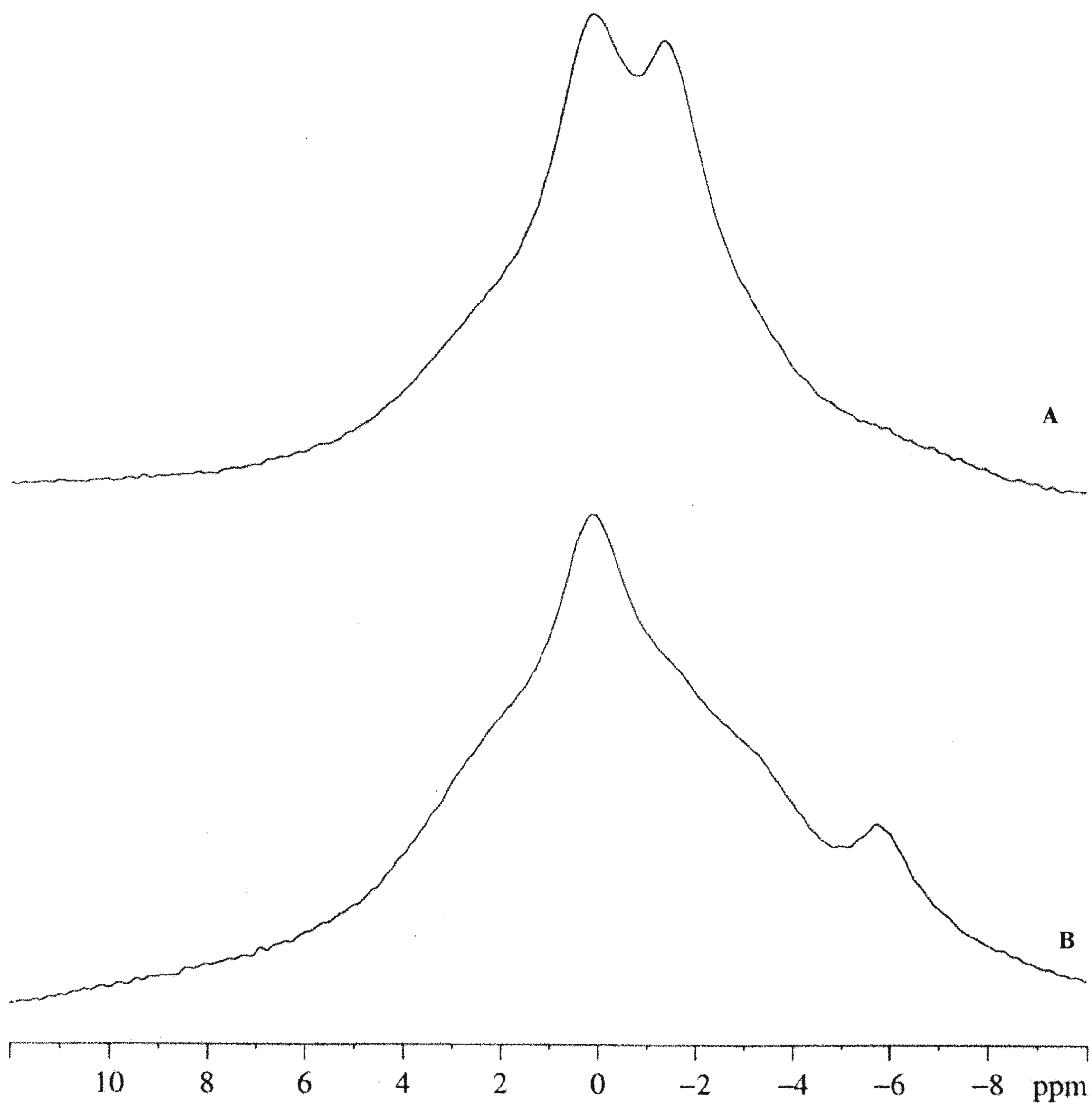

precipitates (figure 4.3). There were a great deal of species in the BF_nBr_{3-n} adduct range (2 ppm to -10 ppm). The MAS data supports the fact that this ligand does not form cations, as suggested by the data in chapter 3 and $ISOXBF_nCl_{3-n}$ samples earlier in this chapter. The precipitates were analyzed by + FAB ms and gave the following signals: 2.5:1:1.5:2.5 solid; $Me_4pn.H^+$ [131 m/z (100 %)] and $Me_4pn.H.HBr^+$ [211 m/z (11.1 %)]; 4:1:3:4 solid; $Me_4pn.H^+$ [131 m/z (100 %)] and $Me_4pn.H.HBr^+$ [211 m/z (12.0 %)].

4.3.4: Bipyr. In both reaction ratios, a yellow precipitate formed upon addition of the $ISOX.BF_nBr_{3-n}$. The vials were centrifuged, and the reactions solutions were studied by nmr. Beyond a small amount of BF_4^-, nothing was detected in the chloroform solutions. The samples were dried, and then the precipitates were analyzed by + FAB ms: 2.5:1:1.5:2.5 solid; $bipyr.H^+$ [157 m/z (37.2 %)], $(bipyr)BF_2^+$ [205 m/z (29.2 %)], $(bipyr)BBr^+$ [246 m/z (21.4 %)], $(bipyr)BFBr^+$ [265 m/z (5.7 %)], and $(bipyr)BBr_2^+$ [327 m/z (100 %)] (figure 4.4); 4:1:3:4 solid; $bipyr.H^+$ [157 m/z (42.9 %)], $(bipyr)BF_2^+$ [205 m/z (18.3 %)], $(bipyr)BBr^+$ [246 m/z (17.6 %)], $(bipyr)BFBr^+$ [265 m/z (5.7 %)], and $(bipyr)BBr_2^+$ [327 m/z (100 %)].

The precipitates were dissolved in nitromethane and studied by ^{19}F and ^{11}B nmr. The spectra for both solutions (figures 4.5 and 4.6) contained the same species: $(bipyr)BF_2^+$; $(bipyr)BFBr^+$; $(bipyr)BBr_2^+$; and BF_4^-. Except for the ratio of $(bipyr)BBr_2^+$:BF_4^- (more BF_4^- in 2.5:1:1.5 solution) there was little difference the two systems. The difluoro and the fluorobromo boron cations' ^{11}B chemical shifts overlap to some degree at 64.21 MHz, so the ^{11}B chemical shift of $(bipyr)BFBr^+$ cation was determined by studying the sample at McMaster (^{11}B frequency = 160.46 MHz).

In addition, ^{11}B MAS nmr spectra were obtained. Figure 4.7 compares ^{11}B MAS nmr spectra of the 4 mole equivalent bipyr plus 4:1:3 $ISOX.BF_nCl_{3-n}$ and 4:1:3 $ISOX.BF_nBr_{3-n}$ systems. The ^{11}B chemical shifts are very dependent upon which halogens are present (11).

Figure 4.4: Positive ion FAB ms spectrum of species formed from bipyr + ISOX.BF_nBr_{3-n} (ISOX:BF_3:BBr_3:bipyr = 4:1:3:4). 200 to 350 m/z range - full spectrum in appendix III.

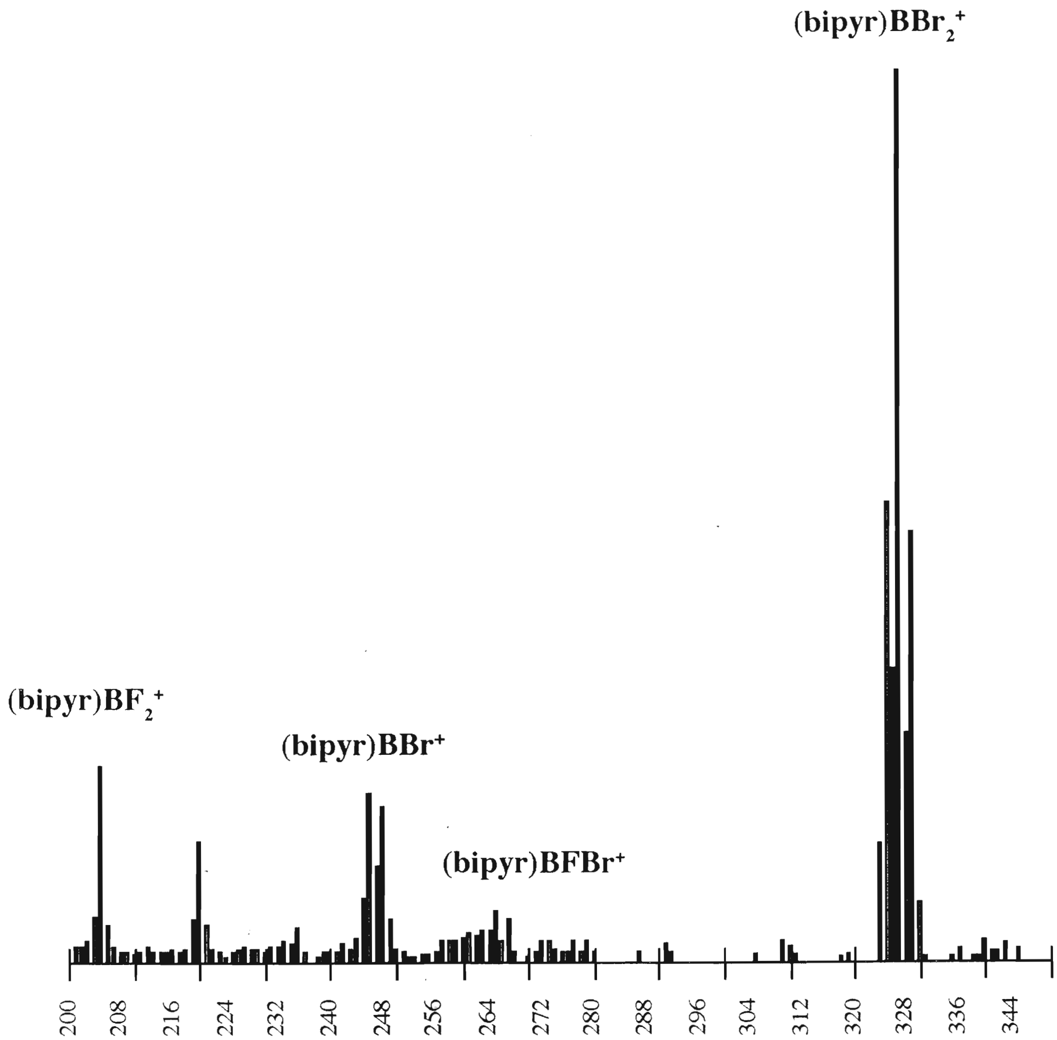

Figure 4.5: 64.20 MHz ^{11}B nmr spectra of species formed from bipyr + ISOX.BF_nBr_{3-n} (ISOX:BF_3:BBr_3:bipyr = 4:1:3:4).

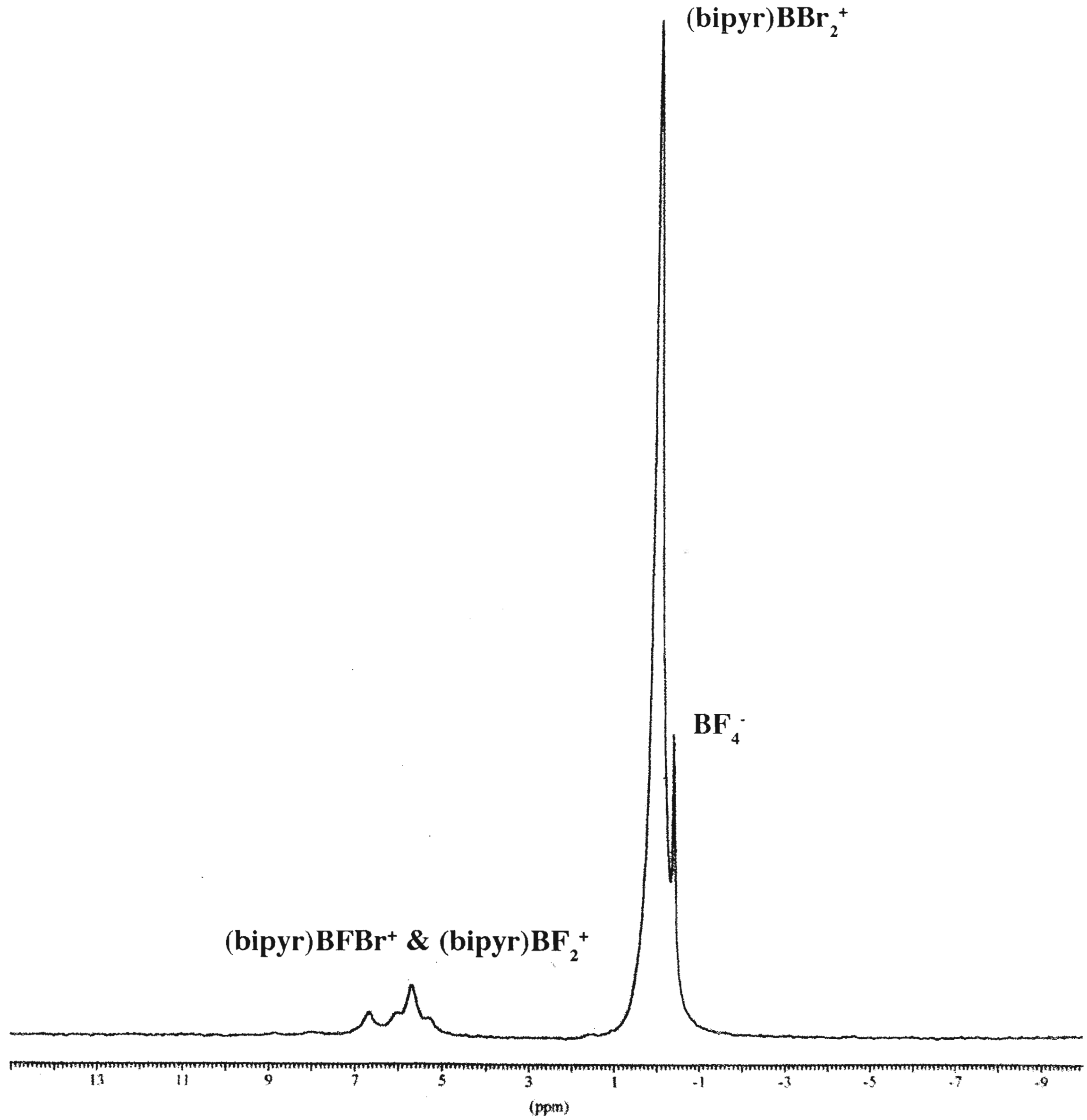

Figure 4.6: 188.31 MHz ^{19}F nmr spectra of species formed from $ISOX.BF_nBr_{3-n}$ + bipyr ($ISOX:BF_3:BBr_3$:bipyr = 4:1:3:4).

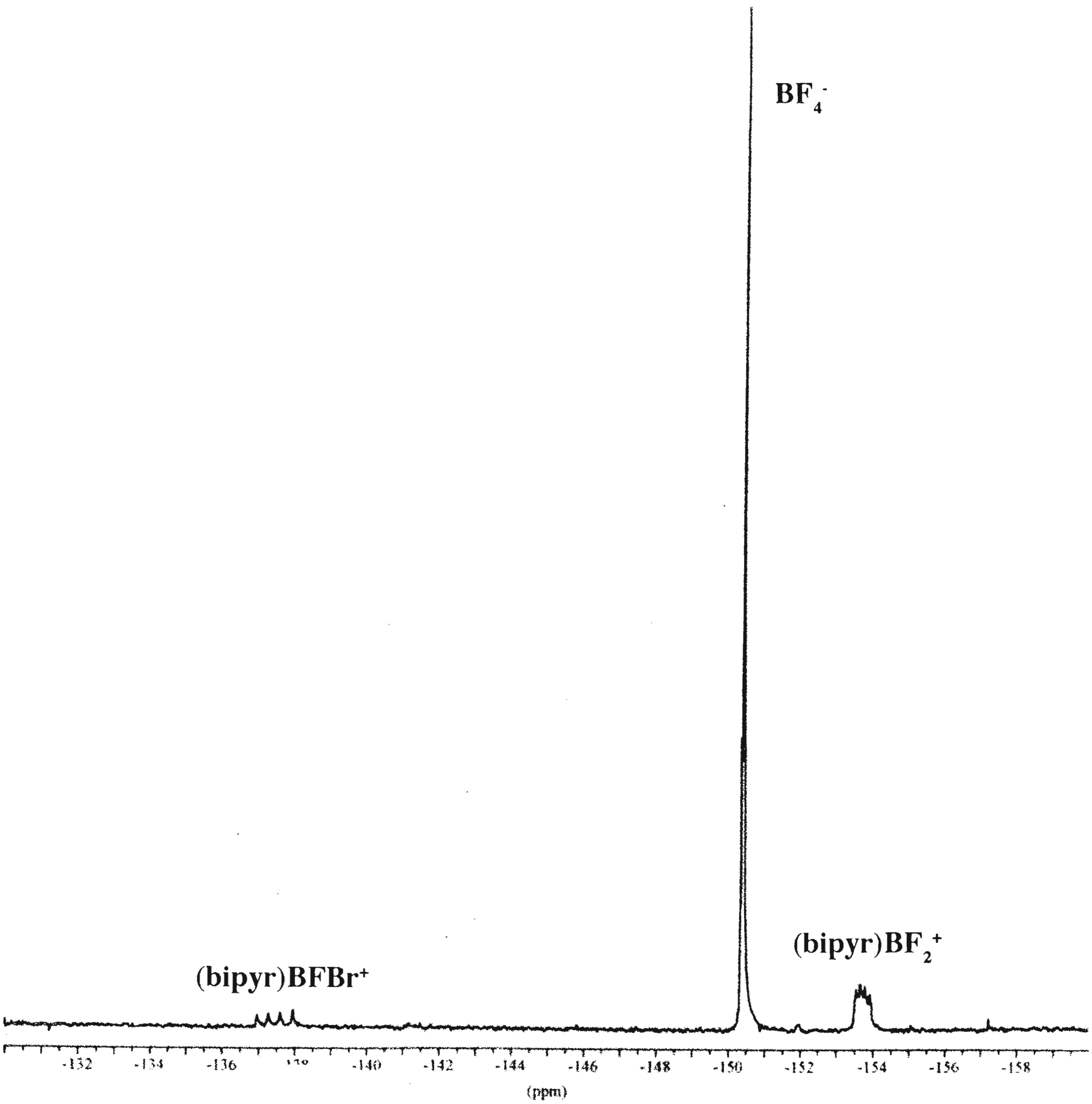

Figure 4.7: 96.29 MHz ^{11}B MAS nmr spectra of species formed from bipyr + ISOX.BF_nX_{3-n}. A ISOX:BF_3:BCl_3:bipyr = 2.5:1:1.5:2.5, B ISOX:BF_3:BBr_3:bipyr = 4:1:3:4.

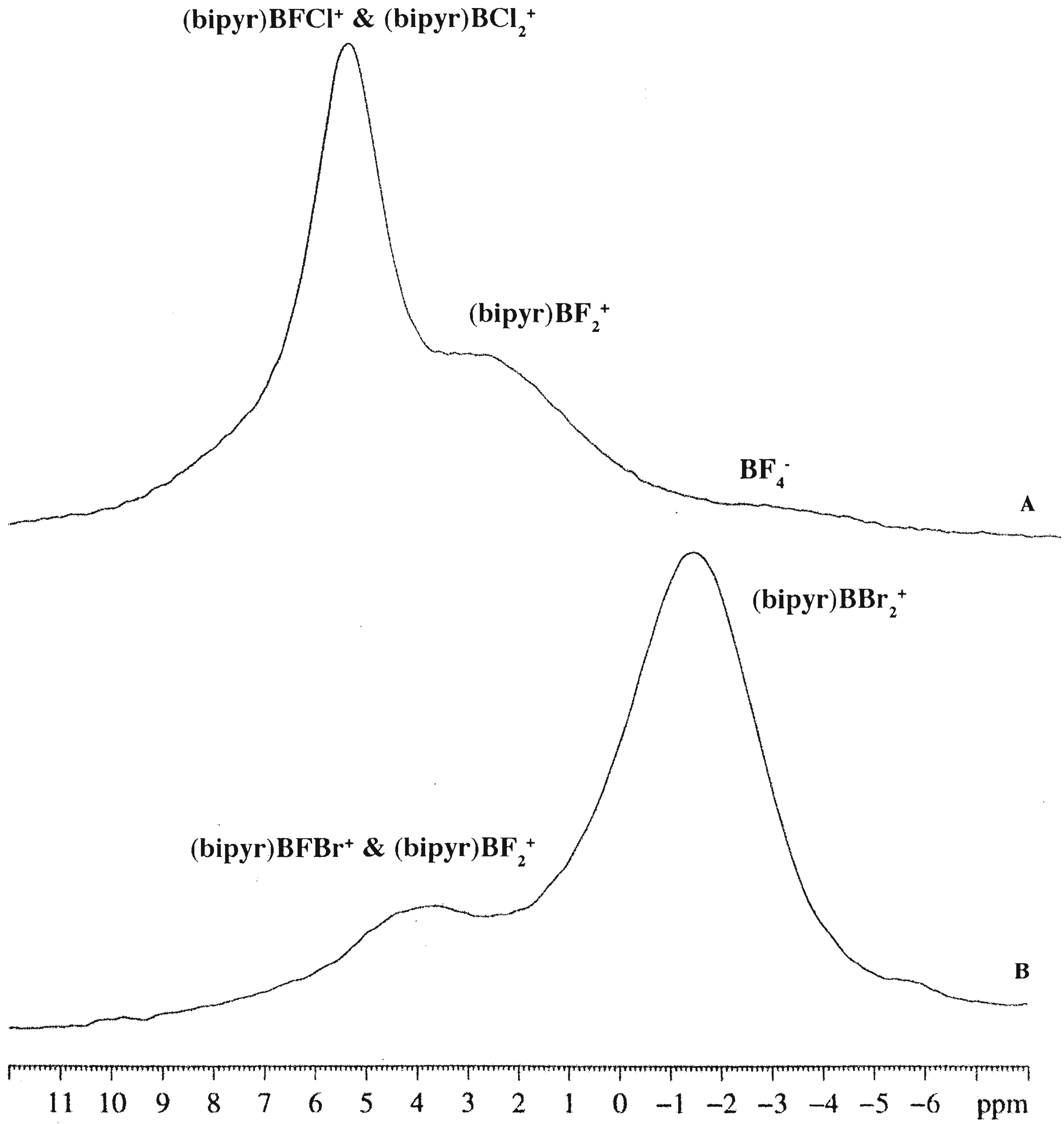

4.3.5: 1,10-Phen. In both reaction ratios, a brown oil precipitates upon addition of the ISOX.BF_nBr_{3-n}. Beyond a very small amount of BF_4^-, nothing was detected in the chloroform phase. The oils were separated from the chloroform, and then analyzed by + FAB ms: 2.5:1:1.5:2.5 oil; 1,10-phen.H^+ [181 m/z (100 %)], (1,10-phen)BF_2^+ [229 m/z (35.3 %)], (1,10-phen)BBr^+ [270 m/z (3.7 %)], (1,10-phen)$BFBr^+$ [289 m/z (8.1 %)], and (1,10-phen)BBr_2^+ [351 m/z (12.3 %)]; 4:1:3:4 oil; 1,10-phen.H^+ [181 m/z (100 %)], (1,10-phen)BF_2^+ [229 m/z (45.8 %)], (1,10-phen)BBr^+ [270 m/z (7.3 %)], (1,10-phen)$BFBr^+$ [289 m/z (16.4 %)], and (1,10-phen)BBr_2^+ [351 m/z (30.8 %)].

The oils were dissolved in nitromethane and studied by ^{19}F and ^{11}B nmr. The spectra for both solutions contained the same species: (1,10-phen)BF_2^+; (1,10-phen)$BFBr^+$; (1,10-phen)BBr_2^+; and BF_4^-. Except for the ratio of (1,10-phen)BBr_2^+:BF_4^- (more BF_4^- in 2.5:1:1.5 solution) there was little difference between the two systems. The ^{11}B signals of the difluoro and the fluorobromo boron cations overlapped at 64.21 MHz, so they were studied at McMaster. The two samples, from their nmr and ms data, had a much more even distribution of cations in solution, when compared with the bipyr system. The product was an oil and it formed overnight, and it is possible the some halogen exchange occurred in the system, before the formation of the desired cations. To try to determine what was occurring, a 4:1:3 ISOX.BF_nBr_{3-n} solution had two 2 molar equivalents of 1,10-phen added to it while monitoring the nmr tube via 160.46 MHz ^{11}B nmr. As expected, all of the mixed ISOX adducts (BF_2Br and $BFBr_2$) reacted with 1,10-phen before the first spectrum was obtained, leading to the (1,10-phen)BF_2^+ and (1,10-phen)$BFBr^+$ cations. Afterwards, the BF_3 and BBr_3 adducts of ISOX reacted, but a much slower rate. This suggests that fluorine and bromine exchange could occur, for the reactions are not instantaneous like in the bipyr system above. An oil was forming at the bottom of the nmr tube after the second spectrum was acquired, so no more quantitative monitoring of the reaction was possible, for two phases exist (the second phase would selectively extract some species).

4.3.6: Terpyr. At both reaction ratios, the products ((terpyr)BF_2^+; (terpyr)$BFBr^+$; (terpyr)BBr_2^+; and BF_4^-) were soluble in chloroform, but the $^1J_{BF}$'s were not resolvable for the species, so the 2.5:1:1.5:2.5 sample had the chloroform removed so that it could be studied in nitromethane by nmr. Upon removal of the chloroform, a brown oil remained. It contained the same species as the reaction solution. Like above, the difluoro and the fluorobromo boron cations overlapped in the 64.21 MHz ^{11}B spectrum, and were dealt with accordingly. The 2.5:1:1.5:2.5 oil was separated from the chloroform before the + FAB ms, but the reaction solution was run for the 4:1:3:4 solution: 2.5:1:1.5:2.5 oil; terpyr.H^+ [234 m/z (100 %)], (terpyr)BF_2^+ [282 m/z (24.2 %)], (terpyr)BBr^+ [323 m/z (2.5 %)], (terpyr)$BFBr^+$ [342 m/z (5.4 %)], and (terpyr)BBr_2^+ [404 m/z (15.3 %)]; 4:1:3:4 solution; terpyr.H^+ [234 m/z (73.9 %)], (terpyr)BF_2^+ [282 m/z (71.1 %)], (terpyr)BBr^+ [323 m/z (11.2%)], (terpyr)$BFBr^+$ [342 m/z (6.0 %)], and (terpyr)BBr_2^+ [404 m/z (100 %)]. The intensity difference of species in the ms spectra is puzzling. However, it has been noted by Z. Yuan (12a) that + FAB ms spectra of the same species in its solid versus solution can give very different D.H^+ intensities. The nmr spectra displayed much more even distribution of fluorobromo boron species than the mass spectra. Terpyr was reacted with 4:1:3 ISOX.BF_nBr_{3-n} solution, like the 1,10-phen, to study the formation of the cations, and the reactions behaved in a similar manner.

4.3.7: 1,8-BDN. 1,8-BDN was reacted at both solution ratios (2.5:1:1.5:2.5 and 4:1:3:4), and as with the ISOX.BF_nCl_{3-n} solutions, the results were very different from other ligands. Upon addition of the ISOX.BF_nBr_{3-n} solutions to vials containing 1,8-BDN, the solutions underwent similar colour changes to those reported in section **4.2.7**. Yet, unlike that system, no $BF_nBr_{4-n}^-$ or $BF_mCl_{4-n}Br_o^-$ (m + n + o = 4) anions were visible in any solution via nmr. Again the only identifiable cation species in the solutions was the (1,8-BDN)BF_2^+ cation at 1.9 ppm. In addition, some trace amounts ISOX.$BFBr_2$ and ISOX.BF_2Br were still present. A + FAB ms displayed two significant species: 1,8-BDN.H^+ [215 m/z (100 %)] and (1,8-BDN)BF_2^+ [263 m/z (6.7 %)]. Two additional experiments using additions of 4 molar equivalents of 1,8-BDN to 4:1:3 ISOX.BF_nBr_{3-n} solutions were performed. The samples were monitored by ^{11}B and ^{19}F nmr and unlike the chloride system, no $BF_nX_{4-n}^-$ anions were found. In addition, 1,8-BDN reacts with the ISOX.BF_nBr_{3-n} system in the following order: ISOX.BF_2Br (minutes) > ISOX.$BFBr_2$ (hours) > ISOX.BF_3 = ISOX.BBr_3 (days). Fluorine-bromine exchange between the ISOX.$BFBr_2$ & ISOX.BF_3 adducts and ISOX.BF_3 & ISOX.BBr_3 adducts. This is likely why in the nearly equimolar fluorine:bromine system, only the (1,8-BDN)BF_2^+ cation was detected.

4.4: Discussion.

4.4.1: Formation of tertiary-amine chelating ligand.boron adducts and dihaloboron cations. ISOX is a much weaker base than pyridine, and the other C=N donors that we have used in the past (13). Other bases have only allowed their BF_3 adduct to be substituted by the added D', but ISOX allowed Me_4en, Me_4pn, and Me_5dien to displace it from all of its adducts in both the ISOX.BF_nCl_{3-n} and ISOX.BF_nBr_{3-n} systems [ie., reaction **4.1**]. This allowed us to form Me_4en.BF_nX_{3-n}, Me_4pn.BF_nX_{3-n}, and

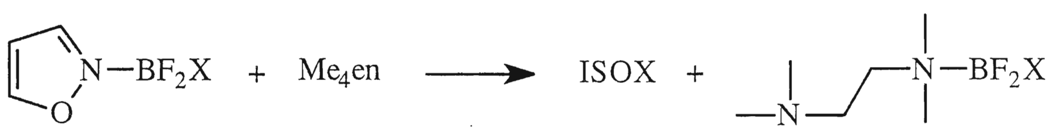

[**4.1**]

Me_5dien.BF_nX_{3-n} systems without the problem of bis (or tris) adducts of Me_4en, Me_4pn, and Me_5dien, which would have occurred if we attempted the formation of a chelated ligand.BF_nX_{3-n} system via our previous methods. The only adduct that we did not detect in chloride solutions was Me_5dien.BF_2Cl; the displacement of the chloride to form the (Me_5dien)BF_2^+ cation must be too rapid.

Upon formation of the Me_4en.BF_nX_{3-n}, Me_4pn.BF_nX_{3-n}, and Me_5dien.BF_nX_{3-n} systems, the Me_4en and Me_5dien ligands can displace X in order to form the desired BF_2^+ [reaction **4.2**] and BFX^+ cations. As in chapter 3, Me_4pn does not form BF_2^+ or BFX^+

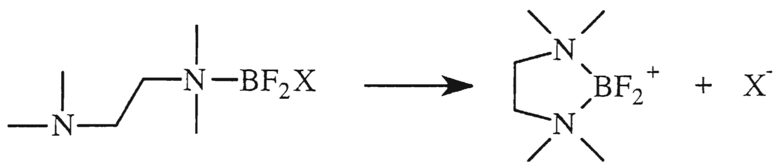

[4.2]

cations. Chelate ring size appears to be important, this will be discussed in the next chapter. Though the $Me_4en.BCl_3$, $Me_5dien.BCl_3$, $Me_4en.BBr_3$ and $Me_5dien.BBr_3$ adducts form in their respective solutions, neither Me_4en and Me_5dien could displace one chloride or bromide ion to form the desired BCl_2^+ or BBr_2^+ cations. This is not surprising, for Me_4en and Me_5dien could not do so with $Me_4en.BF_3$ or $Me_5dien.BF_3$ in any of the systems either (chapters 3, 4, and 6). This is likely due to two factors: 1) that in all three of these adducts, there is no suitable leaving group, like there is with the visible intermediate species (pyr)(DD)BF_2^+ (chapters 3 and 5) or DD.BF_2X (this chapter) for the BF_2^+ cation; 2) that the Me_4en and Me_5dien ligands do not have restricted or no rotation when one of its end (or middle) nitrogen atoms is in the form of an adduct, like 1,10-phenanthroline does (30), to force a halide atom to leave the adduct in order for cation formation to occur (see discussion in chapter 6). If they did, then the desired BF_2^+, BCl_2^+, and BBr_2^+ cations of Me_4en and Me_5dien would have formed from the BF_3, BCl_3, and BBr_3 adducts.

From both ISOX.$BFCl_2$ and pyr.$BFCl_2$, the (Me_5dien)$BFCl^+$ cation formed at a 3:1 ratio. Semi-empirical calculations at the PM3 level on the diastereomers of (Me_5dien)$BFCl^+$ give an energy difference of only 0.011 kJ/mol between them, so the 3:1 ratio must arise from kinetic rather that thermodynamic factors. Differences in steric hindrance in the transition state are certainly important (15), and these may have played a significant part in the ratio of diastereomers.

4.4.2: Formation of dihaloboron cations of aromatic chelating ligands. Unlike the tertiary-amine chelating ligands above, no adducts of the aromatic chelating ligands are stable long enough to be detected. It is not known whether ISOX or a halide is first displaced, though the much faster reaction of the ISOX.BF_nCl_{3-n} system than the pyr.BF_nCl_{3-n} system strongly suggests that ISOX is displaced first. In general, we know that: 1) fluorine-chlorine and fluorine-bromine exchange occurs during reactions; 2) that in systems where steric hindrance of the ligand is a factor, greater ligand steric hindrance correlates with slower reactions; 3) that not all ISOX adducts are equally reactive; 4) that the ratios of cations present is very much dependent on the ability of ISOX to stabilize mixed adducts; and 5) that 1,8-BDN behaves very differently compared to the other rigid ligands.

The formation of BF_4^-, and BCl_4^- anions when ISOX.BF_nCl_{3-n} solutions were reacted with the bipyr, 1,10-phen and terpyr ligands, shows that fluorine and chlorine exchange must be occurring. The formation of these anions was dependent on the ratio of fluorine to chlorine in the reaction solution (high fluorine means more BF_4^-). The formation of these anions likely occurs when the ISOX.BF_3 and ISOX.BCl_3 adducts react with the chelating ligands in order to form the desired BF_2^+ and BCl_2^+ cations. Whether the system is fluorine or chlorine rich, the amounts of tetrahalo boron anions do not charge balance with the amount of +1 cations. Thus, Cl^- must be present to provide additional negative charge. This is supported by the fact that in the fluorine rich ISOX.BF_nCl_{3-n} solutions, no BCl_2^+ cations were observed. In the ISOX.BF_nBr_{3-n} solutions that were reacted with the bipyr, 1,10-phen and terpyr ligands, fluorine and bromine exchanged, for the formation BF_4^- anion was dependent on the ratio of fluorine to bromine in solution (high fluorine means more BF_4^-). The formation of these anions likely occurs when the ISOX.BF_3 and ISOX.BBr_3 adducts react with the chelating ligands in order to form the desired BF_2^+ and BBr_2^+ cations. Unlike the chloride system, the bromine system did not have the BBr_4^- anion form, for its chemical shift is distinctive (57). All of the -1 counter ions for the +1 cations must have been Br^-.

With the ISOX.BF_nCl_{3-n} system, the reactivity of the ligands was bipyr $\approx$ 1,10-phen $\approx$ terpyr >> 1,8-BDN, but with the ISOX.BF_nBr_{3-n} system, the reactivity of the ligands was bipyr >> 1,10-phen $\approx$ terpyr >> 1,8-BDN. This suggests that steric hindrance is a factor in aromatic dihaloboron cation formation, though it can only be noted readily in the ISOX.BF_nBr_{3-n} system. Bipyr is the least sterically hindered ligand and it reacts much more rapidly then the rigid 1,10-phen or bulky terpyr. 1,8-BDN is both rigid and bulky, so it is the slowest of the group.

The ISOX.BF_nCl_{3-n} system reacts too quickly with bipyr, 1,10-phen and terpyr to note which adducts are more reactive: yet in the ISOX.BF_nBr_{3-n} system, the trend was $BF_2Br \geq BFBr_2 > BF_3 > BBr_3$. It is not surprising that the mixed halogen adducts are more reactive then their unmixed relatives, but what is a surprise is that the bromine system reacts more slowly then chlorine system. This might relate to the physical form of the 1,10-phen and terpyr fluorobromo boron cations. These two Lewis bases slowly form oils when they react with the bromine system, while they form insoluble solids when they react with the chlorine system. The oils do appear to have some solubility in chloroform, and do not separate from solution as quickly. Thus, there is no unbalanced equilibrium in order to push the reaction(s) quickly to completion. With bipyr, the formation of the insoluble solid precipitates seems to drive the reactions to completion much more rapidly.

As discussed in chapter 1, the lack of ability of weak or soft bases (ISOX has a $pK_b = 12.7$ (10)) to stabilize mixed halide adducts of BF_nBr_{3-n} has a great effect on the ratio of products produced. Thus, the fluorochloro system had an even distribution of the four ISOX.BF_nCl_{3-n} adducts while the ISOX.BF_nBr_{3-n} system had lesser amounts of the mixed adducts. This lead to the formation of the BBr_2^+ cations in both ISOX.BF_nBr_{3-n} reaction ratios, whereas the BCl_2^+ cations only formed in the higher chlorine reaction ratio.

1,8-BDN, known as 'proton sponge' is a very highly sterically hindered molecule, and behaves very differently from the others. Only the BF_2^+ cation forms. Whether X is Cl or Br, affects how 1,8-BDN reacts with the chloroform in which the reaction is taking place. Within fluorochloro systems, the 1,8-BDN appears to react with chloroform to form carbenes, which then lead to the formation of $BF_nCl_{4-n}^-$ anions via reaction [**4.3**]. This reaction was first noted in our amidine systems (6,12), and it had only been seen in Lewis base deficient systems. In solutions where amidines were added after there was an equal

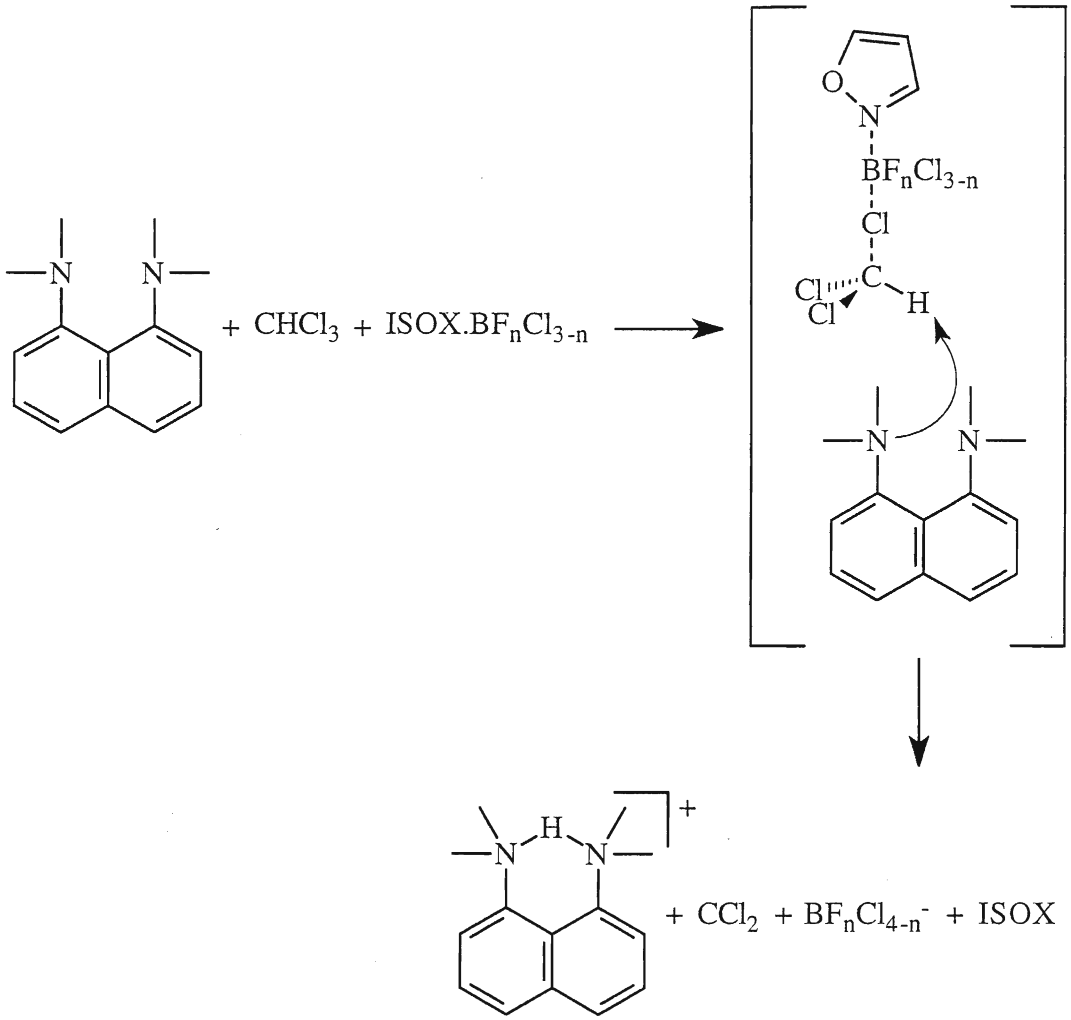

[4.3]

amount of Lewis base and Lewis acid, no $BF_nCl_{4-n}^-$ anions were noted (12,13). This is the first case where there is evidence of $BF_nCl_{4-n}^-$ anions forming in one of our Lewis base rich systems. Figure 4.8 displays ^{11}B nmr monitoring of the formation of the various anions in chloroform-d_1 over a period of days and several additions of 1,8-BDN. It is not possible to determine the reaction pathway that leads to the $(1,8\text{-BDN})BF_2^+$ cation. With the fluorobromo systems, no $BF_mBr_nCl_o^-$ ($m + n + o = 4$) anions were detected, suggesting at least three possibilities: 1) that they are not favoured due to chemical reasons; or 2) that they are formed, but react too fast to be detected; or 3) that they are formed, but exchange too fast on the nmr time scale to be detected by nmr (57). The second reason appears more likely, due to the fact that fluorine-bromine exchange is on going during the

Figure 4.8: 64.20 MHz ^{11}B nmr monitoring of species formed from 1,8-BDN + ISOX.BF_nCl_{3-n} (ISOX:BF_3:BCl_3:1,8-BDN = 4:1:3:4). **A** Initial, **B** after 0.2 mol. equ. of 1,8-BDN, **C** after 0.6 mol. equ., **D** after 2.2 mol. equ., **E** 24 hours after 4 mol. equ..

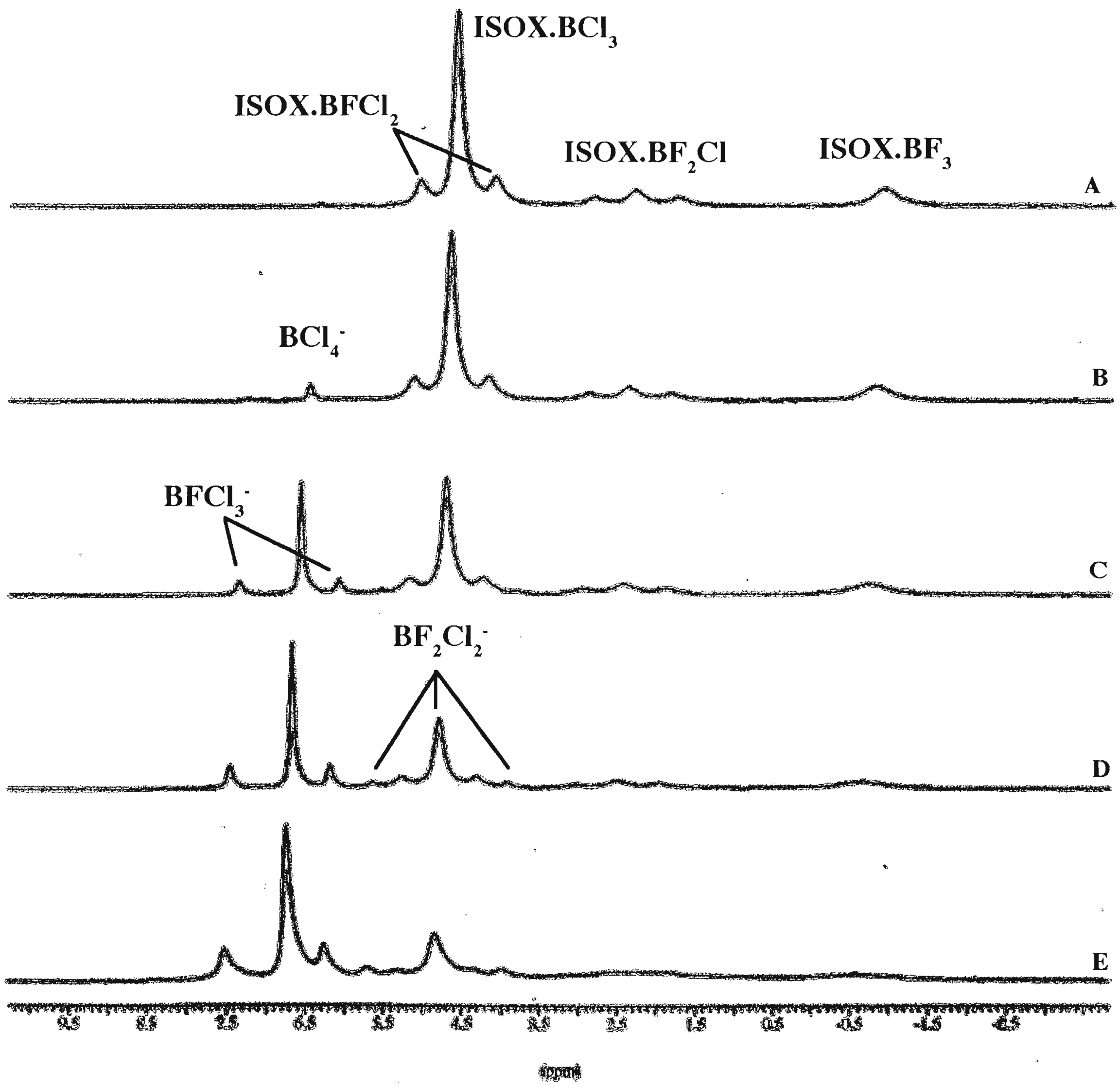

Figure 4.9: 188.31 MHz ^{19}F nmr monitoring of species formed from 1,8-BDN + ISOX.BF_nBr_{3-n} (ISOX:BF_3:BBr_3:1,8-BDN = 4:1:3:4). **A** Initial, **B** after 4 mol. equ. of 1,8-BDN, **C** after 0.8 hours, **D** after 2.4 hours, **E** 5.6 hours, **F** 24 hours.

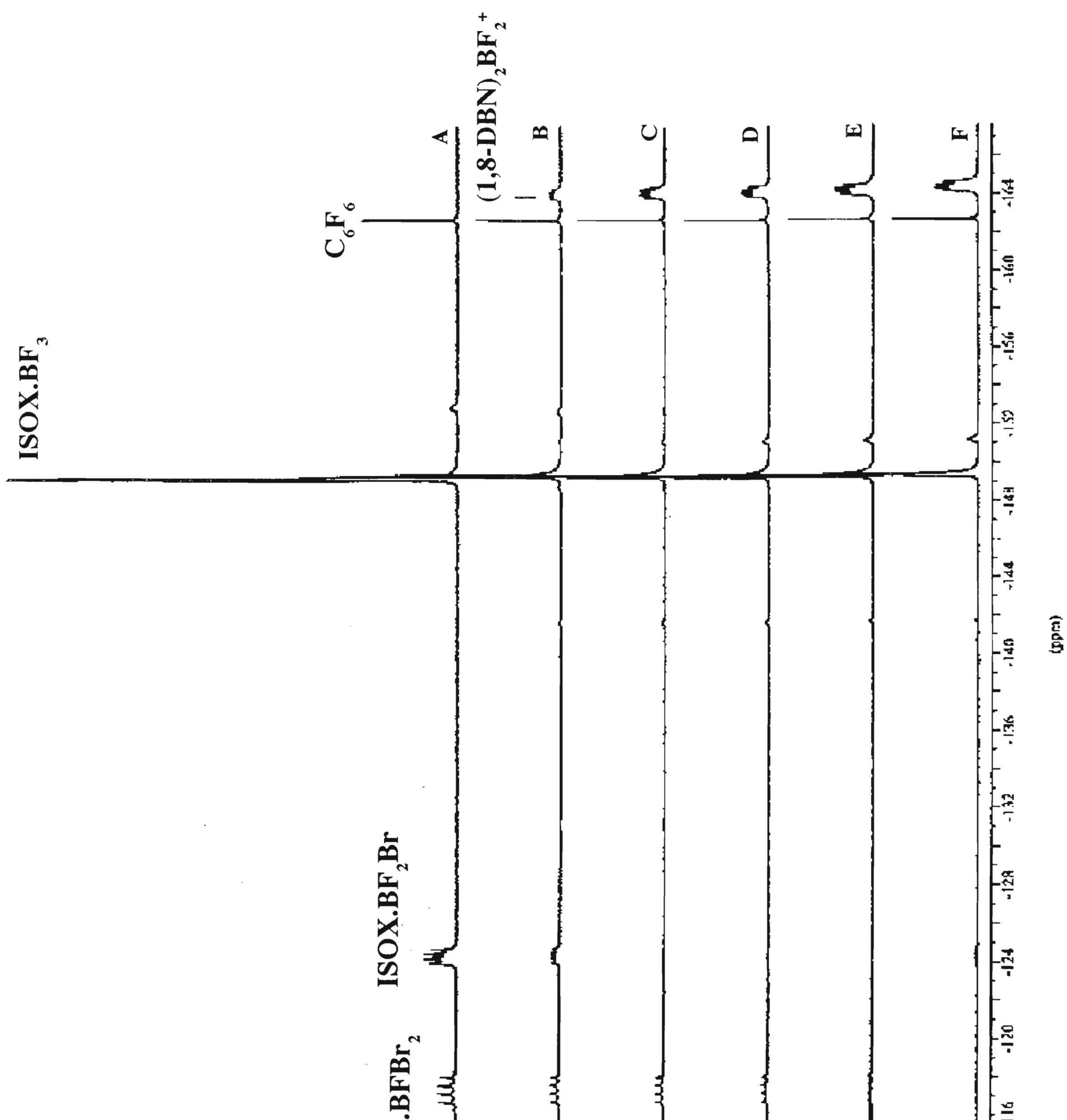

various stages of the reaction. Figure 4.9 displays the formation of (1,8-BDN)BF_2^+ from a ISOX.BF_nBr_{3-n} system.

4.4.3: Trends in + FAB ms. A few trends were noted in the study of chelated dihaloboron cations by + FAB ms that are worth noting: 1) the general ratio of BF_2^+ to BFX^+ to BX_2^+ cations observed by nmr is confirmed by + FAB ms; 2) systems that generate a great deal of adducts, have a high DD.H^+ ion count (DD). It is usually 100 % m/z; 3) DD.BF_3 and DD.BF_2X adducts of t-amines do not break down to give DD.BF_2^+ ions in the + FAB ms (NBA matrix). They tend to generate DD.H^+ ions, instead, so there is no false positive cation identification. This is likely due to the base strengths of the t-amines being in the $pK_b^1 = 4.2$ to 5.0 range (10), which tends to not favour DD.BF_2^+ ion formation (12a). As well, there is a non-coordinated nitrogen site on the chelating ligands that form adducts, so this site can undergo protonation, and this may lead to the destruction of the adducts; 4) Me_4en, Me_4pn, and Me_5dien.BF_nBr_{3-n} samples form DD.HBrH^+ ions in the + FAB ms, but the aromatic ligands do not. PM3 molecular orbital calculations of Me_4en.HBrH^+, Me_4pn.HBrH^+, bipyr.HBrH^+, and 1,10-phen.HBrH^+ were performed using MacSpartan 1.1.7 software. For all ligands, except bipyr, the most stable structure was that of 7 and 8 member rings that contained a Br that was coordinated between the two H-N sites on the bidentate Lewis bases (see appendix 1). Bipyr was more stable as a Br-H.bipyr.H^+, with a weak coordination between the Br and the H^+. Yet, as noted above, the aromatic ligands do not form the DD.HBrH^+ cation. This was likely due to two reasons: 1) the flexibility of the three t-amine ligands. The aromatic chelating ligands (bipyr, 1,10-phen) make 7-member rings, but they can not readily expand, instead the angles of the H-Br-H section of the rings were between 69 and 85 degrees; 2) since the aromatic ligands do not form adducts, there is not the same degree of complexity in the precipitates that are dissolved in the NBA. This leads to much simpler spectra, because the reactions responsible for the DD.HBrH^+ cation cannot occur.

Chapter 5:
Chelating Donor Substitution Reactions of $(pyr)_2BF_2^+.PF_6^-$

5.1: Introduction.

Some $D_2BF_2^+$ salts, such as $(pyr)_2BF_2^+.PF_6^-$ react with various monodentate ligands (13) such as quinuclidine (Q), 1,8-diazabicyclo(5,4,0)dec-7-ene (DBU), and 1,5-diazabicyclo(4,3,0)non-5-ene (DBN). With low-steric-hindrance strong Lewis bases such as DBU and DBN, the reaction did not stop with reaction **5.1**, but gives $(D')_2BF_2^+$ and

$$(D)_2BF_2^+ + D' \longrightarrow (D)(D')BF_2^+ + D \qquad [5.1]$$

other species (13).

This should not be a concern for the reactions performed with chelating donors in this chapter, because they are t-amine or aromatic type ligands, whose monodentate relatives used in previous reactions have not been reported to lead to multiple products (13). Here we extend studies of $(pyr)_2BF_2^+$ to reactions with potentially chelating ligands, for which the thermodynamic benefits of chelation should favour displacement of the second pyr [**5.2**] (19). In addition, this method should allow for the formation of the desired

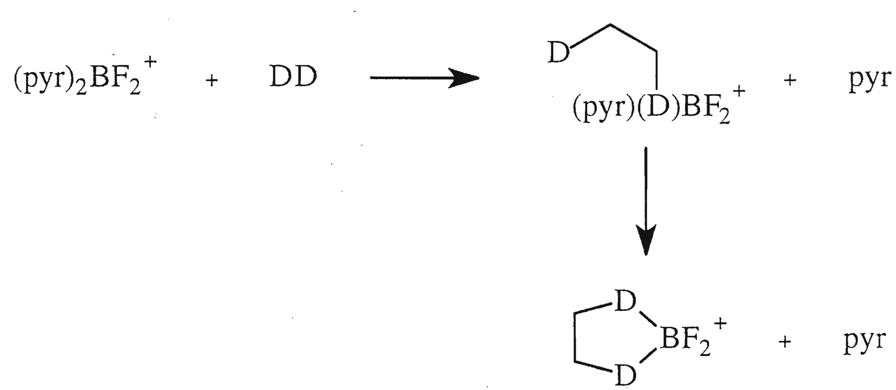

[**5.2**]

chelated fluoroboron cations without the formation of numerous additional species (see chapter 3 and 4). As well, this method, without the presence of B-Cl or B-Br bonds which react with N-H bonds to give HBr or HCl, should allow attachment of Lewis bases that contain NH and NH_2 groups, which can not be dealt with by the methods of chapters 3 and 4.

5.2: Results.

Species were identified by combination of nmr and FAB ms methods as in chapters 3 and 4. Nmr parameters for fluoroboron species detected in this chapter can be found in tables 7.1 and 7.3 (chapter 7).

5.2.1: Survey of reactions of $(pyr)_2BF_2^+.PF_6^-$ with chelating donors. The following survey of reactions by chelating DD donors (contained in tables 1.1a-c), monitored by ^{19}F nmr tests the two experimental factors that were previously examined in the reactions involving $D_2BF_2^+$ salts (12,13): D' concentration; and reaction temperature. The majority of the donors were tested under all 4 survey reactions: 2 & 10 mol. equivalents of DD to $(pyr)_2BF_2^+$ at 293 & 323K. The trends of reactions are noted in table 5.1 and 5.2.

Displacement by DD of both pyr atoms from $(pyr)_2BF_2^+$ in order form $(DD)BF_2^+$ occurred with those t-amine donors that formed 5-membered rings on chelation (table 5.1), just as in chapters 3 & 4. Displacement of the first pyr atom in order to form the non-chelated mixed $(pyr)(DD)BF_2^+$ cations was detected with all t-amine donors except pn and Et_4dien. The % yield of the (pyr)(DD) and $(DD)BF_2^+$ cations increased with DD concentration. Yet, when both the temperature and the DD concentration were high, the % yields lowered and the amounts of impurities increased. Any heating caused the t-amine donors with N-H groups to have lower to no % yields. As for aromatic donors, there was no evidence of pyr displacement or chelation.

5.2.2: Impurities formed by reactions of t-amine donors with $(pyr)_2BF_2^+.PF_6^-$. The fluorine-containing yields in table 5.1 (expressed as ^{19}F signal intensities) are not 100 % for t-amine donors, and this is due to a variety of impurities that formed in solution:

Table 5.1: Yield of $(DD)BF_2^+$ cations at various DD concentrations and reaction temperatures, as % of total signal intensity from B-F region.

	293K		323K	
	2 mol. equ.	10 mol. equ.	2 mol. equ.	10 mol. equ.
en	1.6 %	nr	nr	nr
Me_4en	6.6 %	39.9 %	12.4 %	35.8 %
Me_5dien	8.3 %	40.5 %	14.6 %	36.5 %
Et_4dien	nr	nr	nr	nr
pn	nr	nr	nr	nr
Me_4pn[a]	4.6 %	44.7 %	10.4 %	30.1 %
Me_4dipn[a]	10.3 %	1.2 %	nr	nr
bipyr	nr	nr	nr	nr
1,10-phen	nr	nr	nr	nr
terpyr	nr	nr	nr	nr
1,8-BDN		nr		
pyr_2dien	nr			
$(MeOxz)_2py$	nr			
$(IprOxz)_2py$	nr			
$(BzOxz)_2py$	nr			

[a]% yield for mixed $(pyr)(DD)BF_2^+$ cation; nr = no reaction.

Table 5.2: ^{19}F nmr chemical shifts of impurities formed at various DD concentrations at 293K.

	~ 293K			
	BF_3OH^-		$BF_2(OH)_2^-$	
	2 mol	10 mol	2 mol	10 mol
en	-144.1	-142.6	-137.3	nr
Me_4en	-145.7	nr	-139.0	-137.4
Me_5dien	-144.7	-143.2	-138.4	-138.1
Et_4dien	-143.8	-143.0	-137.2	-138.0
pn	-145.8	-144.2	-139.2	nr
Me_4pn	-145.8	-144.4	-139.2	-137.9
Me_4dipn	-145.1	-143.7	-139.4	nr
bipyr	nr	nr	nr	nr
1,10-phen	nr	nr	nr	-138.0
terpyr	nr	nr	nr	nr

nr = no reaction.

BF_4^- and two significant species in the -142-5 and -137-9 ppm ranges. A variety of experiments were carried out to identify the impurities: 1) samples from various survey reactions were mixed in an nmr tube, and the impurities were found to not be donor specific, i.e., signals of different chemical shifts in the different samples give a single averaged signal when mixed; 2) another nmr tube of combined reaction solutions was mixed with a solution of $Na^+.BF_4^-$ and $Na^+.BF_3OH^-$ in water that was prepared by a literature method, and the species identified by ^{19}F nmr (58). The BF_3OH^- quartet signal at -145.0 ppm [$^1J_{BF}$ = 13.3 Hz] and the adduct from solution at -144.5 ppm [$^1J_{BF}$ = 13.3 Hz] gave a singlet at -143.5 ppm and the other small peaks collapsed into it. This verifies that the major impurity formed in acetone with the presence of t-amine ligands and $(pyr)_2BF_2^+.PF_6^-$ is BF_3OH^-. The other minor impurities peaks are $BF_nOH_{3-n}^-$ based. The second most significantly species (-138 ppm) is identified as $BF_2(OH)_2^-$ (58).

The nature and concentration of impurities detected by ^{19}F nmr changed with: 1) the ratio of t-amine DD to pyr salt; 2) the temperature; and 3) the presence of the N-H bond. With the increase in t-amine donors concentration, BF_3OH^- and related species increased in solution. With increasing temperature, the amount of BF_4^- to BF_3OH^- and related species increased. The presence of N-H bonds on the ligand increased the amount of BF_3OH^- and related species detected. In addition, table 5.2 displays an interesting trend. As the amount of t-amine donor increases in solution, the chemical shifts of both BF_3OH^- and $BF_2(OH)_2^-$ shift to low field.

5.2.3: Impurities formed by $(pyr)_2BF_2^+.PF_6^-$ in acetone. Aromatic donors appeared not to generate any notable amounts of BF_3OH^- impurities, nor do they appear to react with the pyr salt. Solutions containing aromatic donors, and pyr salt solutions where no donor was present underwent a very different set of reactions to those containing t-amines above. Samples of the $(pyr)_2BF_2^+.PF_6^-$ salt in acetone was allowed to decompose while monitored by ^1H, ^1H-^1H COSY, ^{11}B, ^{19}F, and ^{31}P nmr. The following species form over weeks (293 K) or hours (323 K) from the $(pyr)_2BF_2^+.PF_6^-$ salt: pyr.BF_3; BF_4^-, pyr.H^+, BF_3OH^- (very little), $PF_2O_2^-$ (^{19}F chemical shift = -80.4 ppm and ^{31}P chemical shift = -12.3 ppm [$^1J_{FP}$ = 951.3 Hz]) and OPF_2OH (very little) (^{19}F chemical shift = -82.7 ppm and ^{31}P chemical shift = -21.3 ppm [$^1J_{FP}$ = 1068.1 Hz]). The nmr parameters for the P-F compounds agree with those from the literature (59,47). A complex array of reactions occurs, and at very different rates (see figures 5.1, 5.2 and 5.3). The major final species were pyr.H^+, unreacted PF_6^-, BF_4^-, and $PF_2O_2^-$. The main intermediate is pyr.BF_3, which has the same chemical shift as BF_4^- in acetone in the ^{19}F spectra, so it is hidden in many cases.

5.2.4: Detailed studies of Me_4en + $(pyr)_2BF_2^+.PF_6^-$ in acetone. There are many factors affecting the formation of chelated t-amine difluoroboron cations as shown in the survey results described in section **5.2.1**. Me_4en has been used to study reaction **5.2** in more detail to optimize the yield of $(DD)BF_2^+$.

Me_4en at seven different molar equivalents was added to nmr tubes containing $(pyr)_2BF_2^+.PF_6^-$ in acetone at room temperature. A blank (no Me_4en) was also run with the experiments. The results (figures 5.4 & 5.5) show that increasing the amount of Me_4en added to the pyr salt solution increases the rate of $(Me_4en)BF_2^+$ formation. The 32 and 64 mol solutions have estimated final values ($\approx$ 55 %) for their eight day yields, because the $(Me_4en)BF_2^+$ cation precipitated. The precipitate was confirmed by + FAB ms to be the $(Me_4en)BF_2^+$. In some other samples, yields of 60 to 65 % have been attained. Two competing side reactions occur: 1) the formation of BF_3OH^- and related species due to the presence of a t-amine ligand. Note the absence of these species in the blank (figure 5.5); 2) the formation of [pyr.H^+][BF_4^-] due to the decomposition of the $(pyr)_2BF_2^+.PF_6^-$ in acetone.

Figure 5.6 displays the two competing reactions, in addition to the formation of the desired cation in a $(pyr)_2BF_2^+.PF_6^-$ salt solution that contains 8 molar equivalents of Me_4en. At this concentration of Me_4en, and in any solution in which the Me_4en added was greater then one molar equivalent, the formation of the BF_3OH^- and related species was

Figure 5.1: 188.31 MHz ^{19}F nmr spectra of the decomposition products of $(pyr)_2BF_2^+.PF_6^-$ in acetone. The B-F and P-F regions of the spectrum are shown separately.

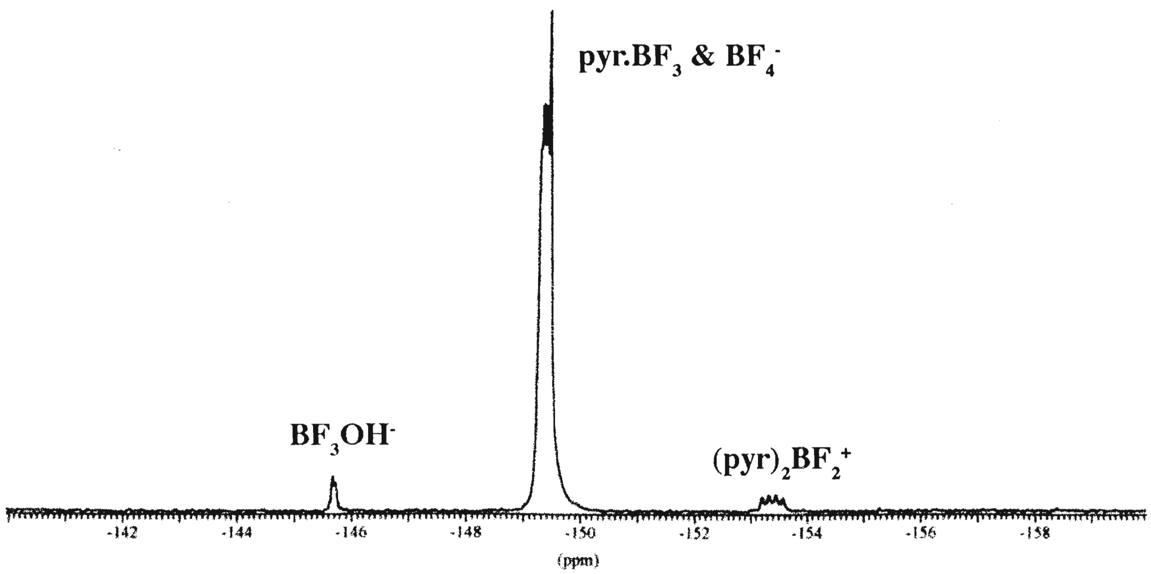

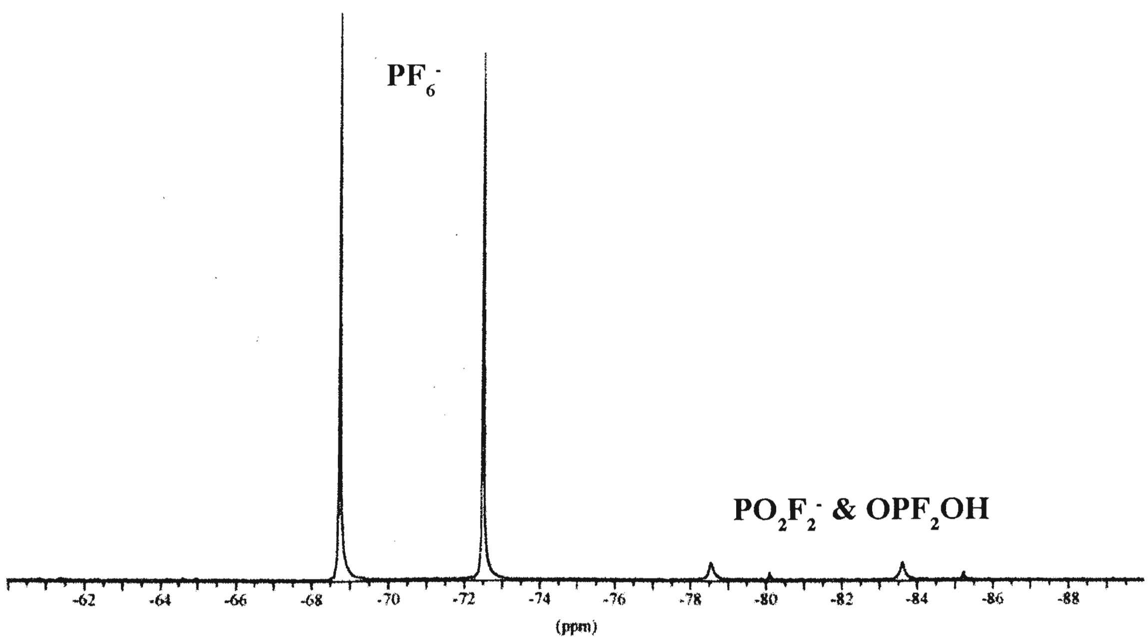

Figure 5.2: 300.13 MHz ^{1}H-^{1}H COSY nmr spectrum of various pyridine containing species during the decomposition of $(pyr)_2BF_2^+.PF_6^-$ in acetone (**A** = $(pyr)_2BF_2^+$; **B** = $pyr.BF_3$; **C** = $pyr.H^+$).

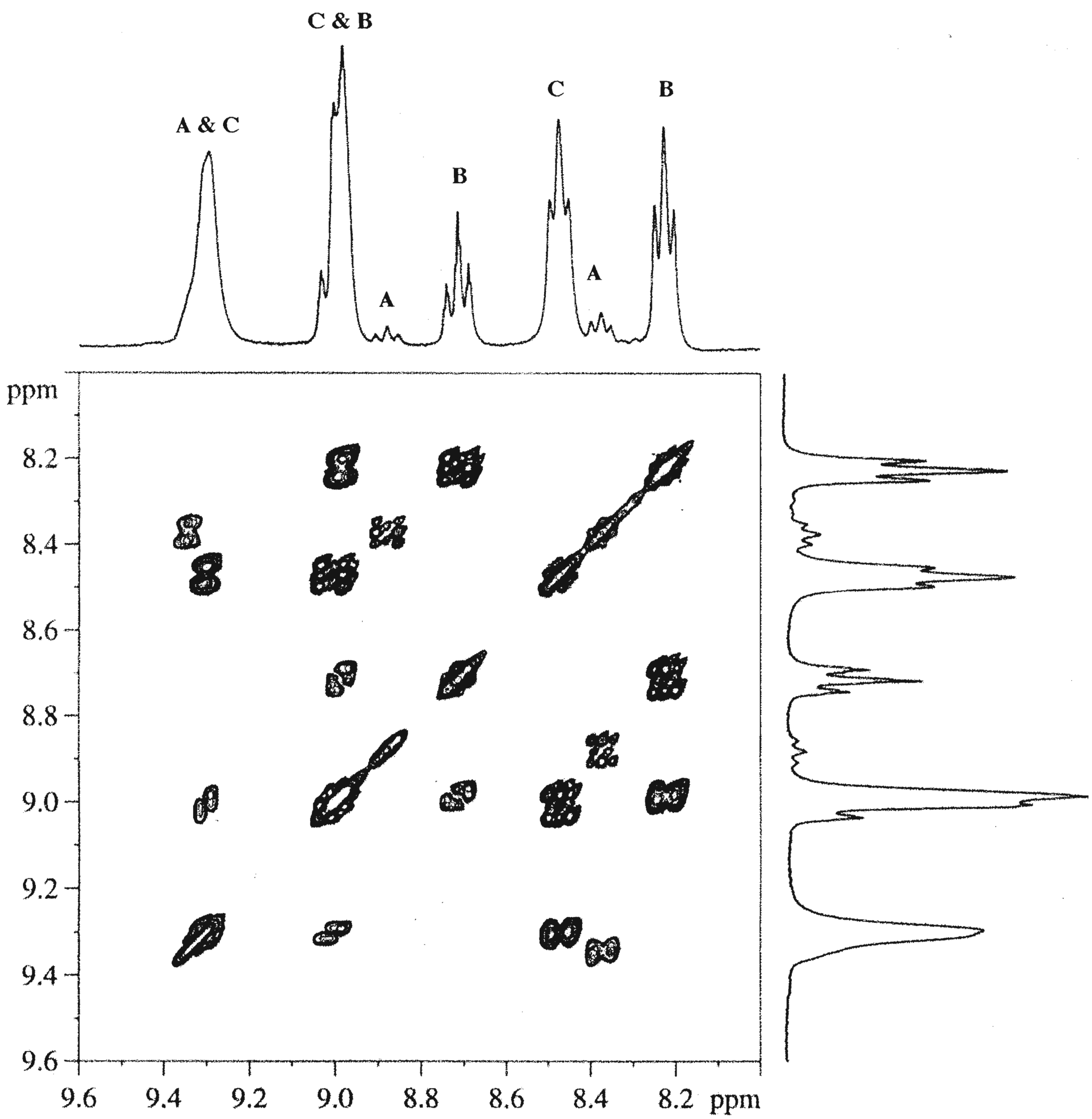

Figure 5.3: 81.01 MHz ^{31}P nmr spectrum of phosphorus containing species present following the decomposition of $(pyr)_2BF_2^{+}.PF_6^{-}$ in acetone.

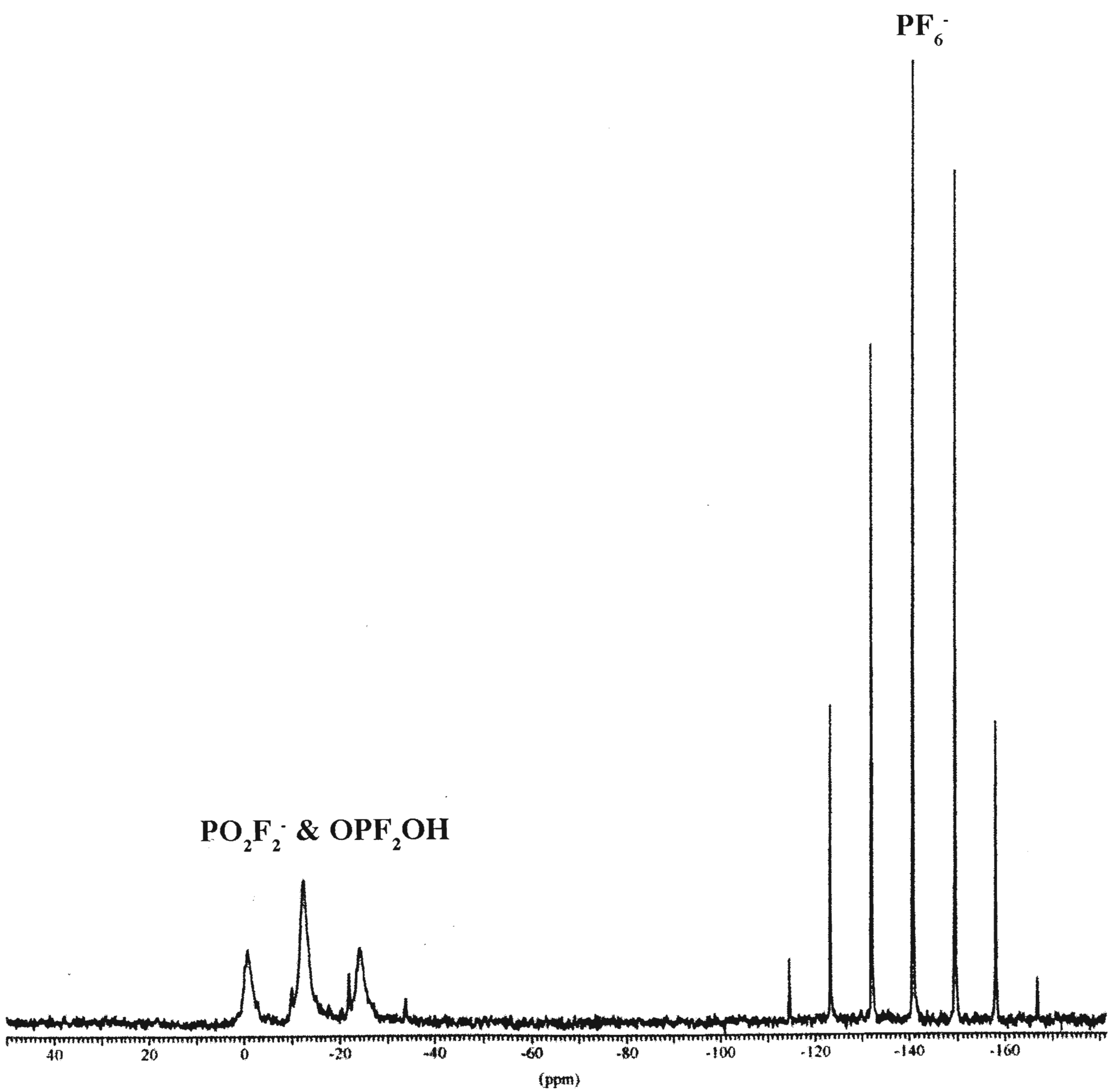

Figure 5.4: % yield (B-F region - relative ^{19}F intensities) of $(Me_4en)BF_2^+$ with increasing amounts of Me_4en added to acetone solutions containing $(pyr)_2BF_2^+.PF_6^-$ (moles Me_4en per mole of $(pyr)_2BF_2^+$). *Estimated value

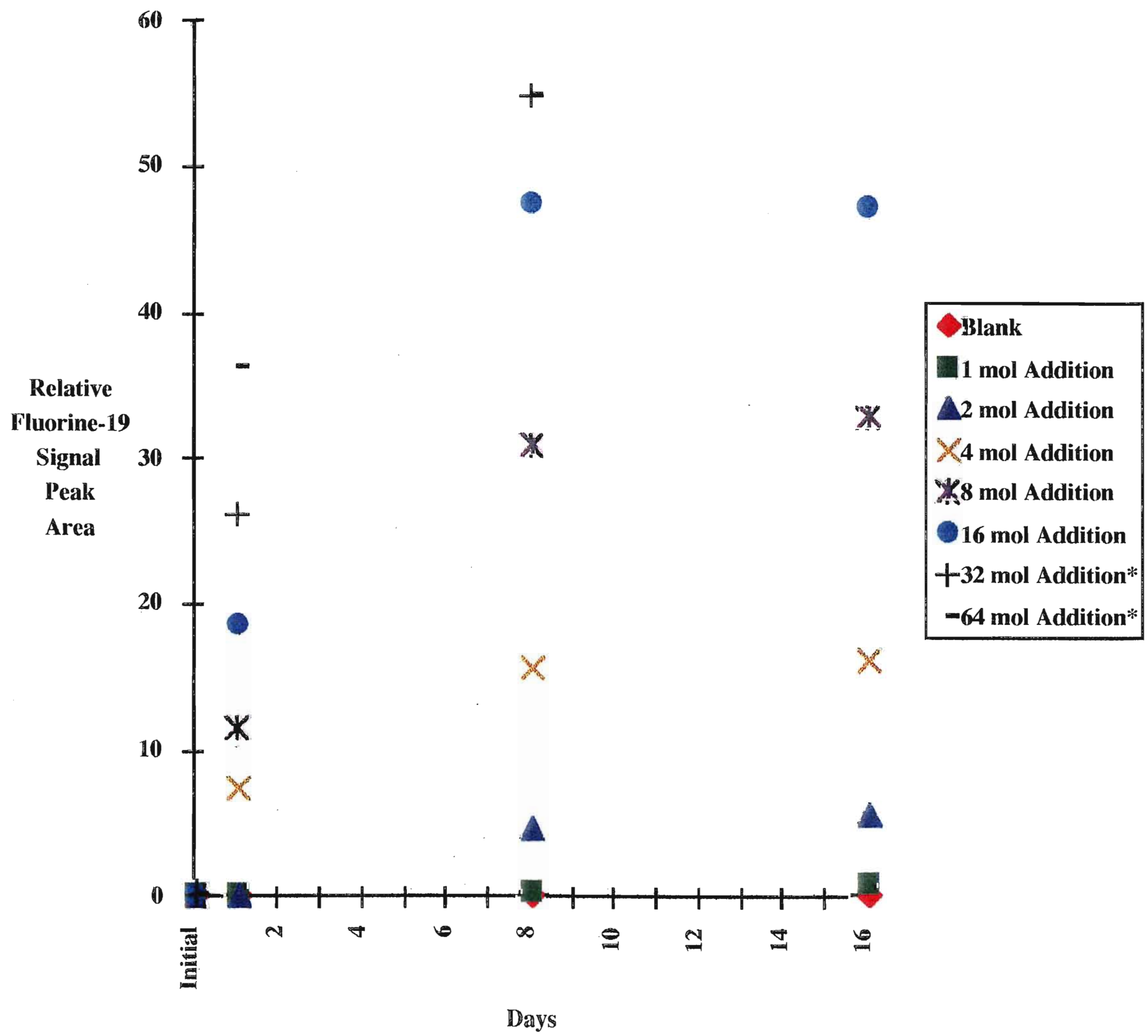

Figure 5.5: 188.31 MHz ^{19}F nmr spectra displaying the increased % yield of $(Me_4en)BF_2^+$ as the amount of Me_4en added to acetone solutions containing $(pyr)_2BF_2^+.PF_6^-$ is increased (**A** = Initial. **B** to **G** after 8 days: **B** = blank (no Me_4en); **C** = 1:1 $Me_4en:(pyr)_2BF_2^+$ mole ratio; **D** = 2:1 $Me_4en:(pyr)_2BF_2^+$; **E** = 4:1 $Me_4en:(pyr)_2BF_2^+$; **F** = 8:1 $Me_4en:(pyr)_2BF_2^+$; **G** = 16:1 $Me_4en:(pyr)_2BF_2^+$).

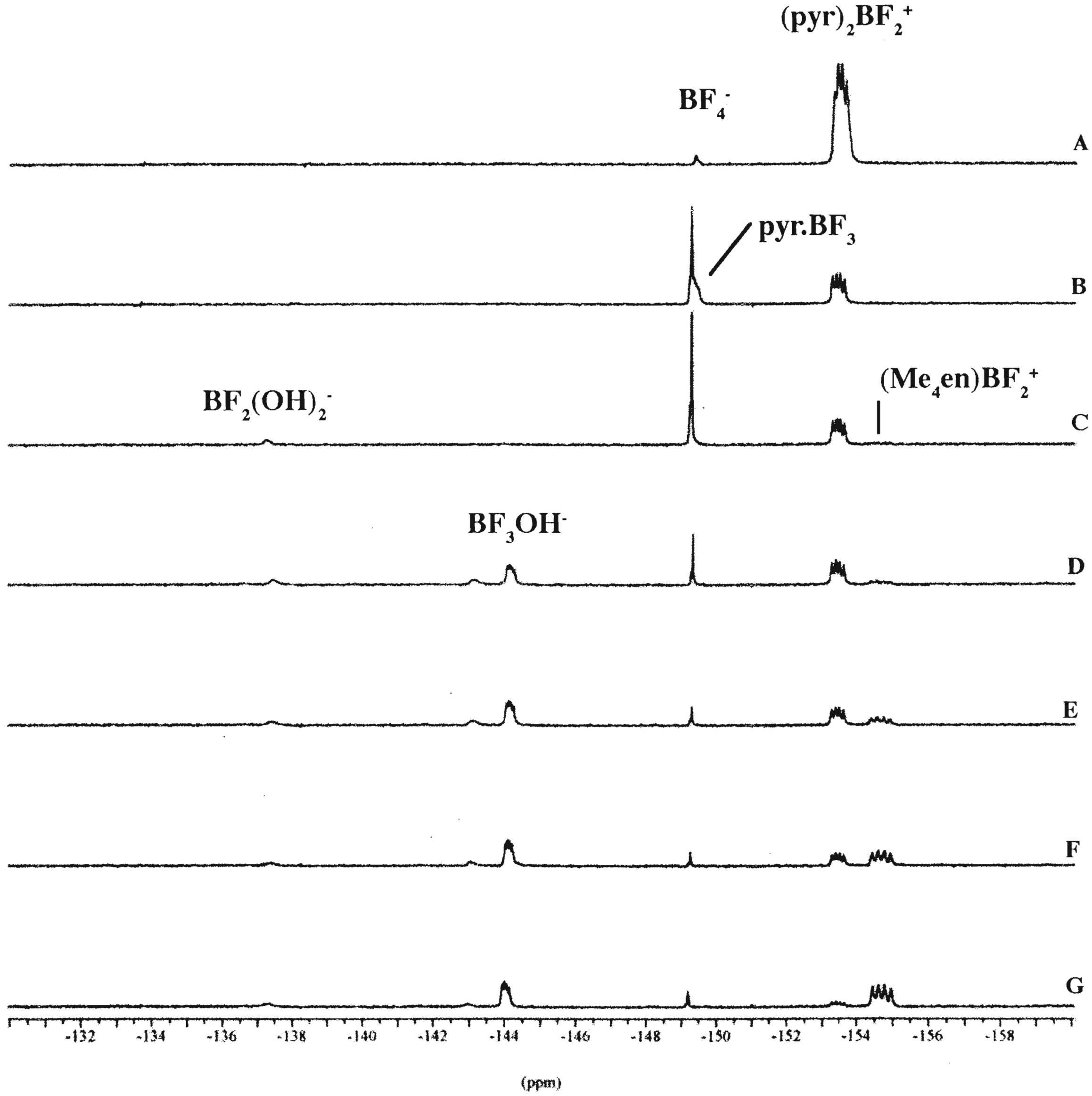

Figure 5.6: % yield (B-F region - relative ^{19}F intensities) of $(Me_4en)BF_2^+$ and other species in an acetone solution containing 8:1 $Me_4en:(pyr)_2BF_2^+.PF_6^-$ over a period of 16 days at room temperature.

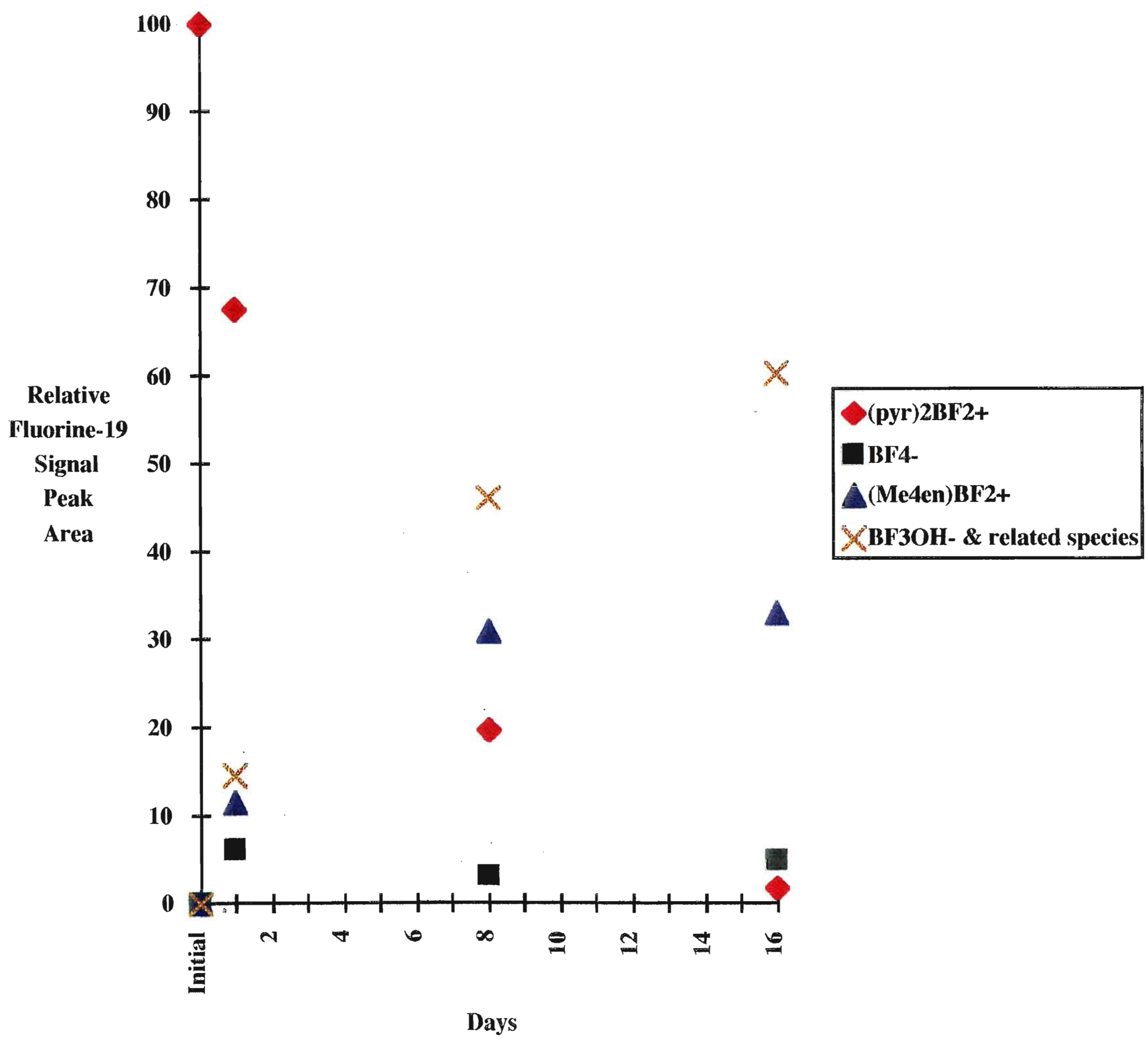

strongly favored over any other reaction at room temperature. In the blank and the one molar equivalent solution, the formation of BF_4^- was strongly favored. Thus, the decomposition of $(pyr)_2BF_2^+$ occurs readily in acetone at room temperature, but if an excess of the Me_4en ligand was present, the normal products $[pyr.H^+][BF_4^-]$ and others do not form readily.

$(Me_4en)BF_2^+$ forms more readily from $(pyr)_2BF_2^+.PF_6^-$ as it increases in concentration. The cation forms faster at 50°C than at room temperature when the same amount of base was used (section **5.2.1**). Although rapid formation of impurities at 323 K can limit the yield, is there a balance in the amount of reagent used and temperature at which the reaction can occur successfully? In figure 5.7, it can be readily seen that at 8 mol equivalents of Me_4en, that temperature does not have a great effect on the rate of reaction for the $(Me_4en)BF_2^+$ cation. All samples at temperatures of 30°C or greater had between 24 and 31 % of the desired cation after 1 day. Only the sample at room temperature has less than this. Temperature does have a great effect on the formation of BF_4^- (figures 5.8 and 5.9). In samples at 50°C or greater, there was no more $(pyr)_2BF_2^+$ left to react with after 1 day. This temperature effect mainly alters the ratio between the unwanted species that were formed, but it does also have an effect on the final yields of all the samples (figure 5.9). Our desired cation forms best at 293 to 303K. On the other hand, if the goal of a reaction was to get a chelated salt quickly, then the use of a 50°C bath would give a useable yield within 24 hours. The sample at room temperature took three weeks to completely consume the $(pyr)_2BF_2^+$.

5.2.5: Me_4en + $(pyr)_2BF_2^+.PF_6^-$ in sulpholane. A maximum yield of 60 to 65 % for $(Me_4en)BF_2^+$ occurs in acetone. Sulpholane was used for similar reactions to those in figure 5.4 to determine whether yield could be improved by changing the solvent. The samples were run at 30°C to insure that the sulpholane did not freeze in the nmr tubes (figure 5.10). As in acetone, $(Me_4en)BF_2^+$ precipitates from sulpholane when it reaches a high concentration, in a solution that is 1:5 (v:v) Me_4en:sulpholane or less. In addition, the

Figure 5.7: % yield (B-F region - relative ^{19}F intensities) of $(Me_4en)BF_2^+$ and other species at various temperatures in acetone solutions containing $8{:}1 Me_4en{:}(pyr)_2BF_2^+.PF_6^-$ after 1 day.

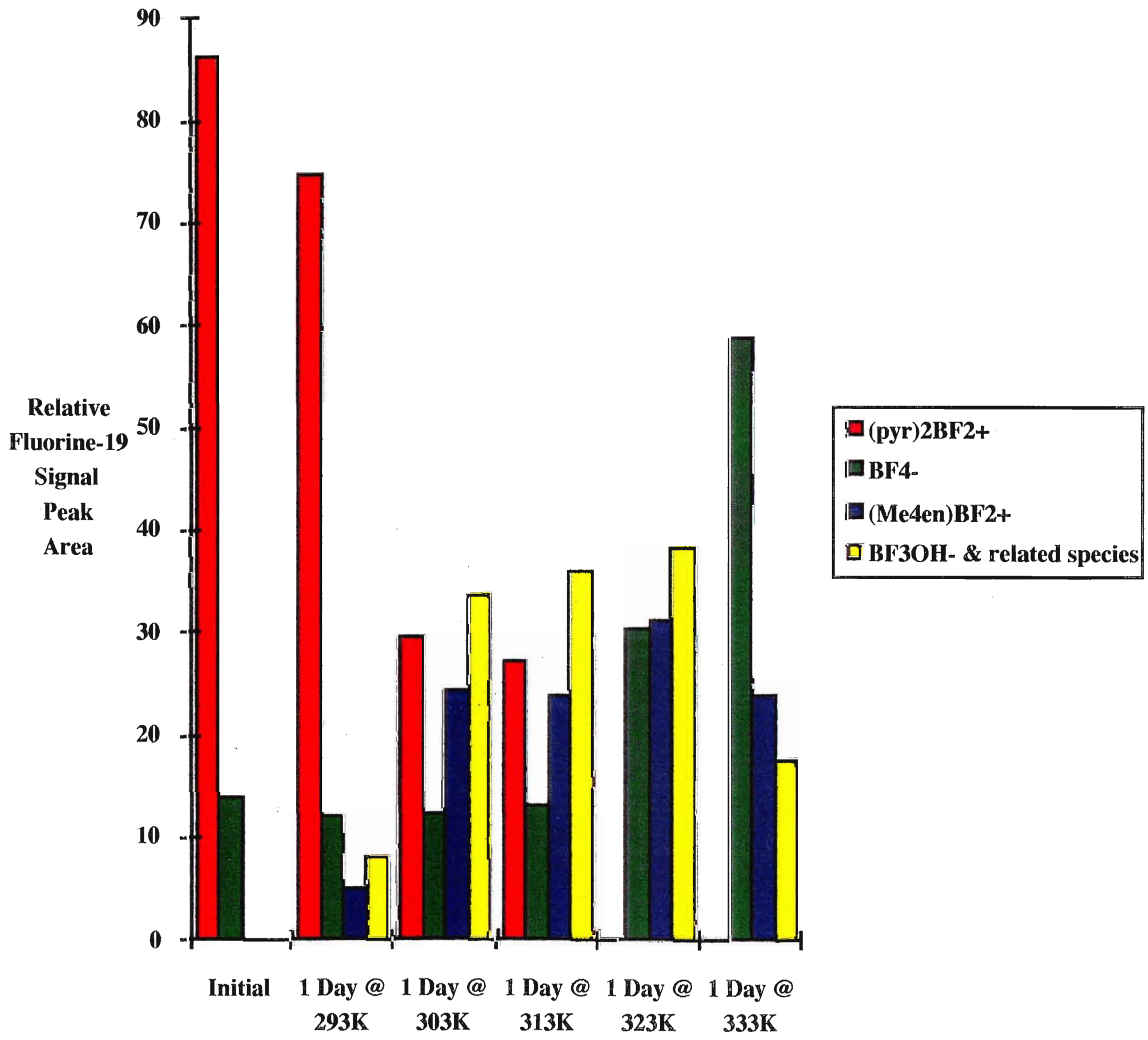

Figure 5.8: Effects of various temperatures on BF_4^- formation from $(pyr)_2BF_2^+.PF_6^-$ in acetone (B-F region - relative ^{19}F intensities).

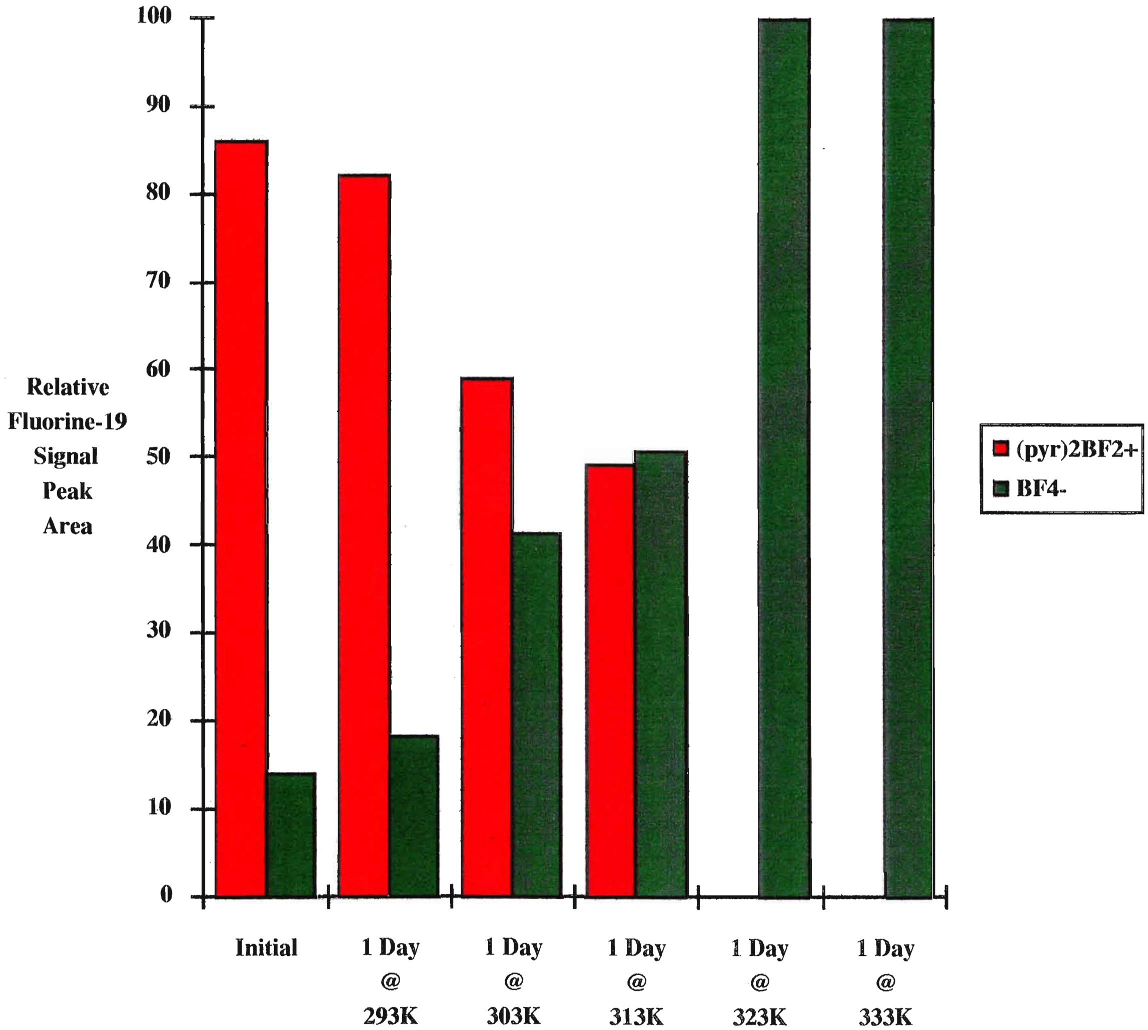

Figure 5.9: Final (between 24 hours and 3 weeks) % yield (B-F region - relative ^{19}F intensities) of $(Me_4en)BF_2^+$ and other species at various temperatures in acetone solutions containing 8:1Me_4en:$(pyr)_2BF_2^+.PF_6^-$.

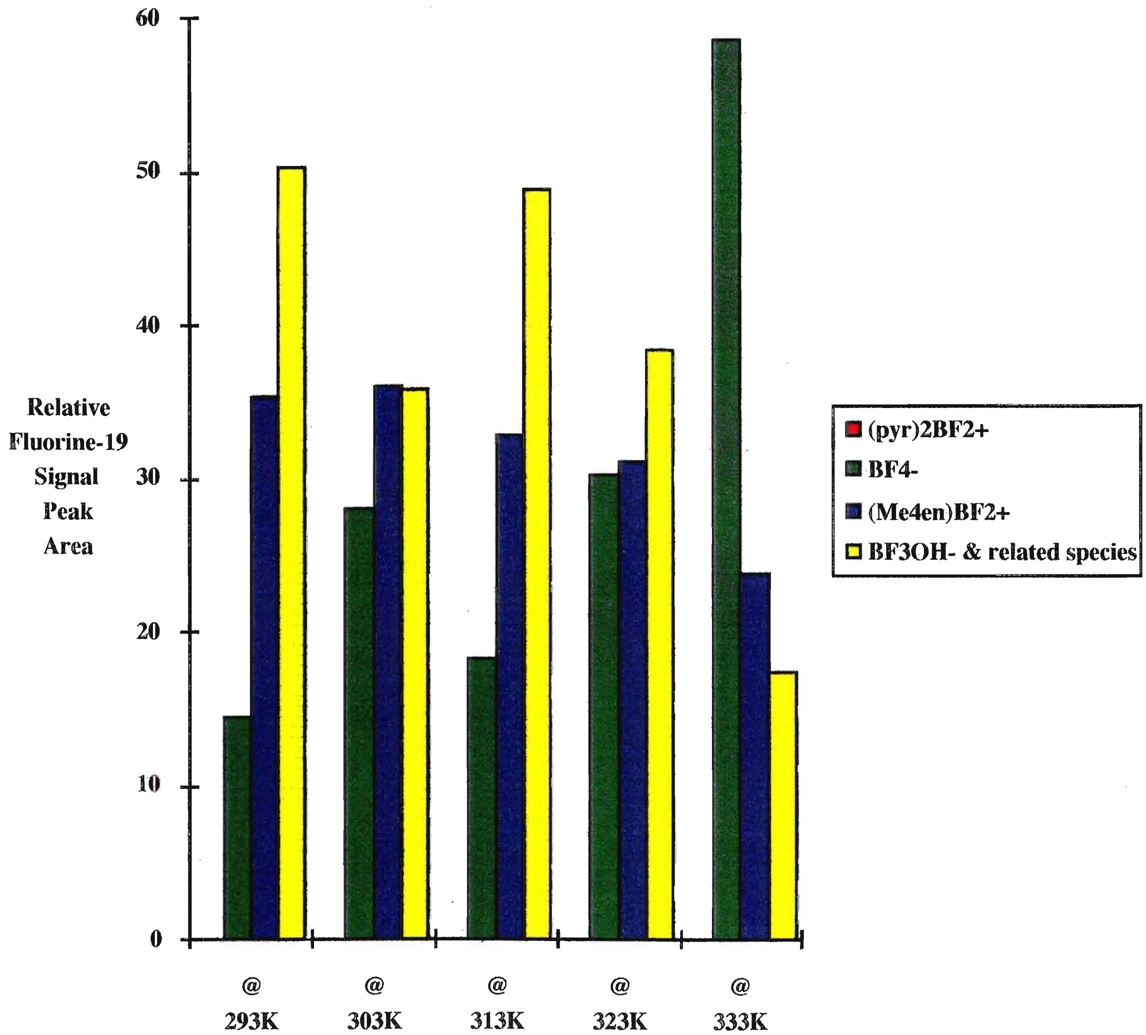

Figure 5.10: % yield (B-F region - relative ^{19}F intensities) of $(Me_4en)BF_2^+$ as the amount of Me_4en added to sulpholane solutions containing $(pyr)_2BF_2^+.PF_6^-$ is increased.

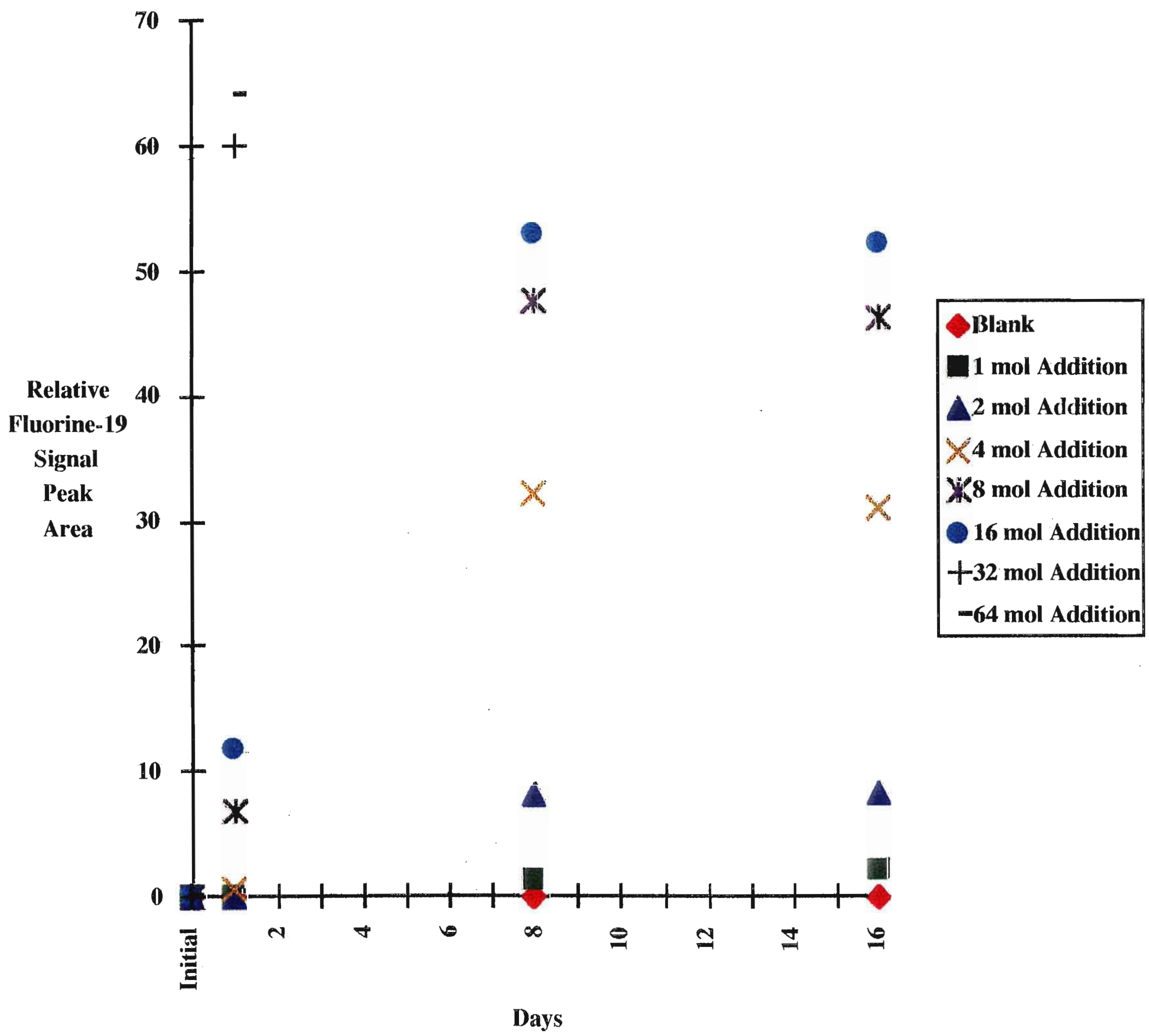

BF_3OH^- signal appears at -144.9 ppm along with the other minor $BF_nOH_{3-n}^-$ based impurities, making this solvent no more suitable than acetone.

5.3: Discussion.

5.3.1: Water. The presence of water appears to be responsible for the various impurities that limit % yields of chelated t-amine fluoroboron cations from $(pyr)_2BF_2^+.PF_6^-$, since the major impurity at room temperature contains an OH group. One possible source of water is due to the limitations of drying acetone (or sulpholane) with 3 Å Molecular Sieves. Acetone is a very difficult solvent to dry, and Molecular Sieves are considered the best drying agent (60). The addition of P_2O_5 or CaH_2 would lead to an array of reactions, but do not dry the acetone (60). Thus, our solvent is the likely cause of the majority of our problems (more on this in section **5.3.4**). The second source of water may have been water adsorbed on the walls of the reaction vessels but, our methods of drying of nmr tubes are currently adequate, for the decomposition of salt was allowed to occur in acetone solution at room temperature and at 50°C in standard glass nmr tubes as well as in Teflon inserts. No difference in the spectra could be detected. Samples prepared with Me_4en also gave reactions that were no different whether they were in glass or Teflon. Thus, moisture on the glassware is not a factor in this research, special tubes are not needed.

5.3.2: Decomposition of $(pyr)_2BF_2^+.PF_6^-$ in acetone solutions. PF_6^- being involved in the decomposition of the salt in an acetone solution is odd, for PF_6^- is normally considered to be kinetically inert. Instead, it reacts until it forms $PF_2O_2^-$ (major species) and OPF_2OH (very minor) (section **5.2.3**). This means that for every PF_6^- that reacts, two BF_4^-'s can be formed and four pyr.H^+ generated (nmr signal intensities agree). PF_6^- is inert to many species (ie., $(pyr)_2BF_2^+$, water, acetone, and bases), but it is not inert to Lewis acids (61). In excess Lewis acids systems, PF_6^- will undergo fluorine exchange reactions (61). The main question becomes how does one generate a Lewis acid in this acetone system? One possibility is protonation of the pyr of $(pyr)_2BF_2^+$ cation by water [**5.3**]. This will lead to the formation of highly reactive $pyr.BF_2^+$, which would react with the PF_6^- anion [**5.4**] to generate PF_5 and $pyr.BF_3$. The PF_5 would rapidly react with

$$(pyr)_2BF_2^+ + H_2O \longrightarrow pyr.BF_2^+ + pyr.H^+ + OH^- \qquad [\mathbf{5.3}]$$

$$pyr.BF_2^+ + PF_6^- \longrightarrow pyr.BF_3 + PF_5 \qquad [\mathbf{5.4}]$$

water, hydroxide, and $(pyr)_2BF_2^+$ to form more $pyr.H^+$, $PF_2O_2^-$, BF_4^-, and OPF_2OH. Phosphorus-fluorine-oxygen reactions are complex and the pathways are numerous (59,62). Thus, it is not surprising that the intermediate species do not appear in the nmr spectra. Heat increases the rate of decomposition of $(pyr)_2BF_2^+.PF_6^-$(figure 5.8).

5.3.3: Decomposition of $(pyr)_2BF_2^+.PF_6^-$ in basic solutions. Samples of the $(pyr)_2BF_2^+.PF_6^-$ salt in acetone with Me_4en was allowed to react while monitored by ^1H, ^{11}B, ^{19}F, and ^{31}P nmr. The samples generate various species. Of these, the main impurity is BF_3OH^- (unless the sample is heated, (see above)). The pathway in which this is formed, is not known, but: 1) it does not involve reactions with the PF_6^- anion; and 2) occurs only in systems where the pK_b^1 of one of the nitrogen atoms on the ligand is 5.0 or lower. The first point makes sense, for if $pyr.BF_2^+$ was generated, it would be quickly coordinated to Me_4en or any other Lewis base in solution. Thus, no PF_5 can be generated. The second point suggests that the formation of BF_3OH^- is base strength dependent. More specifically, it is favoured with bases that have N-H protons. These bases are stronger then their methylated cousins. This indicates that the formation of BF_3OH^- is favoured in a highly basic solution. In N-H systems where the concentration was high, no desired cations were visible, but in systems where there was no N-H protons, the % yield of desired cations increased.

5.3.4: Minimization of Impurities. The major impurities have been identified, and attempts have been made at minimizing them. The following key points appear to be essential for successful formation of chelated t-amine BF_2^+ cations: 1) concentration is a major factor. Samples with concentrations less then 20 mg/ml develop much greater proportions of impurities. Unfortunately, as the dryness of the acetone increases, the solubility of the salt decreases. 20 mg/ml is the maximum concentration in dried acetone; 2) not heating the sample; 3) the use of high concentrations of methylated bases or low concentrations of N-H bonded base will allow for the maximum yields possible (though in some cases, they maximum yield may be very low); 4) the donors be adequately dried (62) to minimize impurities.

Other possibilities are: 1) Drying acetone more thoroughly by making its NaI salt and redistilling it (60); 2) use of other solvents that are easier to dry. However as of yet, none have been found that dissolve the cation better then acetone. Benzene, sulpholane, DMSO, DMF, and nitromethane have been tried and do not. Of them, most will or could react with the salt (DMSO (56), nitromethane and DMF (56)).

5.3.5: Ligand structure, steric hindrance and first pyridine atom displacement. In our 1998 paper (13), it was noted that for Cl^- displacement from $D.BF_2Cl$, the steric hindrance of the D' donor, and especially of D could not be too great. Does the first pyr on $(pyr)_2BF_2^+$ follow this trend as well? In addition, is Cl^- displacement easier then pyr displacement?

Of the fifteen ligands studied in the present work, those that contained NMe_2R, or NH_2R coordinating sites were able to displace the first pyr atom from $(pyr)_2BF_2^+$. Only two ligands did not follow this trend: pn and 1,8-BDN. 1,8-BDN makes sense because of its very high steric hindrance. 1,8-BDN can not get one of its nitrogen atoms in position to displace the first pyr atom from the cation. As for the pn, its lack of reactivity is unexplained.

Et_4dien was unable to displace the first pyr from the cation, which suggests that this ligand was too sterically hindered (see suggestions for future work in chapter 8). Pyr_2dien did not displace pyr either, contrary to expectations based on steric grounds (see suggestions for future work in chapter 8).

The aromatic ligands (bipyr, 1,10-phen, terpyr, $(MeOxz)_2$py, $(IprOxz)_2$py and $(BzOxz)_2$py) were not successful at displacing the first pyr from the cation, and this makes sense for 1,10-phen, for like 1,8-BDN, it is too inflexible to get one nitrogen atom's lone pairs near enough to the boron in the cation. The others, however should have free rotation around their 2-2' (and 6'-2" bonds), would be expected to be able to displace the first pyridine from the salt. However, the $(Oxz)_2$py ligands are fairly sterically hindered by the groups on the 3,3" carbons. Thus, steric hindrance of the D' is a factor, but it does not completely explain the reaction trends. The steric hindrance of the two pyridine atoms on the cation must be greater than a chlorine plus a pyridine on pyr.BF_2Cl, for 1,10-phen, terpyr and bipyr all displaced the chloride and pyr from pyr.BF_2Cl.

5.3.6: Base strength and first pyridine atom displacement. Difference in base strength has also been used to explain chloride displacement trends in our 1998 paper and in earlier work. It is generally considered to be a factor in displacement reactions, though it is not considered as important as steric hindrance. There appears to also be a link between base strength of the end nitrogen and displacement of first pyridine from $(pyr)_2BF_2^+$ (table 5.3). In all cases where the first pyr was displaced, the base strength of the ligand was 4 orders of magnitude greater then those who did not react, but were not eliminated on steric hindrance grounds (ie. bipyr, terpyr, and pyr_2dien). Pn was unusual, for it could have displaced the first pyridine, but the side reactions occurred instead. Thus, steric hindrance appears to be the major factor in first pyridine atom displacement, but base strength could contribute as well.

5.3.7: Chelation ring size and second pyridine atom displacement. Of the five ligands that displaced pyridine to form the unchelated mixed $(pyr)(DD)BF_2^+$ cation, only

Table 5.3: Base strength of outer nitrogen (10) and first pyridine atom displacement.

No Displacement of Pyridine		Displacement of Pyridine	
Ligand	**pK_b[1]**	**Ligand**	**pK_b[1]**
pn	3.4	Me_4pn	4.2
bipyr	9.7	en	4.2
1,10-phen	9.3	Me_4en	5.0
1,8-BDN	1.7	Me_4dipn[a]	4.2
Et_4dien[b]	3.2	Me_5dien	4.6
terpyr[c]	9.7		
pyr_2dien[d]	8.8		
$(MeOxz)_2$py[e]	8.5		
$(IprOxz)_2$py[e]	8.5		
$(BzOxz)_2$py)[e]	8.5		

[a]Estimate from Me_4pn; [b]estimate from Et_3N; [c]estimate from bipyr; [d]estimate from pyridine; [e]estimate from oxazoline.

those ligands that form five-membered rings on chelation did form the desired chelated $(DD)BF_2^+$ cation. This trend was also apparent in the data from chapters 3 and 4. This would at first appear odd, since there are a great deal of six (and seven) membered ring species involving boron in the literature (28,29,37,38,64) and one in this present work: $(1,8\text{-}BDN)BF_2^+$. Yet, when one studies their structures (28,29,37,38), one notes the following trend; that in all the cases noted, except one (64), the ligands are aromatic and rigid, and these two factors are likely very important. In the one case where Me_4pn has been successfully chelated to boron (64) (as a borane + 1 cation), $H_3B.Me_4pn.BH_3$, Me_4pn and I_2 were reacted in dichloromethane for over 16 hours, with a very low yield being attained. This suggests that the three carbon chain of pn based ligands is too long to have the lone pair on the non-coordinated nitrogen close enough to the boron to undergo either an S_N2 or S_N1 type reaction. Carbon chain length does seem odd, for Me_5dien is a much longer over all chain then Me_4pn, but the center nitrogen is still closer then the second one on the Me_4pn.

Chapter 6:
Chelating Donor Reactions with $Et_2O.BF_3$

6.1: Introduction.

Previous studies of the formation of boron difluoroboron cations from $Et_2O.BF_3$ have been discussed at length in chapter 1. The research in this chapter was carried out to examine two questions: 1) were potentially-chelating t-amines as unsuccessful as reported in the formation of $BF_2^+.BF_4^-$ salts? We can identify those BF_2^+ cations by nmr now, since we have prepared them from mixed-halogen adduct systems (chapters 3 and 4); 2) were the aromatic ligands as successful as reported in the formation of chelated $BF_2^+.BF_4^-$ salts? Elemental analysis was the main source of evidence in the past, but it cannot distinguish between a bisadduct ($(BF_3)_2$) and a cation-anion pair ($BF_2^+.BF_4^-$), which are coordination isomers.

6.2 Results - Reactions with $Et_2O.BF_3$.

Nmr parameters for most species discussed in this chapter can be found in chapter 7, but some cation and adduct nmr parameters will be listed here. Reactions were carried out as described in chapter 2 unless otherwise noted. Chloroform was the sole reaction solvent for sections **6.2.1-3**.

6.2.1: <u>Me_4en</u>. In the 1:1 (Me_4en:$Et_2O.BF_3$) solution, both $Me_4en.BF_3$ and $Me_4en.(BF_3)_2$ gave visible ^{19}F nmr signals after 16 hours. The white precipitate that formed, was dissolved in nitromethane and showed the above species as well by nmr. In the 1:2 and 1:3 solutions, only a very small amount of the $Me_4en(BF_3)_2$ bisadduct remained in the solution. The precipitates had the mono and bis BF_3 adduct species visible in the nmr. In no case was the desired $(Me_4en)BF_2^+$ cation detected.

6.2.2: <u>Me_5dien</u>. In the 1:1 solution, both mono-BF_3 adducts(bonded through the end and centre nitrogen sites) gave ^{19}F nmr signals after 16 hours (see chapter 7 for assignment). The precipitate in nitromethane, also contained both mono-BF_3 adducts. A small amount of BF_3OH^- (see chapter 5), BF_4^-, and an unidentified peak at -141.4 ppm were also visible. In the 1:2 solution, only the $Me_5dien.BF_3$ adduct (bonded through the centre nitrogen) remained in solution. The precipitate, dissolved in nitromethane, showed two different species: 1) the bis BF_3 adduct of Me_5dien, with the boron coordinated to the two terminal nitrogen atoms; and 2) the tris-BF_3 adduct. BF_4^- and two very weak unidentified singlets at -144.7 and -141.6 ppm were also present. In the 1:3 solution, no fluorine-containing species remained in the reaction solution. In the precipitate, the tris-BF_3 adduct was present. In addition, the bis BF_3 adduct that has one terminal nitrogen and the central nitrogen atoms coordinated was visible. Some $Et_2O.BF_3$, and some very weak singlets at -148.2, -147.5, -145.5 and -145.0 ppm were also visible. The 1:6 solution, was the same. This method was not successful in forming the desired $(Me_5dien)BF_2^+$ cation.

6.2.3: $\underline{Me_4pn}$. This base behaved just as Me_4en above for solution of 1:1, 1:2 and 1:3 ratios. It did not form the desired $(Me_4pn)BF_2^+$ cation.

6.2.4: Bipyr. The $(bipyr)BF_2^+.BF_4^-$ salt did not form at the 0.5 to 1.0 ml level in either 1:1 ether:acetone, chloroform, or benzene with 1:1, 1:2 and 1:3 bipyr:$Et_2O.BF_3$. In these reactions, the principal product of reaction appears to be bipyr.$H^+.BF_4^-$. Larger volume (10 - 15 ml) reactions using 1:1 ether:acetone or benzene, with active stirring were carried out, and in approximately 50% of the reaction attempts, the bipyr.$H^+.BF_4^-$ salt (^{19}F chemical shift = -150.4 (^{10}B), -150.5 (^{11}B) ppm) did not appear, but a broad peak at -150.2 ppm in nitromethane (no coupling or isotope shifts visible). Based on known chemical shifts of pyridine adducts (15) this peak occurs at the expected chemical shift region for the bis-BF_3 adduct of bipyr. Bipyr was also reacted with ISOX.BF_3 in chloroform, and a similar broad peak at -150.2 ppm was observed.

In all cases, the product(s) of reactions of bipyr with $Et_2O.BF_3$ or ISOX.BF_3 were insoluble in the reaction solvent, so reactions between bipyr and the boron trifluoride donors were carried out in nitromethane. Unfortunately, nitromethane coordinates to BF_3, and displaces Et_2O or ISOX in the presence of bipyr to form a mixture of $CH_3NO_2.BF_3$ (-

141.4 ppm) and $(CH_3NO_2)BF_2^+.BF_4^-$ (1:2 ratio between ^{19}F peaks at -139.9:-150.5 ppm). So the only evidence that the adduct bipyr.$(BF_3)_2$ exists is a ^{19}F chemical shift of -150.2 ppm (and ^{11}B chemical shift of -0.6 ppm). Elemental analysis of the precipitate: C = 46.84 %, H = 2.15 % and N = 10.92 %; is inconsistent with bipyr.$(BF_3)_2$, calculated: C = 41.16 %, H = 2.76 % and N = 9.60 %; or with bipyr.$H^+.BF_4^-$, calculated: C = 49.23 %, H = 3.71 % and N = 11.48 %. Since neither of these values match, elemental analysis can not confirm this species. Bipyr.BF_3 is even further from the found value. Elemental analysis was the only evidence given for formation of (bipyr)$BF_2^+.BF_4^-$ in the literature (28,30), though these conclusions are not supportable based on elemental analysis alone, for the bis-BF_3 adduct is an isomer of this. + FAB ms gave no evidence of a (bipyr)$BF_2^+.BF_4^-$ salt in any sample.

6.2.5: 1,10-Phen. On addition of $Et_2O.BF_3$ to a benzene solution containing 1,10-phen, a white precipitate formed nearly instantly. The precipitate, dissolved in nitromethane, gave ^{19}F chemical signal at -149.8 ppm [$^1J_{BF}$ = 24.4 Hz]) that we assigned to (1,10-phen)BF_2^+ and at 4 times greater intensity, the anion BF_4^- (^{19}F chemical shift = -150.4 (^{10}B), -150.5 (^{11}B) ppm). A ^1H and ^1H-^1H COSY nmr spectra (figure 6.1) in acetonitrile-d_3 showed that only 50 % of the 1,10-phen had reacted with the $Et_2O.BF_3$. The other 50 % of the 1,10-phen appears as 1,10-phen.H^+ in figure 6.1, and BF_4^- anion must be the counter ion. It is not known, whether the 1,10-phen.$H^+.BF_4^-$ salt formed pre or post isolation on the Schlenk line.

A 1:2 solution in benzene was dried after 24 hours, and some of its contents were dissolved in acetonitrile-d_3. The ^{19}F nmr spectrum gave the following 1:2 signals: (1,10-phen)BF_2^+ at -149.2 ppm [$^1J_{BF}$ = 23.4 Hz] and BF_4^- at -149.4 (^{10}B), -150.0 (^{11}B) ppm (figure 6.2). The ^1H and ^{13}C nmr spectra for this sample showed that greater than 95 % of the 1,10-phen had formed the desired cation (^1H and ^{13}C nmr data can be found in tables 6.1 and 6.2, along with the data for the uncoordinated ligand). Positive and negative ion FAB ms spectra of the precipitate showed: + FAB ms; 229 m/z[(1,10-phen)BF_2^+]

Figure 6.1: 300.13 MHz ^{1}H-^{1}H COSY of (1,10-phen)BF_2^+.BF_4^- and 1,10-phen.H^+ in acetonitrile-d_3. **A** (1,10-phen)BF_2^+, **B** 1,10-phen.H^+.

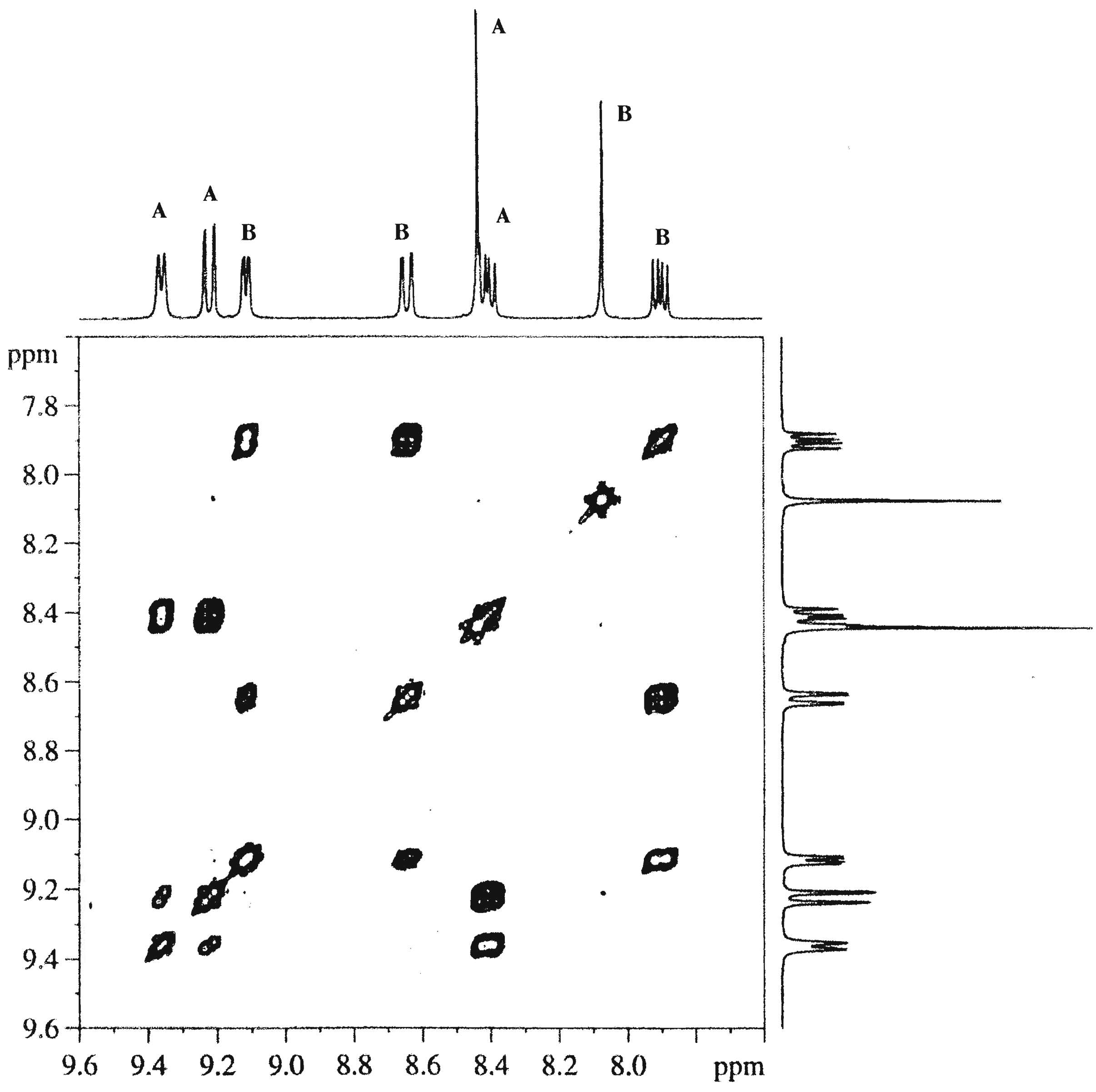

Figure 6.2: 188.31 MHz ^{19}F nmr of (1,10-phen)$BF_2^+.BF_4^-$ in acetonitrile-d_3.

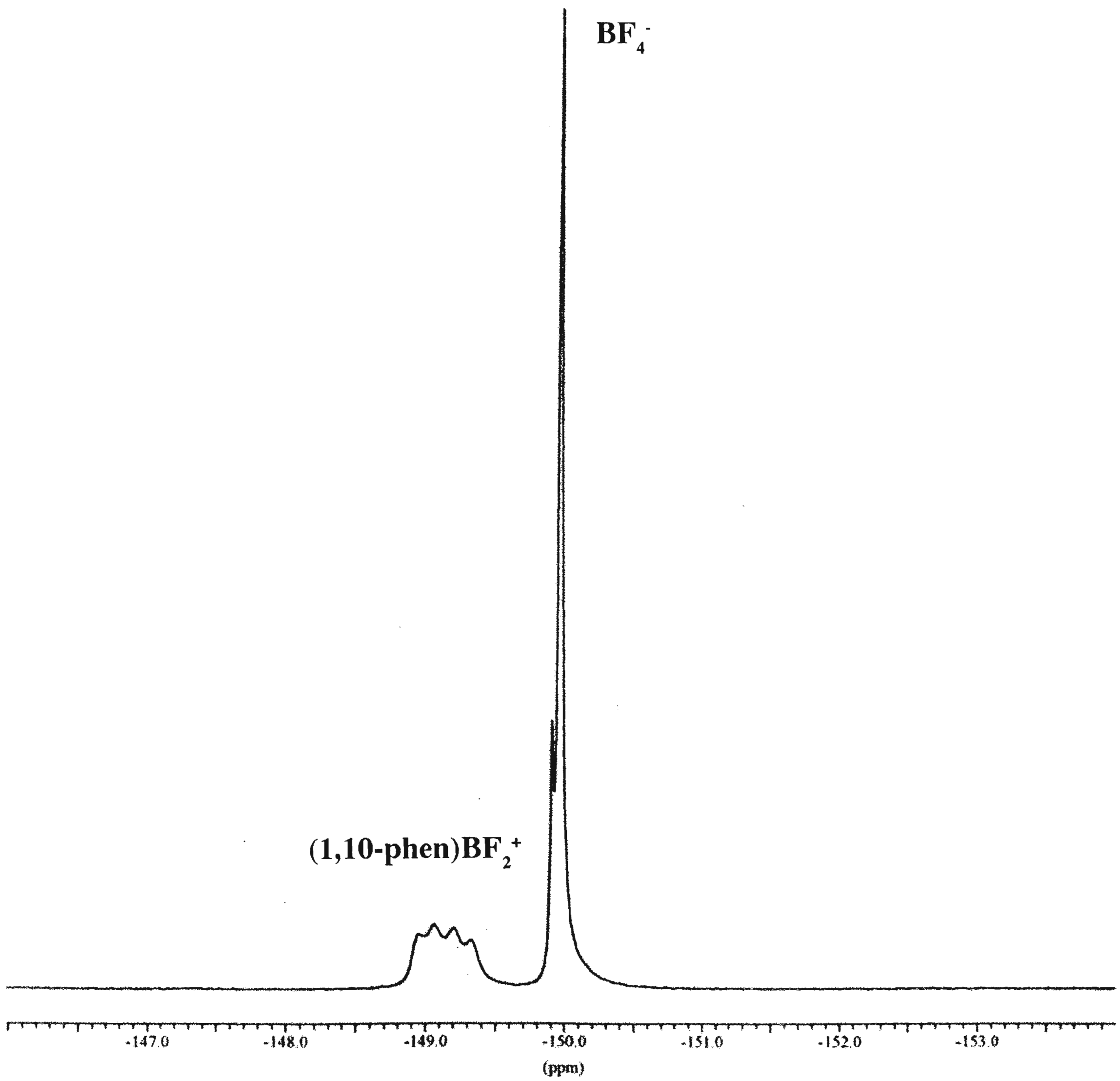

Table 6.1: ^1H nmr parameters of aromatic bidentate ligands and aromatic $(DD)BF_2^+.BF_4^-$ salts.[a]

	^1H Chemical Shifts (ppm)		$^3J_{HH}$ (Hz)	
	Ligand	BF_2^+ Cation	Ligand	BF_2^+ Cation
1,8-BDN	7.30	7.83	14.17 (t)	8.13 (t)
	7.29	8.21	12.77 (d)	8.29 (d)
	6.94	8.15	7.20 (d)	7.89 (d)
	2.75	3.44	(s)	(s)
1,10-phen	9.10	9.36	4.31, 1.61 (dd)	5.23 (d)
	8.25	9.22	8.25, 1.49 (dd)	8.36, 0.72 (dd)
	7.73	8.44	(s)	(s)
	7.62	8.41	8.00, 4.21 (dd)	8.40, 5.41 (dd)

[a]In acetonitrile-d_3

Table 6.2: ^{13}C chemical shifts of aromatic bidentate ligands and aromatic $(DD)BF_2^+.BF_4^-$ salts.[a]

	^{13}C Chemical Shifts (ppm)	
	Ligand	BF_2^+ Cation
1,8-BDN	151.7	139.4
	138.8	136.2
	126.5	131.9
	122.4	128.5
	113.8	122.7
	44.7	52.9
1,10-phen	150.8	146.2
	147.0	145.9
	136.9	129.6
	130.0	129.2
	127.5	128.6
	124.0	126.9

[a]In acetonitrile-d_3

(100 %) and 181 m/z [1,10-phen.H^+] (46.5 %); - FAB ms; 403 m/z [$(BF_4^-)_2$(1,10-phen)BF_2^+] (unknown %) and 87 m/z [BF_4^-] (100 %).

A chloroform solution containing ISOX.BF_3 was reacted with 1,10-phen at a 2:1 ratio, and the (1,10-phen)BF_2^+.BF_4^- salt readily formed. Elemental analysis found: C = 45.70 %, H = 2.83 % and N = 9.01 %; calculated: C = 45.64 %, H = 2.55 % and N = 8.87 %. This result, along with the bipyr results suggest that ISOX.BF_3 and $Et_2O.BF_3$ behave similarly as BF_3 sources.

6.2.6: Terpyr. In the 1:1, 1:2 and 1:3 (terpyr:$Et_2O.BF_3$) solutions in 1:1 ether:acetone or benzene, a pale yellow precipitate formed over a matter of minutes, which was dissolved in nitromethane. The ^{19}F spectra detected the cation (terpyr)BF_2^+ (^{19}F chemical shift = -145.2 ppm [$^1J_{BF}$ = 25.2 Hz]) and an excess (1:6 to 1:20) of BF_4^- (^{19}F chemical shift = -150.4 (^{10}B), -150.5 (^{11}B) ppm). ^1H and ^1H-^1H COSY were performed in acetonitrile-d_3, and showed that only 10 to 30 % of the terpyr had reacted with the $Et_2O.BF_3$. Positive and negative ion FAB ms found: + FAB ms; 282 m/z [(terpyr)BF_2^+] (100 %) and 234 m/z [terpyr.H^+] (58.2 %); - FAB ms; 240 m/z [(BF_4^-)(NBA)] (unknown %) and 87 m/z [BF_4^-] (100 %). Similar results and % yields were found when ISOX.BF_3 was reacted with terpyr. This ligand is very much like bipyr, but unlike bipyr, it does form the (terpyr)BF_2^+.BF_4^- salt, however with a very low % yield. Yet, there was no evidence of a mono, bis or tris adduct of terpyr detected in solution.

6.2.7: 1,8-BDN. In a 1:1 (1,8-BDN:$Et_2O.BF_3$) solution in benzene, a red precipitate formed over 24 hours. The benzene was removed on a Schlenk line, and two precipitates were visible (red and white). In nitromethane, the cation (1,8-BDN)BF_2^+ (^{19}F chemical shift = -162.2 ppm [$^1J_{BF}$ = 29.2 Hz]) and a less than two-fold excess of BF_4^- (^{19}F chemical shift = -150.4 (^{10}B), -150.5 (^{11}B) ppm) were visible. In acetonitrile-d_3, the ^{19}F nmr chemical shifts are slightly different ((1,8-BDN)BF_2^+ = -162.5 ppm [$^1J_{BF}$ = 29.2 Hz] and BF_4^- = -149.9 (^{10}B), -150.0 (^{11}B) ppm). A ^1H nmr spectrum displayed that only 50 % of the 1,8-BDN had reacted with the $Et_2O.BF_3$. This is expected, since the BF_4^-

anion must be generated in the reaction to balance the charge. The other 50 % of the 1,8-BDN species appear to be 1,8-BDN.H^+ and 1,8-BDN.

The 1:2 solution was like the 1:1, except the ^{19}F, ^{1}H and ^{13}C nmr spectra for this sample showed that more than 95 % of the 1,8-BDN had formed the desired cation (^{1}H and ^{13}C nmr data can be found in table 6.1 and 6.2, along with the data for the uncoordinated ligand). Peaks in the ^{1}H chemical shift range were assigned by using ^{1}H {^{1}H} nOe difference nmr. + FAB ms; 263 m/z [(1,8-BDN)BF_2^+] (100 %), 248 m/z [(1,8-BDN - Me)BF_2^+] (9.9 %), 215 m/z [1,8-BDN.H^+] (86.8 %) and 200 m/z [(1,8-BDN - Me).H^+] (4.7 %); - FAB ms; 437 m/z [$(BF_4^-)_2$(1,8-BDN)BF_2^+] (unknown %) and 87 m/z [BF_4^-] (100 %).

6.3: Results - DMSO Solvolysis of (DD)BF_2^+.BF_4^- salts and Related Species.

Two groups (28,30) have reported the formation of (bipyr)BF_2^+.BF_4^- and (1,10-phen)BF_2^+.BF_4^- in the past, but have been unsuccessful at nmr characterization of the cations due to solvolysis by DMSO-d_6. The most recent (30) of the papers determined that solvolysis was occurring, but failed to identify their cations correctly. They labeled $(DMSO)_2BF_2^+$ in their ^{11}B nmr spectra (^{11}B chemical shift = 2.2 ppm, [$^{1}J_{BF}$ = 12.5 Hz]) as (1,10-phen)BF_2^+, while tentatively identifying the true (1,10-phen)BF_2^+ peak as 1,10-phen.BF_3. We here describe the reactions of DMSO with related systems.

6.3.1: Reactions with bipyr species. Nmr tubes containing: a) the product (-150.2 ppm) from section **6.2.4** in DMSO; b) the product (-150.2 ppm) from section **6.2.4** in nitromethane plus a 10 molar excess of DMSO. In addition, samples from 1) a mixed sample of (bipyr)BF_2^+, (bipyr)$BFCl^+$, and (bipyr)BCl_2^+ as the BF_4^- salts in DMSO; 2) a mixed sample of (bipyr)BF_2^+, (bipyr)$BFBr^+$, and (bipyr)BBr_2^+ as the Br^- salts in DMSO; and 3) a mixed sample of (bipyr)BF_2^+, (bipyr)$BFBr^+$, and (bipyr)BBr_2^+ as the Br^- salts in nitromethane, had a 10 molar excess DMSO added, were monitored by nmr. No reactions occurred between any of the bipyr cations and DMSO over 48 hours at room temperature. The cations had their chemical shifts move by varying degrees to high frequency. As for the product from section **6.2.4**, it moved from where it would normally appear at -0.6 ppm (^{11}B) in nitromethane to between 0.0 and -0.3 ppm (^{11}B) in DMSO and 5:1 nitromethane:DMSO.

6.3.2: Reactions with 1,10-phen species. 18 mg of the (1,10-phen)BF_2^+.BF_4^- was placed in 0.5 ml of acetonitrile-d_3. A 4 molar excess DMSO was added, and after the first spectrum was acquired, the low intensity $(DMSO)_2BF_2^+$ intermediate and a large final product DMSO.BF_3 signal were visible (figure 6.3). After 0.2 hours, well over 50 % of the (1,10-phen)BF_2^+ cation was gone from solution. After 1.2 hours, there was no trace of the (1,10-phen)BF_2^+ cation, and the solution was stable, (the integration values were very similar to those taken 14 hours later). Since the solvolysis product was DMSO.BF_3, fluorine exchange occurred between the BF_4^- anion and the DMSO species. Consistent with this, the intensity of the BF_4^- anion decreases over time in the nmr spectra. However, much BF_4^- anion remains; the counter-ion must be protonated base.

A nmr tube containing a mixed sample of (1,10-phen)BF_2^+, (1,10-phen)$BFCl^+$, and (1,10-phen)BCl_2^+ as the Cl^- salts in nitromethane had a large excess DMSO added; and only the (1,10-phen)BF_2^+ reacted with the DMSO to eventually form the DMSO.BF_3 adduct. Another nmr tube containing a mixed sample of (1,10-phen)BF_2^+, (1,10-phen)$BFBr^+$, and (1,10-phen)BBr_2^+ as the Br^- salt (oil in nitromethane) had a large excess of DMSO added and only the (1,10-phen)BF_2^+ reacted with the DMSO to eventually form the DMSO.BF_3 adduct.

6.3.3: Reactions with terpyr species. A nmr tube containing a mixed sample of (terpyr)BF_2^+, (terpyr)$BFBr^+$, and (terpyr)BBr_2^+ as the Br^- salt (oil in nitromethane) had a large molar excess DMSO added and only the (terpyr)$BFBr^+$ cation reacted with the DMSO to eventually form an unknown species in the tricoordination range of the ^{11}B spectrum (~22 ppm). Like its bipyr cousin, the (terpyr)BF_2^+ cation was stable in respect to solvolysis.

Figure 6.3: 64.20 MHz ^{11}B nmr of (1,10-phen)BF_2^+.BF_4^- plus DMSO in acetonitrile-d_3. **A** Initial addition of 4 mole equivalents of DMSO, **B** 0.2 hours, **C** 0.6 hours, **D** 1.4 hours.

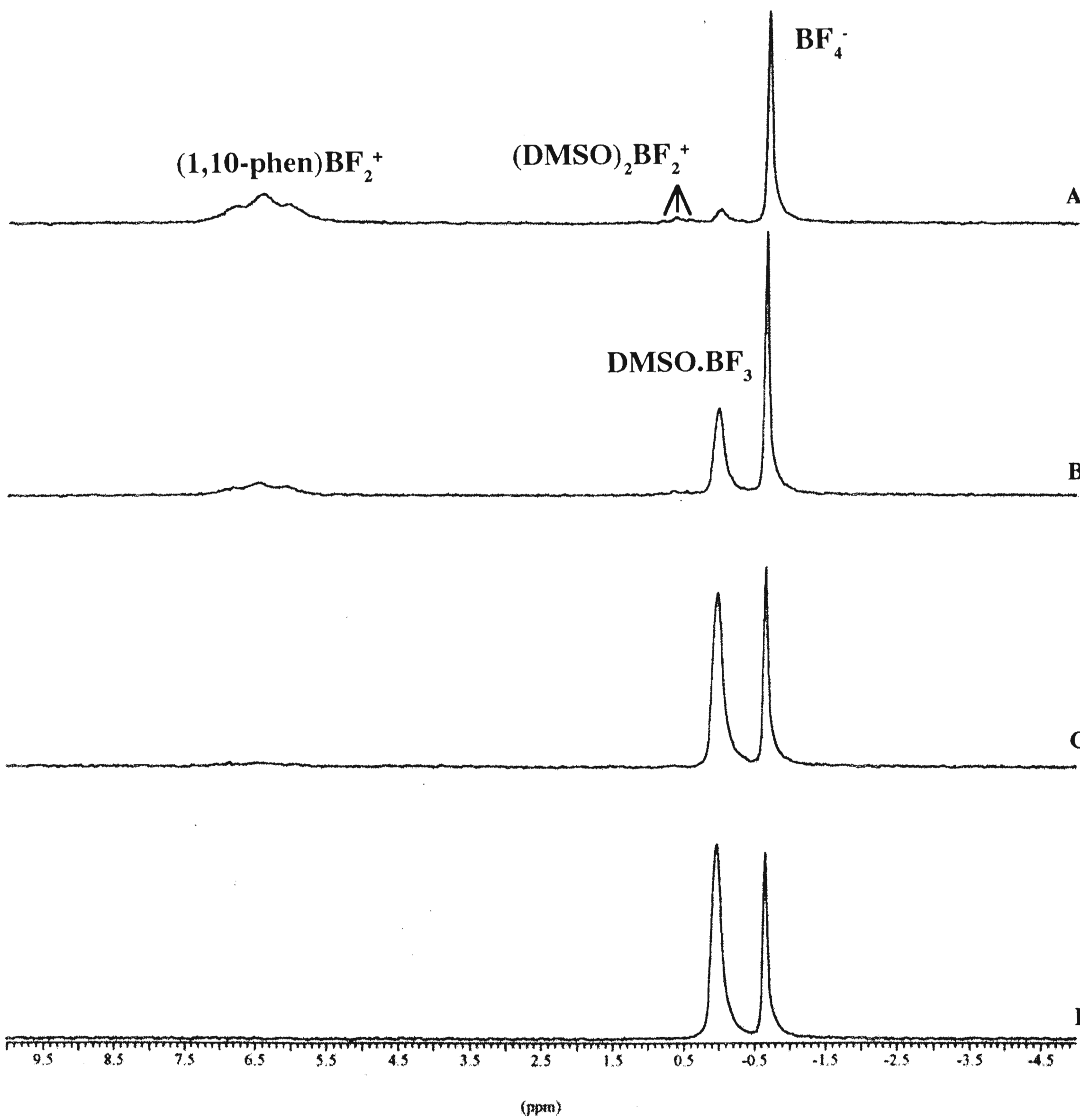

6.3.4: Reactions with 1,8-BDN species. 10 mg of the (1,8-BDN)$BF_2^+.BF_4^-$ salt in 0.5 ml of acetonitrile-d3 did not react with a four molar excess of DMSO over a week. This is expected, because of the cation's steric hindrance. This cation is similar in behavior to the (quinuclidine)$_2BF_2^+$ cation that we have studied in the past (13), which was unreactive with a wide variety of D' donors.

6.4: Discussion.

6.4.1: Solvolysis of bipyr and 1,10-phen species. The product assigned as bipyr.$(BF_3)_2$ in section **6.2.4** has a similar ^{11}B chemical shift in DMSO (0.0 ppm) as reported for (bipyr)BF_2^+ by Axtell et al. (0.6 ppm) (28) and Koch and Madelung (1.6 ppm) (30). (Bipyr)BF_2^+ was successfully synthesized in chapters 3 and 4, and it appears at 5.7 ppm in the ^{11}B nmr spectrum (nitromethane, see chapter 7). In addition, this +1 cation of bipyr is not reactive with DMSO (section **6.3.1**). This suggests that contrary to Axtell et al. and Koch & Madelung's reporting, they did not form the $BF_2^+.BF_4^-$ salt of bipyr, but the bis-BF_3 adduct. As well, Koch & Madelung (30) suggested that (bipyr)BF_2^+ undergoes rapid solvolysis by DMSO, and reacts before it can be detected in solution by nmr, whereas the rigid (1,10-phen)BF_2^+ cation is much more stable towards DMSO. From our results, the opposite is true. Further evidence for bipyr.$(BF_3)_2$ must be gained. An X-ray crystal structure of a pure sample would verify this $(BF_3)_2$ isomer.

6.4.2: Ligand structure and the formation of DD.$(BF_3)_2$ adducts versus (DD)$BF_2^+.BF_4^-$ salts. All the aromatic chelating ligands discussed in chapter 1 that were reported to form the $BF_2^+.BF_4^-$ salts by reaction with $Et_2O.BF_3$ are very rigid (except

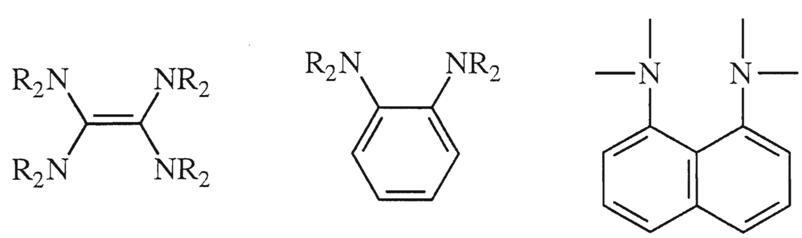

R = H or Me

bipyr, which by my work appears not to be rigid nor form the salt). Upon studying the structures of the t-amines ligands that have been reported successful, they were all rigid (29,36). Thus, of the seven ligands dealt with in this chapter, the four (**1 - 4**) that

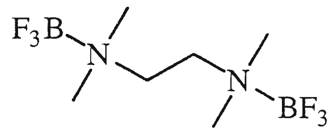

1

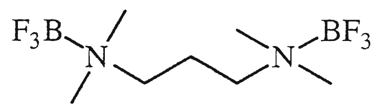

2

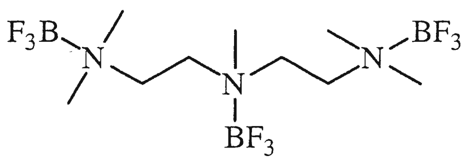

3

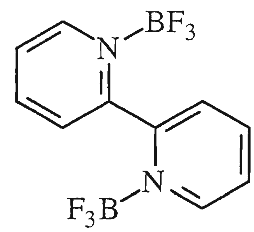

4

successfully formed the bis adduct (or tris) all had some flexibility, or an ability to rotate. This means that the BF_3 groups on the different donor sites did not have to come in contact with one another. The three (**5 - 7**) that did form $BF_2^+.BF_4^-$ salts could not on steric

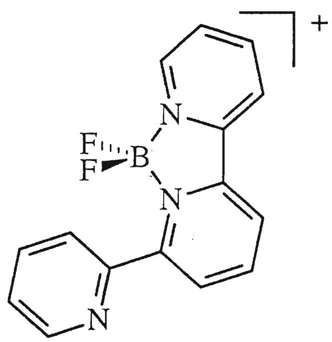

5

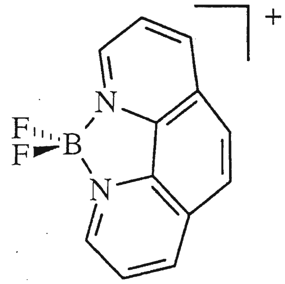

6

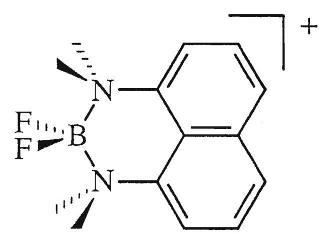

7

grounds, form bis or tris adducts without severe steric hindrance. Though terpyr could in theory form a bis or tris BF_3 adduct, the centre coordination site's BF_3 group would be interacting with one of the outer BF_3 groups or one of the outer pyridine rings, making the bis or tris BF_3 adduct sterically undesirable. The other two ligands (1,10-phen and 1,8-

BDN) are too rigid to form the bis BF_3 adduct. If it is formed, it is likely very short lived (see **6.4.3**).

6.4.3: Possible mechanisms for the formation of $(DD)BF_2^+.BF_4^-$ salts. There are four possible mechanisms of formation of $(DD)BF_2^+.BF_4^-$ salts from $Et_2O.BF_3$ (reactions **6.1** through **6.3**). These mechanisms can be determined with the used of ^{11}B and ^{19}F nmr. The examples are all illustrated with 1,10-phen, without implying a specific mechanism for the 1,10-phen case. In addition, there are certainly other possibilities that could involve impurities (8a), especially H^+. H^+ has been suggested (65) to be responsible for the formation $BF_2^+.BF_4^-$ salts, by acting as a protecting group for one of the donor sites.

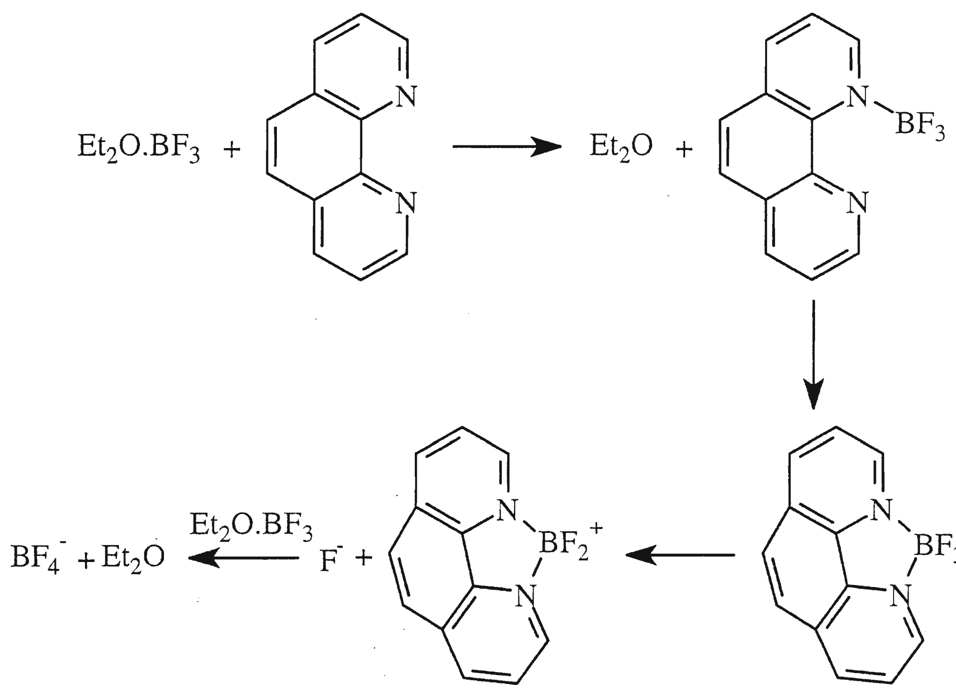

[**6.1**]

The first mechanism, reaction **6.1**, involves the initial coordination of BF_3. The second nitrogen on the ligand then coordinates to the boron, and in doing so, displaces an F^- anion. The boron atom's penta coordination could be detectable by nmr if it is long enough lived. The F^- is coordinated by BF_3 from $Et_2O.BF_3$ or free BF_3, giving Et_2O and

BF_4^-. Fluoride anions have been detected in various systems (12), so this is not impossible. Yet, in those systems where F^- existed, water or alcohol was generally present. In order to determine if this reaction was the method of formation of the cations, some Ph_3SnCl (66) could be placed in the reaction flask. F^- will displace the chlorine, and Ph_3SnF will precipitate to the bottom of the flask.

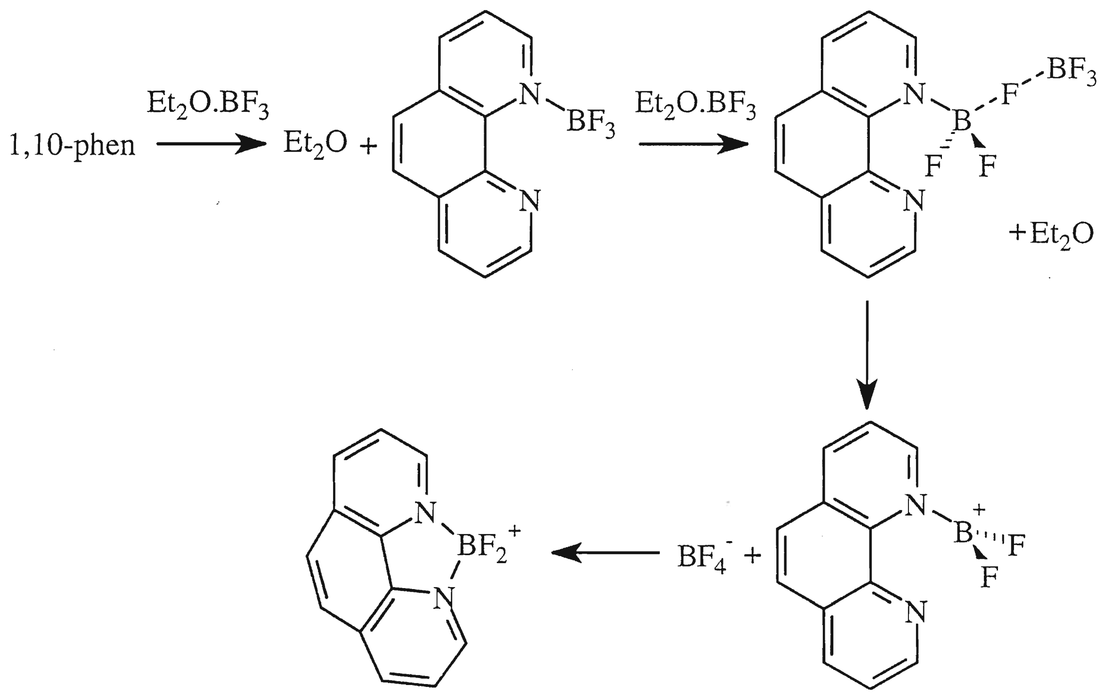

[6.2]

The second and third possible mechanisms (reactions [**6.2** and **6.3**]) involve the same starting point as reaction **6.1**, but instead of the ligand generating a fluoride ion, an $Et_2O.BF_3$ molecule disassociates and the BF_3 removes a fluorine from the tetra-coordinated [**6.2**] or penta-coordinated [**6.3**] BF_3 on the ligand via a fluorine bridge. The ligand is left with a sp^2 boron (as $N.BF_2^+$) [**6.2**] which it quickly chelates or the desired tetrahedral boron [**6.3**]. The tetra versus penta-coordinated boron could be determined via nmr. Fluorine bridges between two boron atoms have been detected by this lab (53a) and theorized by others (67). The conditions of the detection of a fluorine bridge by ^{19}F nmr have involved a very low temperature (118 K). If a sample was prepared, and studied, the chemical shift of the bridged-fluorine is around -110 ppm.

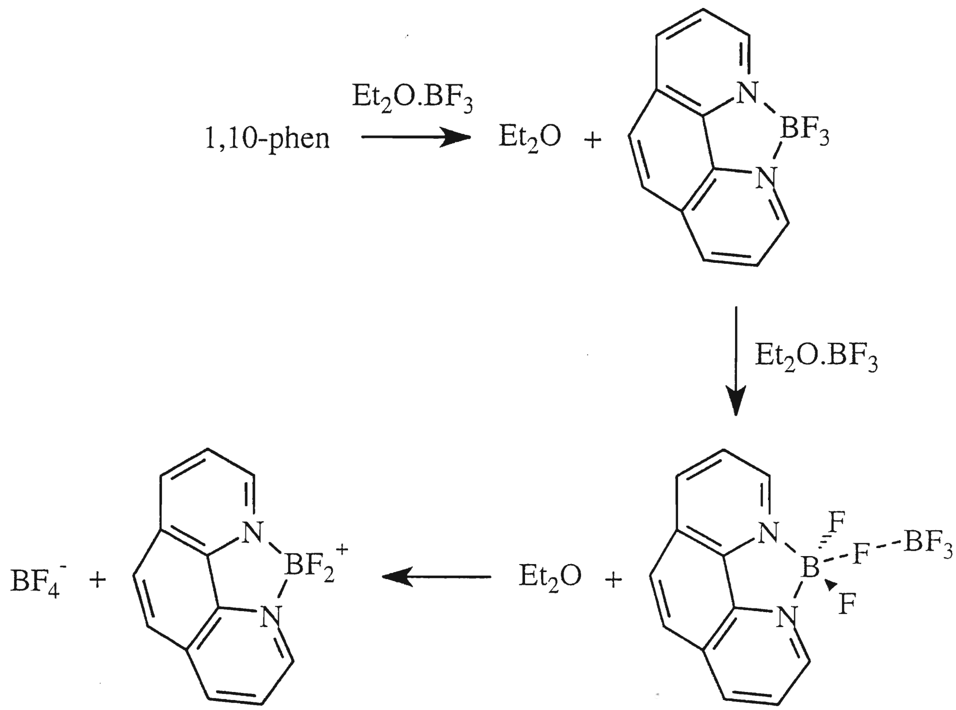

[6.3]

The fourth possible mechanism [6.4] involves the formation of a bis adduct of the bidentate ligand, which undergoes isomerization to the desired $BF_2^+.BF_4^-$ salt. This mechanism, like reactions **6.2** and **6.3**, would have to be proven at low temperature, where the reaction could be slowed down enough to detect the chemical shift changes as the chelating donor goes from bis adduct coordination to chelation.

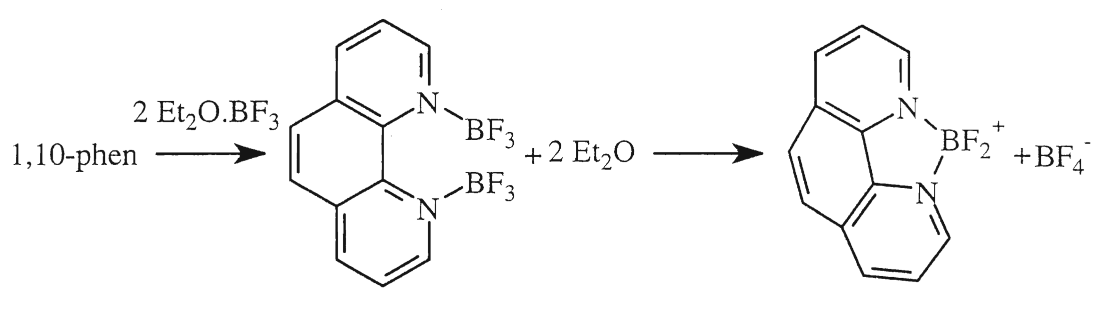

[6.4]

Chapter 7:
Nmr Parameters of Chelated Fluoroboron Cations and Related Species

7.1: Introduction.

It has been noted in many previous studies (6,13-15,55) that steric hindrance plays a large influence in the nmr parameters observed in fluoroboron cations. Using data from these studies (6,13-15,55), one can study the effects of chelation on fluoroboron cations very readily, for the nmr parameters of corresponding species with monodentate ligands are already known.

7.2: Results and Discussion.

7.2.1: Chelated tertiary-amine difluoroboron cations. Table 7.1 contains the chemical shifts of $(en)BF_2^+$, $(Me_4en)BF_2^+$ and $(Me_5dien)BF_2^+$ in acetone, and as the steric hindrance increases around the donor nitrogen atoms, the ^{19}F chemical shifts of the cations move further to high frequency (low field). This is the same trend as observed for

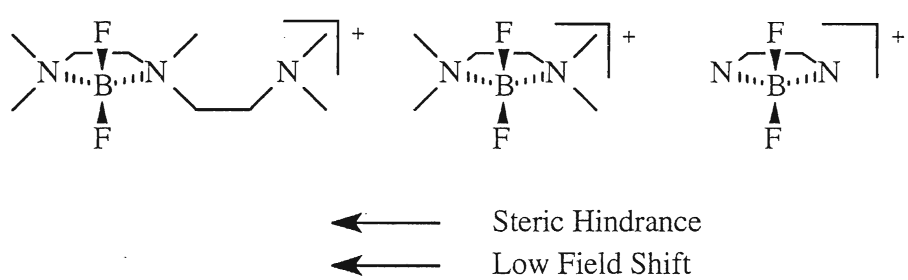

t-amine $(D)_2BF_2^+$ and $D.BX_3$ species (14,16,55). As for ^{11}B chemical shifts, there is no significant difference between the values for $(Me_4en)BF_2^+$ and $(Me_5dien)BF_2^+$ in acetone, chloroform or nitromethane. This shows that the central boron atom is not sensitive to the R groups on the nitrogen atoms.

Beyond the visible effects of steric hindrance on nmr parameters between chelated BF_2^+ cations, what are the visible nmr differences due to chelation? The chelated

Table 7.1: Nmr parameters of chelating t-amine ligand.boron dihalide cations.

	^{19}F Chemical Shift (ppm) in		^{11}B Chemical Shift (ppm) in		$^{1}J_{BF}$ (Hz) in	
	$CDCl_3$	Acetone	$CDCl_3$	Acetone	$CDCl_3$	Acetone
$(en)BF_2^+$		-156.2				32.6
$(Me_4en)BF_2^+$	-156.6	-154.7	3.7	4.4	32.7	31.4
$(Me_5dien)BF_2^{+a}$	-153.9	-152.0	3.5	4.6	32.9	32.9
	-155.1	-153.0			32.9	32.9
$(Me_4en)BFCl^+$	-139.9	-137.5[b]	8.8	9.2[b]	60.5	58.6[b]
$(Me_5dien)BFCl^+$	-137.5[c]	-135.1[bc]	8.8[c]	9.4[bc]	61.0[c]	60.2[bc]
	-140.6[d]	-137.7[bd]	8.8[d]	9.3[bd]	61.0[d]	60.2[bd]

[a]Coupling constants ($^{1}J_{BF}$) obtained from the ^{11}B spectra are somewhat larger than those determined from the ^{19}F spectra: 33.5 Hz in $CDCl_3$, 34.5 Hz in acetone; [b]insoluble in acetone; obtained in 3:1 acetone:sulpholane; [c]minor diastereomer; [d]major diastereomer.

$(Me_4en)BF_2^+$ and $(Me_5dien)BF_2^+$ cations have downfield shifted ^{19}F chemical shifts in chloroform: from -153.9 to -156.6 ppm (table 7.1); which are outside the range (-158.9 to -165.4 ppm) for similar non-chelated $(NR_3)_2BF_2^+$ cations (14). The cause of this is likely steric hindrance or lack of mobility, induced by chelation, but it is not likely due to the methyl groups of the ligands being any closer then in the non-chelated cations (table 7.2). The same downfield shift holds true for the ^{11}B chemical shifts (3.5 to 3.7 ppm versus 1.9 to 2.3 ppm). This strongly suggests that the boron is in a much more sterically hindered environment upon chelation. The PM3 semi-empirical models of $(Me_4en)BF_2^+$, and $(NMe_3)_2BF_2^+$ have been modeled by MacSpartan (figure 7.1 and table 7.2), and they agree with this. The boron atom in $(Me_4en)BF_2^+$ relative to $(NMe_3)_2BF_2^+$ has a shorter (-0.015 Å) N-B bond, and a greatly compressed N-B-N bond angle (-14.17°). $(Me_5dien)BF_2^+$ displays a similar trend (table 7.2). Beyond chemical shift alteration due to chelation, the $^1J_{BF}$'s of chelated t-amine ligands are 3.5 to 6.8 Hz smaller then the unchelated $(NR_3)_2BF_2^+$ cations (36.2 to 39.3 Hz) of similar monodentate ligands. This is odd, for the $^1J_{BF}$'s of $(NR_3)_2BF_2^+$ cations generally increase with steric hindrance, yet this is not noted in the chelated species (either between each other or versus the $(NR_3)_2BF_2^+$ cations). Differences in F-B-F bond angle can also affect nmr parameters (16), and there is little difference (0.213°), between the $(Me_4en)BF_2^+$ and $(NR_3)_2BF_2^+$ models.

$(Me_5dien)BF_2^+$ has a chiral central nitrogen, which causes the boron atom to become prochiral and induces magnetic non-equivalence in the two fluorine atoms. This is notable in the collapsing of the $^2J_{FF}$ coupling in figure 7.3 ($^{19}F\{^{19}F\}$) and the distinctive cross peaks in a ^{19}F-^{19}F COSY nmr spectrum (figure. 7.4) A ^{11}B-^{19}F HETCOR nmr spectrum (figure 7.5), of a solution that had been standing at room temperature for 3 months (and involved the 4-Mepyr rather than the pyr adduct system; the behavior is essentially identical), displays the magnetically nonequivalent fluorine atoms of the $(Me_5dien)BF_2^+$ cation, both correlating to the same ^{11}B 1:2:1 triplet. The $^2J_{FF}$ value of 61.2 Hz, compares readily to others found by this lab and others (16,53) (figure 7.2). Steric

Figure 7.1: Models of $(Me_4en)BF_2^+$ and $(NMe_3)_2BF_2^+$.

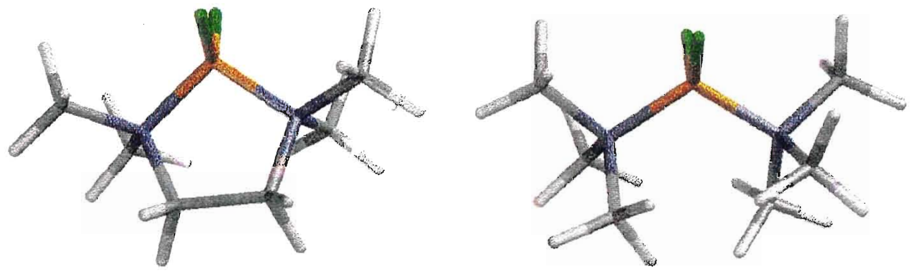

Table 7.2: Values from PM3 calculations on $(DD)BF_2^+$ and related species.

	B-F Length (Å)	N-B Length (Å)	F-B-F Angle (°)	N-B-N Angle (°)	Distance Nearest C to F (Å)
$(Me_4en)BF_2^+$	1.3(39-40)	1.680	109.165	101.796	2.(789-803)
$(Me_5dien)BF_2^+$	1.34(0-2)	1.68(1-3)	109.070	102.152	2.(788-836)[a]
					2.(804-817)[b]
$(NMe_3)_2BF_2^+$	1.343	1.695	109.378	115.966	2.7(44-70)
BF_4^-	1.402		109.471		

[a]fluorine in plane of two methyl groups; [b]fluorine in plane of methyl and long chain.

Figure 7.2: 188.31 MHz ^{19}F nmr spectrum of $(Me_5dien)BF_2^+$ in chloroform. $^1J_{BF}$ and $^2J_{FF}$'s noted.

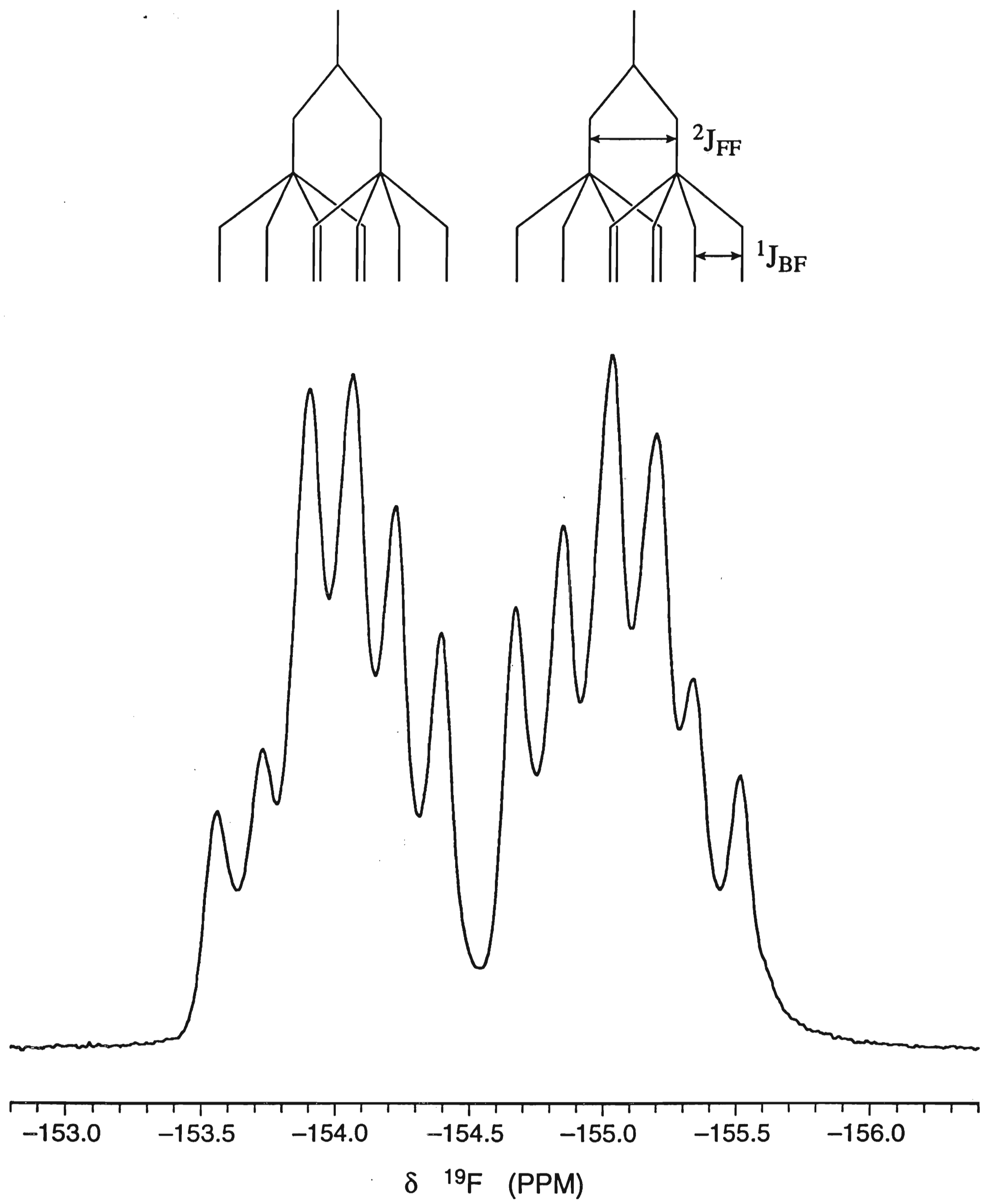

Figure 7.3: 470.53 MHz ^{19}F nmr and $^{19}F\{^{19}F\}$ nmr spectra of $(Me_5dien)BF_2^+$ in chloroform.

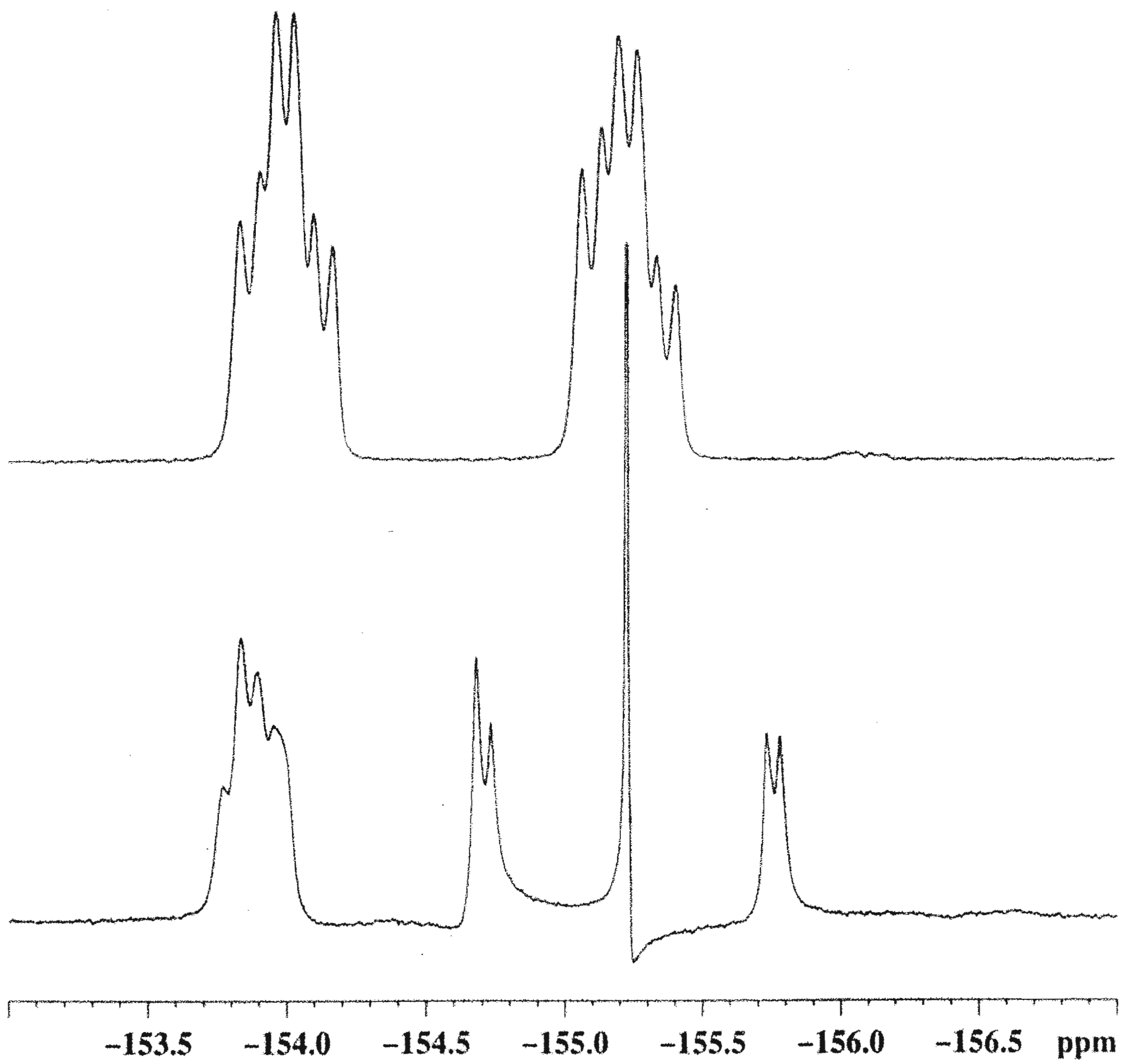

Figure 7.4: 470.53 MHz ^{19}F-^{19}F COSY nmr spectrum of $(Me_5dien)BF_2^+$ present in a solution of $4\text{-Mepyr.BF}_nCl_{3-n}$ following reaction with Me_5dien and standing for 3 months.

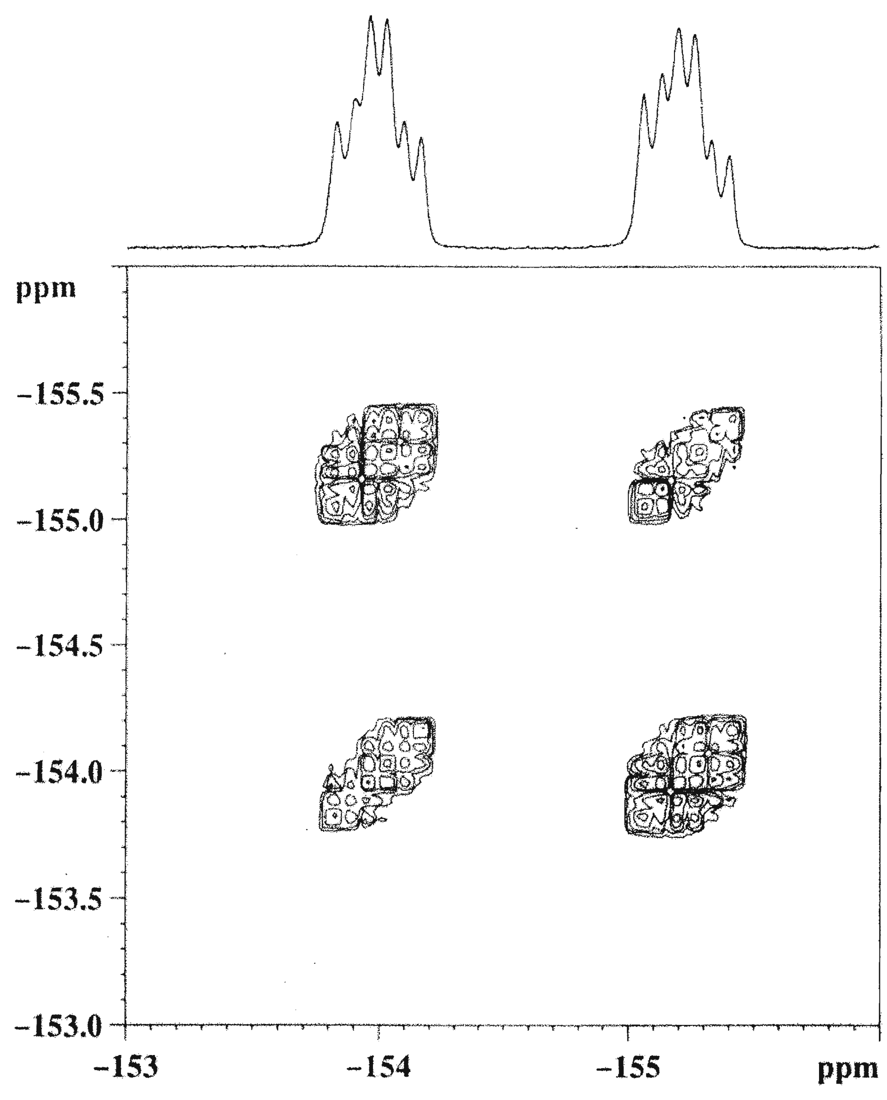

Figure 7.5: 11.7 Telsa partial ^{11}B-^{19}F HETCOR nmr spectrum of species formed from a solution of 4-methylpyridine to which Me_5dien had been added, after standing for 3 months.

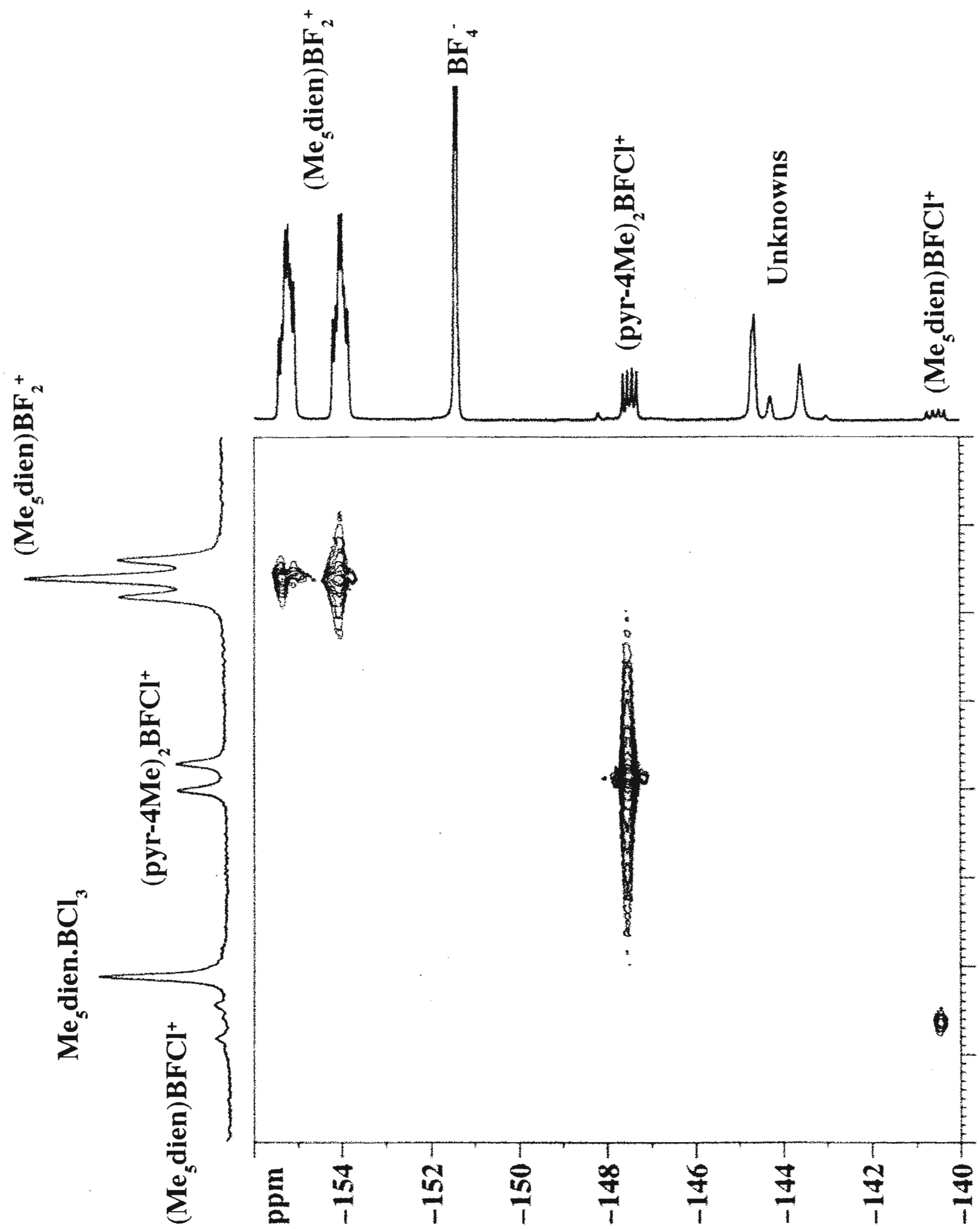

hindrance arguments were used to assign the chemical shifts of the two fluorine atoms: the F in the plane of the two methyl groups is to low frequency of the F in the plane of the methyl and long chain.

7.2.2: Chelated tertiary-amine fluorochloroboron cations. The chelated $BFCl^+$ cations also appear to follow the trend of high-frequency shifting on chelation, though the data is more limited (6,13,14,55). The same holds true whether one looks at the $BFCl^+$ cations in chloroform or acetone:sulpholane (table 7.1). The fluorine of the major diastereometer (**MAJ**) of $(Me_5dien)BFCl^+$ assigned as the structure shown below, has the same environment as $(Me_4en)BFCl^+$, whereas the minor diastereometer of $(Me_5dien)BFCl^+$ (**MIN**) does not, and is more hindered. Due to this, **MAJ** and

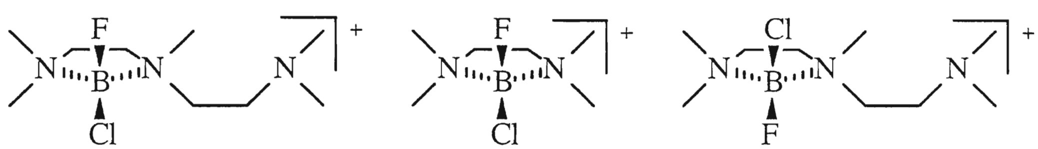

MAJ **MIN**

$(Me_4en)BFCl^+$ have very similar ^{19}F chemical shifts, and **MIN** is approximately 2 ppm down field. We assign the **MAJ** and **MIN** isomers on the same steric hindrance arguments as used for the BF_2^+ cation. ^{11}B chemical shifts (regardless of solvent) in table 7.1 display that the boron atoms in the $BFCl^+$ cations are not sensitive to the R groups on the nitrogen.

7.2.3: Mixed tertiary-amine difluoroboron and fluorochloro cations. The three flexible tertiary-amine chelating ligands (Me_4en, Me_4pn, and Me_5dien) are able to displace chlorine from $pyr.BF_2Cl$ to form the $(pyr)(Me_4en)BF_2^+$, $(pyr)(Me_4pn)BF_2^+$, and $(pyr)(Me_5dien)BF_2^+$ cations respectively (chapter 3). These three donors, along with Me_4dipn, form the mixed $(pyr)(DD)BF_2^+$ cations from $(pyr)_2BF_2^+$ as well (chapter 5). These 4 cations have nmr parameters (table 7.3) that match those of mixed monodentate $(pyr)(NR_3)BF_2^+$ cations (14,15,55). As well, the mixed cations for Me_5dien and Me_4dipn indicate that they bond through one of their end nitrogen sites. The chemical shifts of their mixed species, if they occurred with bonding through their central nitrogen sites, would be

Table 7.3: Nmr parameters of (pyridine)(t-amine).dihaloboron cations.

Species	^{19}F Chemical Shift (ppm)		^{11}B Chemical Shift (ppm)		$^{1}J_{BF}$ (Hz)	
	Acetone	$CHCl_3$	Acetone	$CHCl_3$	Acetone	$CHCl_3$
$(pyr)(Me_4en)BF_2^+$	-158.7	-160.8			29.2	29.0
$(pyr)(Me_5dien)BF_2^+$	-158.7	-160.5			27.4	28.8
$(pyr)(Me_4pn)BF_2^+$	-159.7	-160.0		3.0	28.5	29.3
$(pyr)(Me_4dipn)BF_2^+$	-159.8				28.5	
$(pyr)(NMe_3)BF_2^+$		-162.5[a]		2.0[a]		28.5[a]
$(pyr)(NMe_2Et)BF_2^+$		-159.8[a]				29.7[a]
$(pyr)(NEt_3)BF_2^+$		-150.4[a]				33.0[a]
$(pyr)(Me_4pn)BFCl^+$		-150.1				53.0

[a]From reference 14.

further to high frequency. All the mixed-donor cations display a trend that was noted in our 1998 paper (13): that mixed donor fluoroboron cations that involve pyridine, have chemical shifts that are closer to the other donors' $(D)_2BF_2^+$ than to $(pyr)_2BF_2^+$.

There is one mixed $(pyr)(DD)BFCl^+$ cation in table 7.3, that of Me_4pn. As mentioned above for fully chelated $BFCl^+$ species, there is too little data on mixed $BFCl^+$ cations to determine if the nmr parameters for $(pyr)(Me_4pn)BFCl^+$ behave like those of the mixed-donor difluoroboron cations.

7.2.4: Tertiary-amine.mixed boron trihalide adducts. The adducts of Me_4en, Me_4pn, and Me_5dien formed from the $ISOX.BF_nCl_{3-n}$, $pyr.BF_nCl_{3-n}$ and $Et_2O.BF_3$ systems have similar nmr parameters as adducts formed with monodentate t-amine ligands (16). The ^{19}F chemical shifts and $^1J_{BF}$'s match those of $NMe_2Et.BF_nCl_{3-n}$ the best, suggesting that all the adducts formed by the reactions with $ISOX.BF_nCl_{3-n}$ and $pyr.BF_nCl_{3-n}$ systems, coordinate through only one nitrogen, and Me_5dien coordinates through one of its end nitrogen atoms (table 7.4). These species were assigned by using chemical shift trends based on steric hindrance of tertiary-amine donors (14) and by relative peak intensities. It was only in the excess Lewis acid $Et_2O.BF_3$ systems that the bis and tris BF_3 adducts formed. The ^{11}B chemical shifts of the adducts follow the same trend as ^{19}F, though the specific ^{11}B chemical shifts of NMe_2Et adducts are not available to compare directly.

7.2.5: Chelated aromatic dihaloboron cations. $(Pyr)_2BF_2^+$ has the closest structure of any bismonodentate difluoroboron cation to the $(bipyr)BF_2^+$ cation. Their ^{19}F chemical shifts are similar: $(pyr)_2BF_2^+$ = -155.6 ppm; $(bipyr)BF_2^+$ = -154.4 ppm. The ^{11}B chemical shifts in nitromethane, display a larger effect of chelation: $(pyr)_2BF_2^+$ = 2.7 ppm*; $(bipyr)BF_2^+$ = 5.7 ppm (*value estimated from ref. 15 for nitromethane by adding +1 ppm to the chloroform value). The $(bipyr)BCl_2^+$ and $(bipyr)BBr_2^+$ cations display effects due to chelation in the ^{11}B spectra (see table 7.5), though the BCl_2^+'s is not as pronounced (+0.6 and +3.6 ppm respectively). As seen with the t-amines, chelation has a

Table 7.4: Nmr parameters of t-amine chelating ligand.boron trihalide adducts.

	^{19}F Chemical Shift (ppm) in		^{11}B Chemical Shift (ppm) in		$^{1}J_{BF}$ (Hz) in	
	$CDCl_3$	CH_3NO_2	$CDCl_3$	CH_3NO_2	$CDCl_3$	CH_3NO_2
$Me_4en.BF_3$	-162.3	-157.6	0.1	1.1	15.5	15.4
$Me_5dien.BF_3$[a]	-162.0	-158.8	-0.2		15.9	15.9
$Me_5dien.BF_3$[b]	-160.8	-158.7	-0.2		15.5	
$Me_4pn.BF_3$	-161.2	-159.0	0.1	1.2	15.5	15.1
$NMe_2Et.BF_3$[c]	-161.4				15.7	
$Me_4en.(BF_3)_2$	-158.6	-157.2			15.5	15.1
$Me_5dien.(BF_3)_2$[d]		-158.1				15.5
$Me_5dien.(BF_3)_2$[e]		-156.9				15.5
$Me_5dien.(BF_3)_3$		-151.8(3F)				15.5
		-157.3(6F)				15.0
$Me_4pn.(BF_3)_2$	-160.7	-157.2			15.5	15.5
$Me_4en.BF_2Cl$		-135.1		5.6		43.9
$Me_4pn.BF_2Cl$	-139.4	-137.5	4.6	5.8	44.2	43.3
$NMe_2Et.BF_2Cl$[c]	-139.7				44.1	
$Me_4en.BFCl_2$		-123.3		9.4		70.3
$Me_5dien.BFCl_2$	-126.9	-124.9	8.4	9.4	70.2	70.8
$Me_4pn.BFCl_2$	-128.4	-126.8	8.4	9.5	69.8	69.2
$NMe_2Et.BFCl_2$	-129.2				70.1	
$Me_4en.BCl_3$			10.2	11.1		
$Me_5dien.BCl_3$			10.0	11.1		
$Me_4pn.BCl_3$			10.1	11.2		

[a]Coordination at an end nitrogen; [b]Coordination at middle nitrogen; [c]From ref. 14 [d]Dicoordination at both end nitrogen atoms; [e]Dicoordination at the middle and one end nitrogen. ^{19}F chemical shifts of the centre and end coordinated BF_3 overlap with a separation of only 0.05 ppm at 188.31 MHz.

Table 7.5: Nmr parameters of aromatic ligand.dihaloboron cations.

	^{19}F Chemical Shift (ppm) in		^{11}B Chemical Shift (ppm) in		$^{1}J_{BF}$ (Hz) in	
	$CDCl_3$	CH_3NO_2	$CDCl_3$	CH_3NO_2	$CDCl_3$	CH_3NO_2
$(pyr)_2BF_2^{+}$[a]	-155.6		1.7	(2.7)	22.9	
$(bipyr)BF_2^{+}$	-154.4	-155.7		5.7		23.5
$(1,10\text{-phen})BF_2^{+}$		-149.8		7.0		24.4
$(terpyr)BF_2^{+}$	-146.0	-145.2	5.0	6.0	b	25.2
$(pyr)(2\text{-Mepyr})BF_2^{+}$[a]	-147.5		2.1	(3.1)	25.4	
$(pyr)_2BFCl^{+}$	-146.9		6.2		47.8	
$(bipyr)BFCl^{+}$	-142.3	-143.6	7.4	8.4	~ 55	51.7
$(1,10\text{-phen})BFCl^{+}$	-139.4	-139.1	8.7	9.8	b	52.9
$(terpyr)BFCl^{+}$	-129.8	-128.0	7.6	8.7	49.9	49.1
$(pyr)_2BFBr^{+}$[a]	-142.4		4.9	(5.9)	58.1	
$(bipyr)BFBr^{+}$		-137.5		6.1		61.5
$(1,10\text{-phen})BFBr^{+}$		-135.3		7.1		63.2
$(terpyr)BFBr^{+}$	-126.7	-125.1		5.4	b	60.6
$(pyr)(2\text{-Mepyr})BFBr^{+}$[a]	-129.4		5.2	(6.2)	62.1	
$(pyr)_2BCl_2^{+}$			8.4			
$(bipyr)BCl_2^{+}$			7.8	8.8		
$(1,10\text{-phen})BCl_2^{+}$			9.1	10.2		
$(terpyr)BCl_2^{+}$			8.0	9.0		
$(pyr)_2BBr_2^{+}$[a]			2.6	(3.6)		
$(bipyr)BBr_2^{+}$				0.0		
$(1,10\text{-phen})BBr_2^{+}$				0.6		
$(terpyr)BBr_2^{+}$			-1.4	-0.9		

[a]Values from ref. 15. Calculated ^{11}B chemical shift based on the changes of between chloroform and nitromethane are in (); [b]unresolved.

large effect on the ^{11}B chemical shifts of BX_2^+ cations, though the environment for the fluorine atoms (BF_2^+ cation) does not appear to be affected greatly. With the mixed halide cations of bipyr, there is some difference from $(pyr)_2BFX^+$ between chemical shifts in the ^{11}B and ^{19}F spectra, but the data is too limited to note whether it is the effects of chelation or that this is due to these species being mixed halide cations. The $^1J_{BF}$'s for the three fluoroboron bipyr cations do not differ greatly from the pyr species (only 0.6 to 3.9 Hz), unlike the chelated t-amine species did above. This data is marginal, because data from different solvents had to be compared.

$(bipyr)_2BF_2^+$ is the closet relative to the $(1,10\text{-phen})BF_2^+$ cation. The extra rigidity of 1,10-phen, and the addition of the third aromatic ring apparently cause the significant ^{19}F and ^{11}B chemical shift difference between the two (see table 7.5). The same trend exists for the mixed and diheavy halide cations. The $^1J_{BF}$ values display little difference on chelation.

The $(terpyr)BF_2^+$ cation and the other bidentate terpyr species are much closer akin to $(pyr)(2\text{-Mepyr})BF_2^+$ and related cations in steric hindrance of the donor, and the selected ones displayed in table 7.5 show the same trends as pyr and bipyr do above. In comparing terpyr and bipyr cations' ^{19}F chemical shifts, it can be readily seen, as could be observed between pyr and 2-Mepyr (15), that a coordinated pyr that has an R group at the 2 site is much more sterically hindered then pyr itself.

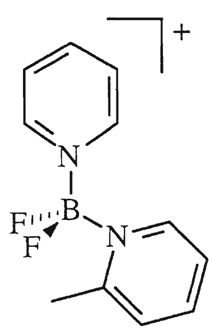

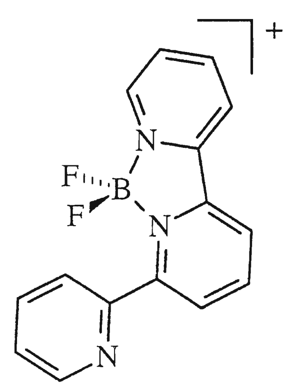

7.2.6: (1,8-BDN)BF_2^+. 1,8-BDN, though it has an aromatic backbone and reacts more akin to aromatic ligands, has nmr parameters that are more similar to those of t-amine ligands. The $(NR_3)_2BF_2^+$ that is the most similar to (1,8-BDN)BF_2^+ is $(Me_3N)_2BF_2^+$ (11,14,55). When one compares the nmr parameters in chloroform, the following trends are noted: $(Me_3N)_2BF_2^+$ = -165.4 ppm (^{19}F) 1.9 ppm (^{11}B) [$^1J_{BF}$ = 36.2 Hz] (55); (1,8-BDN)BF_2^+ = -164.4 ppm (^{19}F) 1.9 ppm (^{11}B) [$^1J_{BF}$ = 30.3 Hz]: very similar, except for the decrease in the $^1J_{BF}$ value. This is not surprising when one looks that the similar steric hindrance around the boron atom in both compounds. This is further

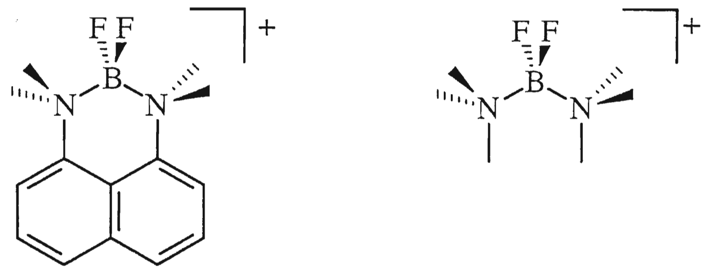

evidence that high frequency shifts in the ^{19}F and ^{11}B spectra of the chelated t-amine ligands (section **7.2.1**) were indeed due to steric hindrance caused by chelation. As for the difference in coupling constants, the fact that chelation of boron by t-amine ligands leads to lower coupling constants (section **7.2.1**), makes this observation consistent with the other results, though not readily explainable. Yet, since this is the only six-membered ring in this study, the conclusions are still tentative. More six-membered rings must be made to be certain of both the chemical shift and coupling constant observations.

7.2.7: Trends and problems in MAS nmr of chelated dihaloboron cations. ^{11}B, $^{11}B\{^1H\}$ and ^{19}F MAS nmr have been attempted on various insoluble materials. The ^{11}B MAS nmr spectra of insoluble materials formed from the reaction of Me_4en, Me_4pn and Me_5dien with solutions of ISOX.BF_nBr_{3-n} are poorly resolved. Yet, they do confirm from the chemical shifts of the broad signals that the insoluble materials contain the expected $BF_nBr_{2-n}^+$ cations (10 to 2 ppm) and BF_nBr_{3-n} adducts (2 to -10 ppm), and the relative intensities vary in the expected manner with changes in the proportions of F to Br. ^{11}B

chemical shifts in the solid state are similar to those in solution (16) for analogous species, but with a notable (2 to 5 ppm) shift to low frequency (high field).

High-power proton decoupling was applied, but it had little effect on the resolution. The broadening in ^{11}B was apparently due to ^{11}B-^{19}F dipolar interactions, and high-power ^{19}F decoupling would be needed to improve resolution. In addition, broadening due to dipolar interactions can be improved by spinning the samples faster (> 12.5 KHz) then is currently possible at Brock. ^{19}F MAS nmr was informative with test samples early in this work, but our depth sequence did not work after some probe problems, so interference from the probe background was too great to get usable spectra. ^{19}F solid state chemical shifts, like ^{11}B, are similar to solution values, but a slight high field shift.

Chapter 8:
Conclusions and Future Work

8.1: Conclusions.

Polydentate tertiary-amine donors that form 5-membered rings upon bidentate chelation were found to chelate effectively when the BF_2 source contained two leaving groups (a heavy halide and a Lewis base), i.e., pyr.BF_2X (X = Cl or Br), ISOX.BF_2X and $(pyr)_2BF_2^+$. Chelation by a tertiary-amine donor is a two-step reaction and the two rates appear to be very dependent on the two possible leaving groups on the central boron atom. The order of increasing ease of displacement for the donors is: pyr < Cl < Br < ISOX. Chelation by tertiary-amine donors leads to nmr parameters that are significantly different then their $(D)_2BF_2^+$ relatives. Those polydentate tertiary-amine donors that would form 6-membered rings upon chelation do not chelate by any of the four methods. Yet they give valuable information on the minor and major pathways for chelation by those that form 5-membered rings upon bidentate chelation. Polydentate tertiary-amine donors, when mono-coordinated, have nmr parameters like those of D.BF_nX_{3-n} and (pyr)(D)BF_2^+ relatives.

Polydentate aromatic ligands chelate effectively when the BF_2 source contained a weak Lewis base, e.g., ISOX.BF_3, ISOX.BF_2X and $Et_2O.BF_3$. Though the chelation by an aromatic donor is a two-step reaction, the rate of chelation by aromatic ligands appears to be dependent on the displacement of the first ligand from the boron. The order of increasing ease of displacement for the donors is: pyr < Cl < ISOX ≈ Br < Et_2O. In systems were a BF_3 source was present without a heavy halide, chelation occurs readily only with rigid aromatic donors.

1,8-BDN, due to its extreme steric hindrance, formed only the $(DD)BF_2^+$ cation, though, its base strength lead to some novel species to be detected.

No tridentate chelation by Me_5dien nor terpyr appeared to occur via the syntheses methods in this work.

8.2: Future Work.

The data contained in this work suggests that bidentate chelation of boron by tridentate ligands is dependent directly on the steric hindrance of the end nitrogen atoms. Many further chelating ligands would extend this work, and these three should be studied: N,N,N',N",N"-pentamethyldipropylenetriamine (Me_5dipn); N,N,N",N"-tetraethyl, N'-methyldiethylenetriamine (Et_4Medien); and N'-methyl, N,N"-dipyridinediethyleneamine (pyr_2Medien) (which are methylated bases from table 1.1). They should be reacted with the pyr.BF_nCl_{3-n} and ISOX.BF_nCl_{3-n} systems to determine: 1) if Me_5dipn ligand will confirm the observation that six member rings involving boron with tertiary-amine chelating ligands do not form; 2) Et_4Medien will test the theory that the end nitrogen atoms on tridentate ligands lead to the formation of mixed and fully chelated BF_2^+ cations, for NEt_3 does not displace chlorine from pyr.BF_2Cl, yet the ISOX.BF_2Cl adduct should allow the formation to the desired chiral (Et_4Medien)BF_2^+ cation; 3) pyr_2Medien should favour coordination at the outer nitrogen atoms, as Me_5dien does. Its central nitrogen and pyridine nitrogen atoms' BF_3 adducts to would be ~ 10 ppm apart in the ^{19}F spectrum. In addition all three ligands will give more insight into nmr parameters of chelated donors. For example, (pyr_2Medien)BF_2^+ should have a ^{19}F chemical shift of approximately -156 ppm, ^{11}B chemical shift of 5 ppm and a $^1J_{BF}$ of approximately 28 Hz if it follows current trends.

1,8-DBN behaves very differently from our other systems, and some simple but important reactions should be attempted. One series of experiments would involve reacting 1,8-DBN with BCl_3 and BBr_3 to determine if the BF_2^+ cation is just preferred in our systems, or is it the only dihaloboron cation that can form from proton sponge. The BCl_2^+ cation has been reported to form by Axtell et al. (28). In addition, carbene trapping experiments with the ISOX.BF_nCl_{3-n} system (where $BF_nCl_{4-n}^-$ ions form, and we presume carbene formation) should be attempted to verify our theory. The reaction would be monitored via ^1H nmr.

Certain ligands in our study chelated only in the presence of heavy halides or did not chelate at all under our conditions. The following experiments should be attempted to make BF_2^+ cations: 1) The isolation of bipyr, terpyr and Me_4pn (chelated ligand)$BF_2^+.I^-$ salts. The method for the Me_4pn is given in chapter 5; 2) bipyr and terpyr, could be reacted with ISOX.BF_3 in the presence of I_2. The addition of I_2 should allow the chelation of boron (or in the case of terpyr, the yield should increase); 3) forming the (chelated ligand)$BF_2^+.BF_4^-$ salts should also be attempted by reacting the above donors and (1,10-phen)$BF_2^+.BF_4^-$. (1,10-phen)BF_2^+ undergoes displacement by DMSO, so it should allow some or all of these donors to cause a similar displacement.

No tridentate chelation occurs via our methods: the MISO.BF_nBr_{3-n} system (MISO $pK_b = 15.0$ (10)) is a possible method of making the fully coordinated BF^{+2} cation of Me_5dien and the other tridentate bases; it is a much weaker donor then ISOX. The reacting of I_2 with isolated bidentate BF_2^+ cations of tridentate donors is another possibility (see above).

Look into ion exchange separation of solutions/precipitates containing cations: 1) so the t-amine cations can be isolated from their many adducts made by the above method and from each other; 2) so that selected cations can be used in chemical reactions without other species being present.

Further research involving the decomposition of the $(pyr)_2BF_2^+.PF_6^-$ salt with and without the presence of base should be performed. The formation of the fluorinated $(2F\text{-}pyr)_2BF_2^+.PF_6^-$ and $(3F\text{-}pyr)_2BF_2^+.PF_6^-$ salts, in addition to the $(pyr)_2BF_2^+.BPh_4^-$ salt will assist in this probing. Substitution reactions that involve the use of the fluorinated donors 2F-pyr and 3F-pyr, and other ligands should be performed to further probe the decomposition of the $(pyr)_2BF_2^+$ in a basic system. Kinetics simulations on the data presented in chapter 5 could also be performed to determine if the reactions to form (chelating ligand)BF_2^+ species occur via an S_N2 or S_N1 type reaction(s). Two phase reactions between insoluble $(pyr)_2BF_2^+$ salts and bases that react for low % yields could be attempted (i.e.., en, pn, etc.). The products of these reactions could be studied by MAS nmr. For aromatic reagents that have not successfully reacted in acetone, the following experiment can be attempted: mix a $(pyr)_2BF_2^+$ salt and the donor; heat mixture to the melting point of the donor under vacuum; keep reaction mixture at a set temperature for X minutes (during which, the removal of pyridine via vacuum occurs); extract chelated salt and/or cool mixture; study via solution or MAS nmr (63).

The most demanding of possible experimental future work involves experimentally determining the mean(s) in which DD forms $(DD)BF_2^+.BF_4^-$ from $Et_2O.BF_3$. This may be performed by molecular modeling like other studies involving fluorine exchange (67).

References

1. Cotton, F.A. & G. Wilkinson, Advanced Inorganic Chemistry, 5th Ed., John Wiley & Sons, Toronto (1988).

2. (a) King, R.B., Inorganic Chemistry of Main Group Elements, VCH Publishers, Inc., New York (1995), (b) Main Group Elements Hydrogen and Groups I-IV, Vol. 1, M.F. Lappert, University Park Press, Baltimore (1972).

3. N.N. Greenwood and A. Earnshaw, Chemistry of the Elements, Pergamon Press, New York (1984).

4. N.N. Greenwood and R.L. Martin, Q. Rev. Chem. Soc., **8**, 1 (1954).

5. J.S. Hartman and J.M. Miller, Ad. Inorg. Chem. Radiochem., **21**, 147 (1978) and references within.

6. J. S. Hartman, Z. Yuan, A. Fox, and A. Nguyen, Can. J. Chem., **74**, 2131 (1996).

7. (a) I. Hermeca, F. Möller and K. Eiter, Synthesis, 591 (1972), (b) D.H.R. Barton, J.D. Elliott, and S.D. Géro, J. Chem. Soc., Perkin Trans. 1, 2085 (1982).

8. (a) A.F. Janzen, Coord. Chem. Rev., **130**, 355 (1994), (b) X. Ou., R. Wallace and A.F. Janzen, Can. J. Chem., **71**, 51 (1993).

9. (a) M.J. Bula, D.E. Hamilton and J.S. Hartman, J. Chem. Soc. Dalton Trans., 1405 (1972), (b) D.E. Hamilton, J.S. Hartman, and J.S. Miller, Chem. Commun., 1417 (1969).

10. D.R. Perrin. Dissociation Constants of Organic Bases in Aqueous Solutions, Butherworths, London (1965).

11. M.J. Farquharson, M.Sc. Thesis, Brock University (1985).

12. (a) Z. Yuan, M.Sc. Thesis, Brock University (1988), (b) J.A.W. Shoemaker, B.Sc. Thesis, Brock University (1997).

13. J.S. Hartman, E.I. Ilnicki, J.A.W. Shoemaker, W.R. Szerminski, and Z. Yuan, Can. J. Chem., **76**, 1317 (1998).

14. M.J. Farquharson and J.S. Hartman, Can. J. Chem., **67**, 1711 (1989).

15. M.J. Farquharson and J.S. Hartman, Can. J. Chem., **74**, 1309 (1996).

16. A. Fox, J.S. Hartman and R.E. Humphries, J. Chem. Soc., Dalton Trans., 1275 (1982).

17. M.J. Farquharson, Unpublished Report, Brock University (1985).

18. F.A. Cotton, G. Wilkinson, C.A. Murillo and M. Bochmann, Advanced Inorganic Chemistry, 6th ed, John Wiley & Sons, Toronto (1999).

19. E.C. Constable, Metals and Ligand Reactivity, 2nd ed, VCH, New York (1996).

20. M.F. Richardson et al, Inorg. Chem., **32**, 1913 (1993).

21. (a) G. Fraenkel and W.R. Winchester, J. Am. Chem. Soc., **110**, 8720 (1988), (b) D. Hoffmann et al, J. Am. Chem. Soc., **116**, 528 (1994), (c) M. Kotowski, S. Begum, J.G. Leipoldt and R. van Eldik, Inorg. Chem., **27**, 4472 (1988), (d) E. Kimra, T. Koike, M. Kodama and D. Meyerstein, Inorg. Chem., **28**, 2998 (1989), (e) J.L. Atwood, K.D. Robinson, C. Jones, and C.L. Raston, J. Chem. Soc., Chem. Commun., 1697 (1991), (f) L.G. Hubert-Pfalzgraf, V. Abada, and J. Vaissermann, J. Chem. Soc., Dalton Trans. **20**, 3437 (1998).

22. D. Hoffmann and D.B. Collum, J. Am. Chem. Soc., **120**, 5810 (1998).

23. (a) S. Han, G.L. Geoffroy and A.L. Rheingold, Inorg. Chem., **26**, 3428 (1987), (b) J. Premkumar and R. Ramaraj, J. Chem. Soc., Dalton Trans. 21, 3667 (1998).

24. (a) G. La Monica, G.A. Ardizzoia, F. Cariati, S. Cenini and M. Pizzotti, Inorg. Chem., **24**, 3920 (1985), (b) T.W. Duma and R.D. Hancock, J. Coord. Chem. , **31**, 135 (1994).

25. N.S. Hosmane et al, Organometallics, **17**, 2784 (1998).

26. A.M. Shedlow and L.G. Sneddon, Inorg. Chem., **37**, 5267 (1998).

27. (a) K. Issleib, H Oehme and K Mohr, Z. Chem, **13**, 141 (1973), (b) D.J. Fuller, D.L. Kepert, B.W. Skelton and A.H. White, Aust. J. Chem., **40**, 2097 (1987).

28. D.D. Axtell, A.V. Campbell, P.C. Keller and J.V. Rund, J. Coord. Chem., **5**, 129 (1976).

29. T. Onak, H. Rosendo, G. Siwapinyoys, R. Kubo and L. Liauw, Inorg. Chem., **18**, 2943 (1979).

30. K.R. Koch and S. Madelung, Polyhedron, **10,** 2221 (1991).

31. R.M.K. Deng and K.B. Dillon, Polyhedron, **11**, 397 (1992).

32. G.E. Ryschkewitsch and T.E. Sullivan, Inorg. Chem., **9**, 899 (1970).

33. S.A. Genchur, G.L. Smith and H.C. Kelly, Can. J. Chem., **49**, 3165 (1971).

34. (a) H. C. Brown, B. Singaram and J.R. Schwier, Inorg. Chem., **18**, 51 (1979), (b) H. C. Brown and B. Singaram, Inorg. Chem., **18**, 53 (1979).

35. B. Singaram and G.G. Pai, Hetrocycles, **18,** 387 (1982).

36. (a) N. Wiberg and J. W. Buchler, Chem. Ber., **96**, 3000 (1963), (b) N. Wiberg and J. W. Buchler, J. Am. Chem. Soc., **85**, 243 (1963).

37. (a) J. Barluenga <u>et al</u>, J. Am. Chem. Soc., **120**, 2514 (1998), (b) F. Li, <u>et al</u>, J. Am. Chem. Soc., **120,** 10001 (1998), (c) X. Song, J. Nolan and B.I. Swanson, J. Am. Chem. Soc., **120,** 11514 (1998); (d) J. Karolin, L. B.-A. Johannson, L. Strandberg, and T. Ny, J. Am. Chem. Soc., **116**, 7801 (1994).

38. N. M. D. Brown and P. Bladon, J. Chem. Soc. (A), 526 (1969).

39. J.B. Lambert, H.F. Shurvell, D. Lightner and R.G. Cooks, <u>Introduction to Organic Spectroscopy</u>, Macmillan Publishing Company, New York (1987).

40. H. Friebolin, <u>Basic One- and Two-Dimensional NMR Spectroscopy</u>, 2nd ed., VCH, New York (1993).

41. J.K.M. Sanders and B.K. Hunter, <u>Modern NMR Spectroscopy</u>, 2nd ed., Oxford University Press, Toronto (1993).

42. A.E. Derome. Modern NMR Techniques for Chemistry Research, Pergamon Press, Toronto (1987).

43. F.A. Bovey, Nuclear Magnetic Resonance Spectroscopy, 2nd ed., Academic Press, Inc., Toronto (1988).

44. C.A. Fyfe, Solid State NMR for Chemists, C.F.C. Press, Guelph (1983).

45. Bruker nmr reference tables, Bruker Spectrospin Canada Ltd.

46. Multinuclear NMR, J. Mason, Ed., Plenum Press, New York (1987).

47. S. Berger, S. Braun and H. Kalionwski, NMR Spectroscopy of the Non-Metallic Elements, John Wiley & Sons, Toronto (1997) and reference within.

48. J.M. Miller, Mass Spec. Rev., **9**, 319 (1989).

49. K. Balasnmugam, J.S. Hartman, J.M. Miller, and Z. Yuan, Can. J. Chem., **67**, 685 (1989).

50. E. De Hoffmann, J. Charette, and V. Stroobant, Mass Spectrometry, John Wiley & Sons, Toronto (1996).

51. (a) R.G. Wilson, J. Appl. Phys. **54**, 6879 (1983), (b) A-M. Lanzillotto and C.W. Magee, J. Vac. Sci. Technol. A, **8**, 963 (1990), (c) M.C. Peak, H.B Im, O.J. Kwon and S.W. Kang, Sur. Coatings Technol., **43/44**, 986 (1990), (d) L. Kaabi et al, Nuc. Instr. and Meth. Phys. Res. B, **120**, 68 (1996).

52. C.G. Eisenhardt, S. Ring, H.-W. Jochims, and H. Baumgärtel, Chem. Phys., **216**, 427 (1997).

53. (a) J.S. Hartman & P. Stilbs, J. Chem. Soc. Chem. Comm., 566 (1975), (b) M. Appel & W. Beck, J. Organomet. Chem., 319 (1987).

54. G.J. Schrobilgen, M.Sc. Thesis, Brock University (1971) and references within.

55. M. J. Farquharson and J. S. Hartman, J. Chem. Soc., Chem. Comm., 256 (1984).

56. P. Ragogna and W.R. Szerminski, unpublished research in Hartman Research Group (1998).

57. J.S. Hartman and G.J. Schrobilgen, Inorg. Chem., **11**, 940 (1972).

58. (a) R.E. Mesmer and A.C. Rutenberg, Inorg. Chem., **12**, 699 (1973); (b) K. Kuhlmann and D.M. Grant, J. Phys. Chem., **68**, 3208 (1964).

59. K.O. Christe, D.A. Dixon, G.J. Schrobilgen, and W.W. Wilson, J. Am. Chem. Soc., **119**, 3918 (1997).

60. A.J. Gordon and R.A. Ford, The Chemist's Companion, John Wiley & Sons, Toronto (1972).

61. (a) S. Brownstein and J. Bornais, Can. J. Chem., **47**, 605 (1969), (b) S. Brownstein, Can. J. Chem., **47**, 605 (1969).

62. K.O. Christe, D.A. Dixon, H.R.A. Mercier, J.C.P. Sanders, G.J. Schrobilgen, and W.W. Wilson, J. Am. Chem. Soc., **116**, 2850 (1994).

63. A.F. Janzen et al, University of Manitoba, unpublished research (1998).

64. G.E. Ryschkewitsch and T.E. Sullivan, Inorg. Chem., **9**, 899 (1970).

65. J.S. Hartman, A.F. Janzen and X. Ou. Paper 57, 79th Annual Canadian Chemical Conference, St. John's Newfoundland, June 23-26 (1996).

66. M. Jang and J.F. Janzen, J. Fluorine Chem., **66**, 129 (1994).

67. A.F. Janzen, X. Ou, and M.G. Sowa, J. Fluorine Chem., **83**, 27 (1997).

Appendix I: Structural values from PM3 level molecular modeling experiments

	H_f (kJ/mol)	ΔH_f[a] (kJ/mol)	N-H (Å)	H-Br (Å)	Br-H (Å)	H-N (Å)	Bond Angle H-Br-H
$Me_4en.HBrH^+$ chelated	30.806		1.080	1.769	1.769	1.080	91.421
$BrH.Me_4en.H^+$	31.462	0.656	1.099	1.739	2.344	1.013	93.496
$Me_4en.H^+$ and BrH	33.538	2.732	1.010		1.477		
$Me_4pn.HBrH^+$ chelated	28.392		1.068	1.806	1.834	1.062	105.240
$BrH.Me_4pn.H^+$	27.977	-0.415	1.062	1.819	1.818	1.062	126.822
$Me_4pn.H^+$ and BrH	31.057	2.665	1.057		1.477		
$bipyr.HBrH^+$ chelated	48.537		1.067	1.777	1.777	1.067	79.686
$BrH.bipyr.H^+$	48.467	-0.070	1.096	1.735	2.679	0.993	84.964
$bipyr.H^+$ and BrH	50.557	2.020	1.000		1.477		
$1,10\text{-}phen.HBrH^+$ chelated	49.688		1.068	1.754	1.754	1.068	69.250
$BrH.1,10\text{-}phen.H^+$	49.688	0.0	1.068	1.754	1.754	1.068	69.267
$1,10\text{-}phen.H^+$ and BrH	51.922	2.234	0.998		1.477		

[a]Relative to chelated species

Appendix II: Models of chelated DDH.BrH+ species.

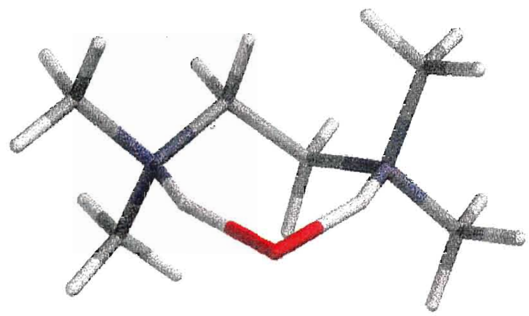

Me4en.H.BrH+

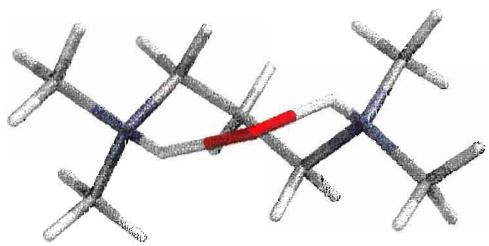

Me4pn.H.BrH+

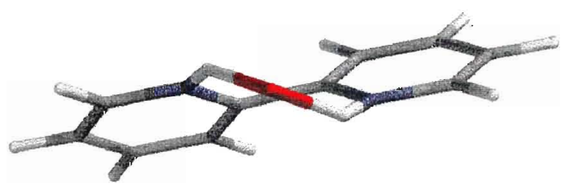

bipyr.H.BrH+

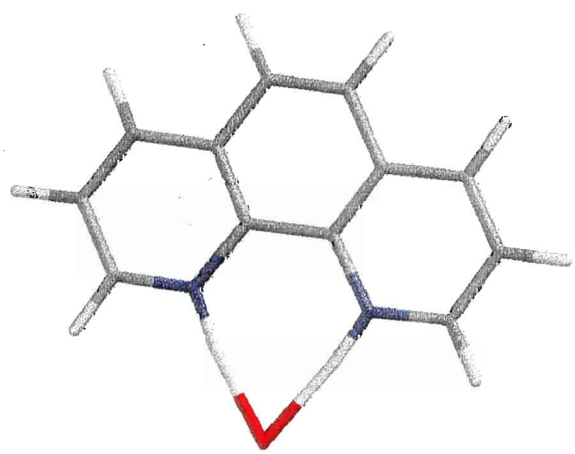

1,10-phen.H.BrH+

Appendix III: Positive ion FAB ms spectrum of species formed from bipyr + $ISOX.BF_nBr_{3-n}$ ($ISOX:BF_3:BBr_3:bipyr = 4:1:3:4$). 50 to 820 m/z range.